ASSEMBLY AND REGULATION OF SIGNALING PROTEINS AT FISSION YEAST MICROTUBULE ORGANIZING CENTERS

By

Joshua A. Rosenberg

Dissertation

Submitted to the Faculty of the

Graduate School of Vanderbilt University

in partial fulfillment of the requirements

for the degree of

DOCTOR OF PHILOSOPHY

in

Cell and Developmental Biology

August, 2007

Nashville, Tennessee

Approved:

Professor Kathleen L. Gould

Professor James G. Patton

Professor Todd R. Graham

Professor Laura A. Lee

Professor Susan R. Wente

ACKNOWLEDGEMENTS

I would first and foremost like to thank my mentor Kathy Gould. I appreciate her endless patience and guidance without which, I would not have been able to succeed. She has always encouraged me to be a critical and independent thinker in order to become a better scientist. I have been constantly challenged throughout my graduate career and been pushed farther than I thought I could or wanted to go. I would not change that experience for anything. Without it I could not have grown as a person or scientist and I thank Kathy for not giving up on me when it would have been easy to.

One thing that attracted me to the Gould lab was the incredible working environment that Kathy has created. She has been constantly been able to attract people that are equally fun and hardworking. This creates a certain "esprit de corps" within the lab which actually makes the long hours fun and enjoyable

Sir Isaac Newton said "If I have seen further, it is by standing on the shoulders of giants." I would like to thank some friendly giants whom I have stood in the shadows of. First of all, I would like to thank Srinivas Venkatram who has been a great friend and a second mentor to me. He always took time out of his day to discuss my project and experimental design. His scientific discussions have been invaluable to my graduate career. Second, I would like to thank my friend Ben Wolfe who has served as model of what a graduate student should be: dedicated, hard working, free thinking and independent. Greg Tomlin who started the Ppc89 project which has been a cornerstone in my graduate career.

I am confident the lab will be in good shape with some great scientists and

friends. Dawn Clifford-Hart is an excellent post-doc whom I look to for advice and guidance, both inside and outside of the lab. My across the bench buddy, Rachel H. Roberts-Galbraith, has helped me through some tough times in the lab and is always there to listen to me complain, thanks. Claudia Kale, I pass the senior graduate student torch to you, I hope it finds you well. One reason that the lab runs like clockwork is the excellent technicians Anna Feoktistova and Liping Ren. Their technical skills are unmatched in any lab.

I would also like to thank my committee members Susan Wente, Jim Patton, Todd Graham and Laurie Lee. I appreciate their help and advice with my project and never losing faith that I could become a scientist.

I would like to thank my parents for fostering a learning environment and always encouraging me to further pursue my academic interests. They have always been supportive of all of my choices and have constantly been there for me.

Last but certainly not least I would like to thank the endless patience, compassion and support of Alison without whom I would have never been able to get through grad school in one piece. Your compassion and nurturing have done more for me than you will ever know and I am so happy we are taking this journey through life together.

TABLE OF CONTENTS

Page

LIST OF FIGURES

LIST OF TABLES

Table Page

LIST OF ABBREVIATIONS

A	alanine
aa	amino acid
ade	adenine
ATP	adenosine triphosphate
C	Celsius /carboxyl
Cdk	Cell division cycle
Cdk	Cyclin-dependent kinase
CFP	Cyan fluorescent protein
DAPI	4,6-diamino-2-phenylindole
DIC	Differential contrast interference
DNA	Deoxy ribonucleic acid
ECL	Enhanced chemiluminescence's
EDTA	ethylenediaminetetraacetic acid
eGFP	Enhanced green fluorescent protein
EM	Electron microscopy
eMTOC	Equatorial microtubule organizing center
FACS	Fluorescent-activated cell sorting
FRET	Fluorescence resonance energy transfer
G1	GAP 1
G2	GAP 2
GDP	Guanosine diphosphate
GFP	Green fluorescent protein
GDP	Glutathione-S-transferase
GTP	Guanosine triphosphate
h	Hour
HA	influenza hemaglutinin epitope
HCL	Hydrochloric acid
his	histidine
IgG	Immunoglobulin G
iMTOC	Interphase microtubule organizing center
kDa	Kilodalton
KGY	Kathy Gould yeast
kV	Kilo volts
leu	Leucine
M	Mitosis/mitochondria
MBP	Maltose binding protein
MT	Microtubule
MTOC	Microtubule organizing center
N	amino
NaCL	Sodium chloride
NE	Nuclear envelope
nm	Nanometer
nmt	No message in thiamine promoter

NP-40	Nonidet P-40
ORF	Open reading frame
^{32}P	phosphorous-32
PAGE	Polyacrylamide gel electrophoresis
PBST	Phosphate buffered saline w/ tween
PCM	Pericentriolar material
PCR	Polymerase chain reaction
pH	Potential of hydrogen
Pro	Proline
PVDF	Polyvinylidene Fluoride
rpm	Revolutions per minute
^{35}S	Sulfur-35
S	Synthesis phase
Sc	*Saccharomyces cerevisiae*
SDS	Sodium dodecyl sulfate
Ser	Serine
SIN	Septation initiation complex
Sp	*Schizosaccharomyces pombe*
SPB	Spindle pole body
TAP	Tandem affinity purification
TBS	Tris-buffered saline
TBS-T	Tris-buffered saline w/ tween
Thr	Threonine
TNT	Transcription/Translation *in vitro* system
Trp	Tryptophan
UV	Ultraviolet
YE	Yeast extract
YFP	Yellow fluorescent protein
μg	Microgram
μm	Micrometer
γ-TuC	Gamma tubulin complex
APC	Anaphase promoting complex
Cdk1	Cyclin dependent kinase 1

CHAPTER I

INTRODUCTION

The eukaryotic cell cycle

Understanding the regulation of how cells grow and divide is one of the most important and basic biological questions. Many of the components involved in cell cycle regulation have been identified using biochemical and genetic screens in model organisms yet the actual coordination is still not fully understood. Understanding the pathways that regulate the cell cycle will give us greater insight into this fundamental biological process and also help us determine what happens in cancer states where cells loose their regulation.

The eukaryotic cell cycle (Figure 1) consists of a round of DNA synthesis (S-phase) flanked by two rounds of cell growth known as GAP phases (G1 and G2). The final stage of the cell cycle is mitosis (M-phase) where the duplicated DNA is segregated and cells divide in a process known as cytokinesis (Murray and Hunt, 1993). During the cell cycle there are monitoring mechanisms in place, known as checkpoints, to ensure that the complex functions that take place during S and M phases do so with a high degree of fidelity (Hartwell and Weinert, 1989). These monitoring processes take place during the GAP phases of the cell cycle and do not allow the cell to proceed into the subsequent phase of the cell cycle until any errors are repaired.

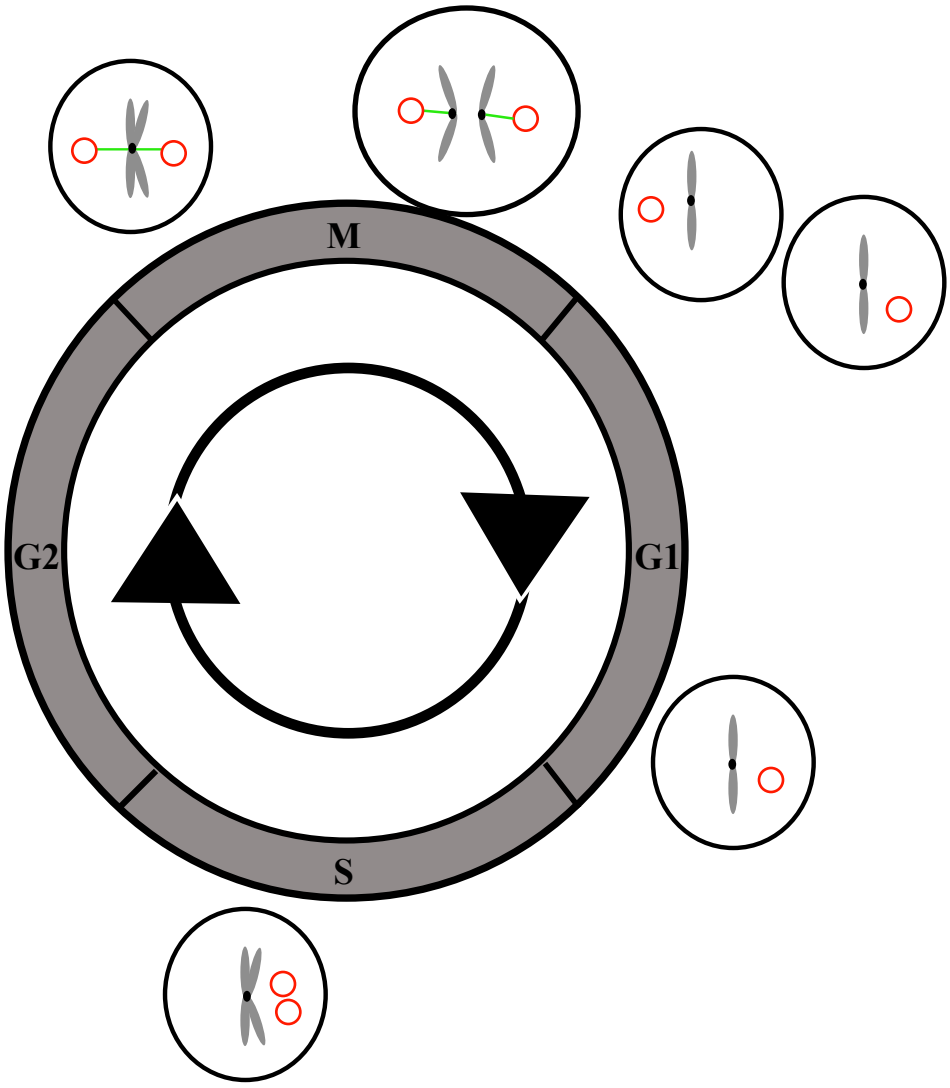

Figure 1. The eukaryotic cell cycle. The cell cycle is divided into four distinct phases: G1, S, G2 and M. During S phase the chromosomes are duplicated as well as the centrosome (red circle). As cells progress in to M-phase the centrosomes migrate to opposite poles of the cell and set up the mitotic spindle (green line). Cytokinesis produces two identical cells with the same DNA.

Cdk regulation

The master regulators of the cell cycle are the highly conserved Cyclin-dependent kinases (Cdks). Cdks require association with a cyclin subunit, as their name implies, in order to be active and properly target substrates for phosphorylation. Specificity of cyclin-Cdk complex activity is achieved by the presence of certain cyclins at specific stages of the cell cycle which are then quickly degraded. Since different Cdk complexes are needed at specific stages to drive the cell cycle forward, the cell cycle can also be thought of as a Cdk cycle. In higher eukaryotes, there are multiple Cdks each of which is dedicated to promote a specific stage of the cell cycle. The activity and specificity of Cdks in a particular cell cycle stage is achieved through association with different cyclin regulatory proteins (Nigg, 1995). In higher eukaryotes, D type cyclins associate with Cdk4 and Cdk6 to promote G1 progression. Subsequently S-phase is promoted by Cdk2 associating with E and A cyclins. For progression from G2 to M phase Cdk1 complexes with A and B cyclins.

In both budding yeast (*Saccharomyces cerevisiae*) and fission yeast (*Schizosaccharomyces pombe*) there is only one Cdk (*Sc* Cdc28 and *Sp* Cdc2) responsible for driving the cell cycle. However, these Cdks still interact with multiple cyclin subunits, as in higher eukaryotes. In *S. pombe,* Cdc2 interacts with cyclins Cig1, Cig2, Puc1, and Cdc13 for G1 progression, yet Cdc13 is the most studied and best understood *S. pombe* cyclin (Figure 2A).

Cdks and their cyclin subunits are highly regulated to ensure that each stage of the cell cycle occurs only once. This is achieved through transcriptional control and proteolytic degradation of subunits. Proteins required for one stage are produced in the

A

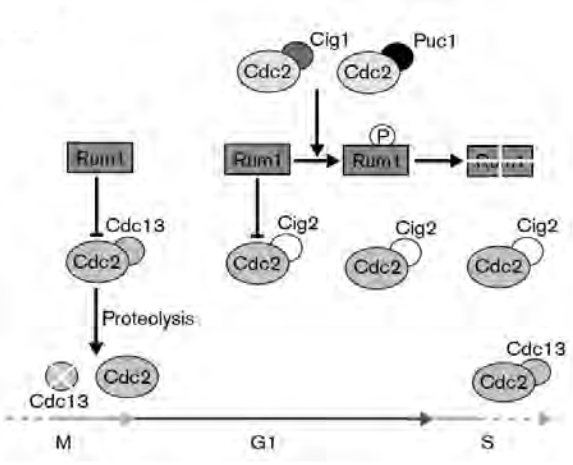

B

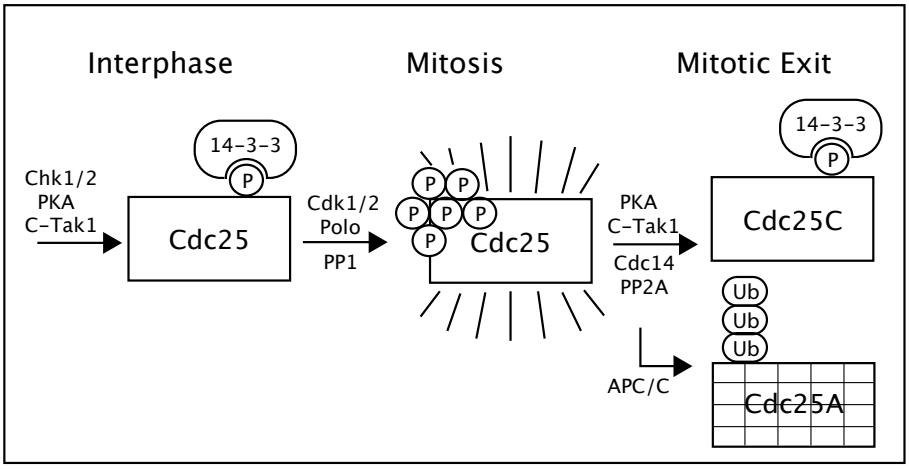

Figure 2. Regulation of Cdk1 and Cdc25. (A) Model of cell-cycle-specific regulation of Cdc2 in *S. pombe*. Cdc2 activity is regulated through its association with four different cyclins: Cig1, Cig2, Puc1 and Cdc13. Cdc2 activity is inhibited when cells exit mitosis by degradation of its associated cyclin Cdc13. Accumulation of the Cdc2 inhibitor Rum1 ensures that Cdc2 activity is kept low throughout late M-phase and G1-phase. Phosphorylation carried out by Cig1- and Puc1-associated Cdc2 targets Rum1 for degradation. In the absence of Rum1, Cdc2–Cig2 activity rises and induces entry into S-phase. Cdc13 accumulates during S-phase and it remains associated with Cdc2 until it is degraded upon exit from M-phase. Adapted from (Moser and Russell, 2000). (B) During interphase and in times of checkpoint activation, Cdc25 is tethered in the cytoplasm through its phosphorylation-dependent interaction with 14-3-3 molecules. At the G2/M transition, Cdk2, acting as a mitotic initiation trigger, phosphorylates Cdc25 and frees it from 14-3-3, in turn, allowing the response site to be dephosphorylated by PP1. Cdc25 activity is further stimulated by the mitotic kinases, Cdk1 and Polo, which together either stimulate Cdc25 activity (Cdc25C) or protect it from proteolysis (Cdc25A). These mitotic phosphorylations are reversed by phosphatases (Cdc14, PP2A), turning off the positive amplification loop and resetting Cdc25 activity and levels to those seen in interphase. Adapted from (Wolfe and Gould, 2004).

previous stage and then quickly degraded once their function is performed. This degradation ensures that downstream phosphorylation events only happen once per cell cycle and further assures that progression through the cell cycle is irreversible (Murray and Kirschner, 1989).

Cdk1 regulation in *S. pombe*

In interphase, the Cdk1 complex is inactive due to inhibitory phosphorylation by the Wee1 kinase. The Cdc25 dual specific phosphatase, an activator of Cdk1, is also inactive during interphase and is held in the cytoplasm by its phosphorylation-dependent interaction with 14-3-3 proteins (Figure 2B). Because this temporal and spatial regulation, Cdc25 cannot remove the inhibitory phosphorylation on Cdk1 during interphase. Activation of Cdc25 occurs when Cdk2 kinase becomes active at the G2/M transition and phosphorylates Cdc25 at its N-terminal region. This phosphorylation causes disassociation of Cdc25 with 14-3-3 which exposes the site of inhibitory phosphorylation and allows its removal (Margolis *et al.*, 2003). The now active form of Cdc25 can enter the nucleus to remove the inhibitory phosphorylation on Cdk1, thereby activating it. Cdk1 then enters into a positive feedback loop where it further phosphorylates Cdc25 on its N-terminal region and also phosphorylates and inactivates Wee1. Another kinase that acts on Cdc25 not mentioned previously is polo-like kinase, which contributes to the positive feedback loop by phosphorylating Cdc25 at the G2/M boundary (Figure 2B). These phosphorylation events further stimulate Cdc25 activity and protect it from ubiquitin-mediated proteolysis. With Cdc25 remaining active, Cdk1 can drive cells into mitosis.

Cdk1 activity is needed for progression into mitosis and its inactivation is needed for mitotic exit. As cells progress through mitosis, Cdc25 becomes dephosphorylated as Cdc14 phosphatases become active in late mitosis (reviewed in (Stegmeier and Amon, 2004; Wolfe and Gould, 2004). This dephosphorylation allows two inhibitory events on Cdc25 to take place. First, Cdc25 is recognized by the anaphase promoting complex (APC) an E3 ubiquitin ligase and is subsequently ubiquitinated to enable ubiquitin mediated proteolysis (Figure 2B). Second, Cdc25 leaves the nucleus and rebinds 14-3-3 that keeps Cdc25 sequestered in the cytoplasm. These events help to turn off the positive amplification loop of Cdk1 activation. Furthermore, once the APC becomes active, cyclin B is degraded by ubiquitin-mediated proteolysis that further attenuates Cdk1 activity. These events together decrease Cdk1 activity thereby allowing cells to exit from mitosis.

Fission yeast, *Schizosaccharomyces pombe*, as a model organism

Model unicellular organisms such as fission yeast *S. pombe,* have enabled researchers to elucidate many of the mechanisms of the eukaryotic cell cycle. Rod shaped fission yeast grow by elongation from the tips and divide by medial fission at a constant size through actomyosin ring constriction, much like in higher eukaryotes (Feierbach and Chang, 2001). Therefore, the cell cycle stage can be determined visually (Nurse *et al.*, 1976). This organism has been particularly useful in the field of cell cycle research because of its facile forward and reverse genetics, the sequencing of its genome (Wood *et al.*, 2002) and its use as a biochemical and cytological system. Furthermore, genetic screens have allowed the visual identification of mutant alleles that function at

discrete points in the cell cycle, termed cell division cycle (cdc) mutants, which continue to grow without dividing resulting in cells that are longer than wild-type cells (Nurse, 1975; Nurse *et al.*, 1976; Nasmyth and Nurse, 1981). *S. pombe* has discrete phases of the cell cycle much like that of higher eukaryotes except that it spends approximately 70%, of its life in G2. This in contrast to human cells which spend about 20% of their cell cycle in G2 and *S. cerevisiae* cells that do not have a defined G2 phase. Furthermore, many of the regulatory elements that control cell size and progression through the cell cycle are conserved from yeast to higher eukaryotes. This flexibility and functional significance of *S. pombe* make it a powerful system in which to study the eukaryotic cell cycle.

Signaling cytokinesis in fission yeast

When *S. pombe* cells enter into mitosis, the duplicated DNA is properly segregated and the cell is divided into a mother and daughter cell, a process termed cytokinesis. This process is highly regulated so that cytokinesis happens only after the genetic material is divided. In order for cytokinesis to happen in *S. pombe* and all other eukaryotes, an actin and myosin based ring forms at the specified cleavage plane. This actomyosin ring constricts after mitosis is complete and new cell membrane material is added to the cleavage furrow. Once the ring fully constricts, the cell is split into two cells with the same size, shape and genetic material.

One difference between higher eukaryotes and fission yeast is that in the yeast cell, as the actomyosin ring constricts, a septum formed of β-1,3-glucan and β-1,6-glucan that is needed to separate the cytoplasm of the mother and daughter cell (Humbel *et al.*,

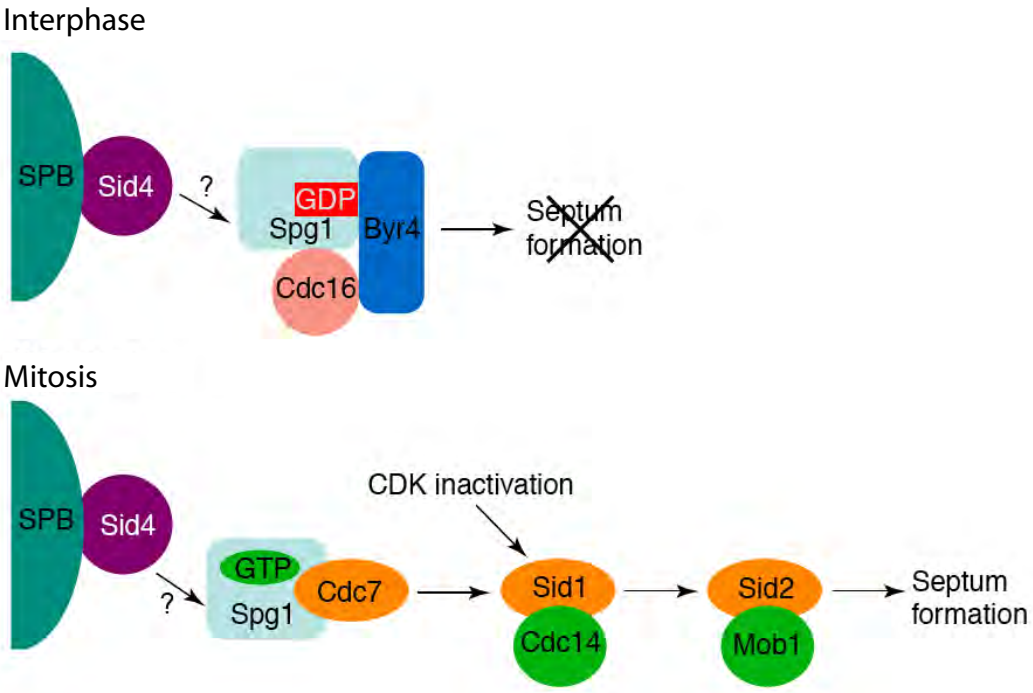

Figure 3. A model for the order of function of the SIN in *S.pombe*. Sid4 is constitutively localized to the SPB and is required for localization of both positive and negative regulators of the SIN; however, the identity of the SIN components with which Sid4 interacts directly is not clear. In interphase, the Cdc16p–Byr4p GTPase-activating protein (GAP) keeps Spg1p in the inactive GDP-bound form. Upon entry into mitosis, Spg1p is converted to the active GTP-bound form, which then binds to and recruits Cdc7p to the SPB. Following CDK inactivation in anaphase, Cdc7p recruits the Sid1p–Cdc14p kinase complex to the SPB. Sid1p–Cdc14p could then promote activation of the SPB-localized Sid2p–Mob1p kinase complex, which then translocates to the cell-division site to trigger initiation of cell division. Adapted from (McCollum and Gould, 2001).

2001). The coordination of ring constriction and septation in fission yeast is carried out by a GTPase-regulated signaling cascade called the septation initiation network (SIN) (Figure 3) (reviewed by (McCollum and Gould, 2001; Simanis, 2003; Krapp *et al.*, 2004b). Two proteins, Cdc11 and Sid4, function to anchor the signaling network to the spindle pole body (SPB), the yeast homolog of the centrosome, during the cell cycle (Bardin and Amon, 2001; McCollum and Gould, 2001; Simanis, 2003; Krapp *et al.*, 2004b). Sid4 is the most upstream component of the SIN but it is not know how Sid4 localizes to the SPB. It could be that Sid4 directly localizes to the SPB itself or there could be a tether that links the Sid4 to the SPB. The SIN is composed of three kinases (Sid1, Sid2 and Cdc7), a two-component GAP (Byr4 and Cdc16) and the small GTPase Spg1 (Figure 3). All of the components, except for Cdc16 and Byr4, are positive regulators of the SIN where loss of function of these proteins result in repeated rounds of nuclear division without septation. Loss of function of the negative regulators of the SIN, Cdc16 and Byr4, result in multiple septa formation without nuclear division (Fankhauser *et al.*, 1993; Song *et al.*, 1996).

Microtubule organizing centers structure, function and duplication

The SPB, the yeast analog of centrosome, serves as a signaling center for the SIN, the primary role for this organelle is to serve as the major microtubule organizing center (MTOC) in yeast where it anchors and nucleates microtubules (MTs) throughout the cell cycle (Figure 4A and Figure 15). In interphase, MTOCs serve as one of the areas for cytoplasmic MT organization. In mitosis, MTOCs nucleate the mitotic spindle that is needed for proper sister chromatid separation. MTOCs in yeast (SPBs) appear

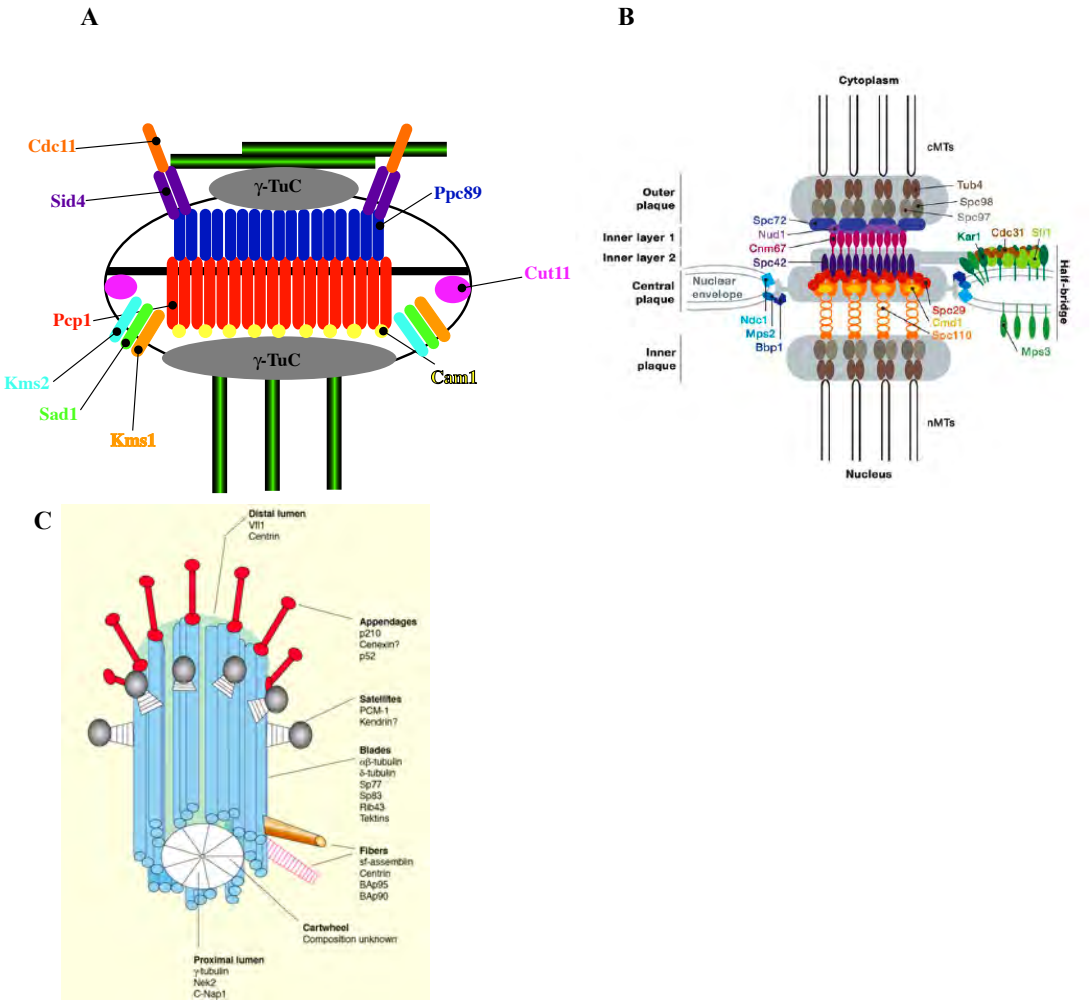

Figure 4. Protein composition and morphology of major MTOCs. (A) A speculative model of the *S. pombe* SPB showing the hypothesized locations of known components (generated from the literature). It appears as a tri–laminiar structure outside the nuclear envelope until G2/M when it is incorporated within the nuclear envelope. (B) A schematic diagram of the S. cerevisiae SPB with known positions of protein components and both cytoplasmic and nuclear MTs shown. The SPB is always incorporated in the nuclear envelope. Adapted from (Jaspersen and Winey, 2004). (C) The higher eukaryotic centriole. This diagram shows the main ultrastructural features and locations of known protein components. The proximal side is the site of new centriole formation in G1/S and the fibers associated there connect the mother and daughter centrioles until disengagement. The satellite accessory proteins link the γ-TuRC to centrioles in interphase. Adapted from (Marshall, 2001).

morphologically different from MTOCs in higher eukaryotes (centrosomes), their functions are highly analogous (Adams and Kilmartin, 2000). To date there are three structural proteins common to *S. cerevisiae*, *S. pombe* and higher eukaryotic MTOCs: centriolin (*Sp* Cdc11, *Sc* Nud1), centrin (*Sp* and *Sc* Cdc31) and kendrin (*Sp* Pcp1, *Sc* Spc110) (Marshall, 2001). Furthermore, all MTOCs are made up of multiple coiled-coil proteins that enable many proteins to pack close together and form higher ordered structures. Coiled-coiled proteins also serve as scaffolding proteins to localize protein complexes for signaling cell cycle transitions, anchoring and nucleating MTs and for cytokinesis (as discussed above) (Doxsey *et al.*, 2005a). These proteins are appear to make up the majority of proteins localizing to the pericentriolar material (PCM) surrounding the centrosomes.

Higher eukaryotic centrosomes

In higher eukaryotes the major MTOC, the centrosome, lies outside the nucleus in interphase and appears as two perpendicular cylinders each known as a centriole. The centrioles are surrounded by a protein dense matrix called the pericentriolar material (Figure 4C). Previously the PCM material was thought to be amorphous but with recent advances in electron microscopy and studies in *Caenorhabditis elegans,* the PCM has emerged as a coiled-coil protein dense lattice surrounding the centrioles (Kirkham *et al.*, 2003; Leidel and Gonczy, 2003; Wong and Stearns, 2003; Dammermann *et al.*, 2004; Leidel *et al.*, 2005). The PCM's full composition is not yet been fully determined but it is thought that some of the coiled-coil proteins in the PCM connect the γ-tubulin ring complex (γ-TuRC) to the centrioles (Luders and Stearns, 2007). Purification of this

matrix of proteins has not been achieved probably because the PCM is a dense nucleation of proteins loosely associated with the centrioles, which have a defined structure. The PCM therefore probably is washed away with biochemical purification or does not sediment with the centrioles.

In each centrosome, the centrioles can be distinguished from one another because the mature mother centriole has spoke-like appendages at its distal end whereas the daughter centriole does not. Each centriole is formed by nine MT triplets called blades that are arranged into a cylinder (reviewed in (Bettencourt-Dias and Glover, 2007). The centriolar MTs are made up of α and β tubulin in the same way that cytoplasmic and spindle MTs are. However, centriolar MTs undergo post-translational modifications such as polyglutamylation and acetylation, which contribute to MT stability and therefore to centriolar maintenance (Urbani and Stearns, 1999). The MT blades surround a central cartwheel structure of unknown composition. Within the cartwheel structure is the lumen of the centriole in which γ-tubulin and centrin (*Sp* and *Sc* Cdc31) localize (Marshall, 2001).

As mentioned above, mother centrioles have blade like appendages on their distal ends; however, these are not the only accessory structures seen on centrioles. On the other end of the centriole from the spoke-like appendages, the proximal end, are fibers which connect the mother and daughter centrioles until centriolar disengagement. There are also structures called satellites that are found within the PCM and are connected to centrioles through striated stems. The function of these satellites has not been fully elucidated, they could play a role as adaptor proteins for γ-tubulin ring complex proteins found in the PCM to connect to the centrioles (Kubo *et al.*, 1999). One of the

components of the satellites is kendrin (pericentrin) whose yeast homologues, *Sp* Pcp1and *Sc* Spc110, connect the γ-tubulin complex to the core of the SPB (Flory *et al.*, 2000). While much of the descriptive work on centrioles and centrosomes has been accomplished the field is now focusing on characterizing the function of many of these proteins utilizing model organisms that are genetically and biochemically tractable such as *C. elegans*.

Work in the past twenty years has focused on understanding the composition of the centrosome but studies focusing on centrosomal duplication have fascinated scientists since the organelle was first discovered. The centrosome duplication cycle is much like that of DNA: it happens only once during the cell cycle and it is semi-conservative (Beisson and Wright, 2003). In G1, cells start out with a single centrosome (two centrioles surrounded by PCM) outside the nucleus. As cells transition from G1 to S-phase, the centrioles separate and the daughter centriole begins to grow starting out as a disk like structure adjacent to the proximal side of the mother centriole. This centriolar duplication is concurrent with DNA replication. As cells transition from S-phase into G2, the daughter centriole begins to elongate until it reaches its maximal length seen at the G2/M border. At this point there are two centrosomes next to each other formed by semi-conservative duplication wherein each centrosome there is an old and new centriole perpendicular to one another. As cells enter into mitosis the phosphorylation of centrin triggers the centrosomes to separate from one another (Lutz *et al.*, 2001). Then the centrosomes migrate to opposite poles of the cell, a process mediated by kinesin MT motor proteins (Boleti *et al.*, 1996). At the same time the mitotic spindle MTs are nucleated and anchored by the γ-TuRC localized to the PCM. These MTs from opposite

poles bind to one another as well as to kinetochores to form a bipolar mitotic spindle. After DNA segregation and cytokinesis the mother and daughter cells both contain one centrosome to start the centrosomal duplication in the subsequent cell cycle.

The events in centrosomal maturation are highly regulated by multiple kinases working at specific stages of the cell cycle to influence centriolar duplication, maturation and separation. Interestingly, studies have shown that entry into S-phase is initiated by Cdk2 paired to either cyclin E or A and is needed for duplication of both DNA and centrosomes (Hinchcliffe *et al.*, 1999; Lacey *et al.*, 1999). One of the many targets of Cdk2 in higher eukaryotes is the murine kinase Mps1, which has also been implicated in *S. cerevisiae* SPB duplication (discussed below). However, unlike in DNA replication, if cells arrest in S phase, centrosomes can undergo multiple rounds of duplication (Hinchcliffe *et al.*, 1999). Therefore, it seems that while DNA and centriole duplication are under the control of the same kinases, licensing their duplication is under a different set of regulators.

Once again, recent studies in *C. elegans* have identified a complex of proteins consisting of the kinase ZYG-1 and proteins SAS-5, SPD-2, SAS-6, and SAS-4 that are needed for centriole duplication/maturation (Leidel and Gonczy, 2005). With these studies, a picture is beginning to emerge as to how centrioles of higher eukaryotes mature and duplicate. Starting in G1, SPD-2, a protein implicated in PCM assembly and centriole formation, is recruited to the centriole in a CDK2 dependent manner (Dammermann *et al.*, 2004; Cowan and Hyman, 2006). In turn, SPD-2 recruits ZYG-1, a kinase that shares homology to human NIMA kinase NEK8 and polo like kinases PLK1 and PLK4, to the centriole. The substrates of ZYG-1 are unknown but it does recruit SAS-5 and SAS-6,

two proteins needed for the growth of the central tube of the daughter centriole prior to S-phase (Delattre *et al.*, 2004; Leidel *et al.*, 2005). Another protein component in this complex is SAS-4, that is needed to recruit the MTs that surround the central tube (Kirkham *et al.*, 2003). Depletion of SAS-4 results in smaller centrosomes and stunted centrioles (Kirkham *et al.*, 2003; Leidel and Gonczy, 2003). Interestingly, through fluorescence recovery after photobleaching (FRAP) experiments, SAS-4 was found to recover only after cytokinesis and only once per cell cycle (Leidel and Gonczy, 2003). These experiments show that protein recruitment for daughter centriole formation happens only once per cell cycle and formation of the daughter centriole happens shortly after cytokinesis in G1-phase.

A recent study gave insight into the purpose of centriolar disengagement and its role in centriolar duplication. This study showed that centriole disengagement in G1 requires the activity of the protease separase and the APC in anaphase. Furthermore, the disengagement seen in G1 "licenses" centriole duplication in the subsequent cell cycle (Tsou and Stearns, 2006). Therefore, it seems that centriolar engagement blocks centriolar re-duplication and could explain one mode of regulation for centriolar duplication which appears to be distinct from DNA duplication.

The details listed above paint a picture of how the centrosome is needed to duplicate and form a bipolar spindle, one fact remains: the centrosome is not needed for MT organization in interphase or for forming functional spindles in mitosis (Szollosi *et al.*, 1972; Brenner *et al.*, 1977; de Saint Phalle and Sullivan, 1998). This is not to say that centrosomes are not needed for cell cycle progression. Laser ablation studies elucidated that acentriolar cells (where the PCM is still intact) can still undergo mitosis yet these

cells display chromosome segregation defects. Also, these cells arrest in the subsequent G1 phase. If one of the poles is ablated in cells that are in prometaphase, the cells can still go through mitosis and the cell that receives the centrosome continues to cycle whereas the acentrosomal cell arrests in G1 (Khodjakov and Rieder, 2001). There are a few theories as to why these cells arrest in G1. One is that since there are no centriolar proteins acting as scaffolds, Cdk2/cyclin E mislocalizes and therefore cells cannot enter into S-phase. Another theory is that there might be a centrosome check point mediated by p53 where cells that do not have the proper amount of centriolar proteins arrest until centrioles are repaired (Doxsey *et al.*, 2005c). The exact mechanism of cell-cycle arrest due to ablation of centrioles remains unclear, these studies do show that there are multiple roles for the centrosome. One of these roles is as a signaling center, organizing and concentrating signal transduction pathways needed for cell cycle progression. Second, the centrioles are not needed for MT organization and nucleation but some factors in the PCM are responsible for this function, i.e. γ-TuRC and PCM proteins.

The centrosome is not only implicated in the G1/S transition but also in the G2/M transition. As described above, Cdk1 activity is needed for entry into mitosis and Cdk1 is found localized to centrosomes in prophase. An inhibitor kinase, Chk1, is found localized to centrosomes in interphase but not in mitosis (Forrest *et al.*, 1999; Kramer *et al.*, 2004). Chk1 keeps Cdc25 phosphatase inactive and therefore keeps the Cdk1 positive amplification feedback loop off. By inhibiting Chk1 activity, centrosomal Cdk1 becomes active and cells prematurely enter into mitosis (Kramer *et al.*, 2004). The previously described ablation studies show that centrosomes are not required for entry into mitosis yet these studies do show that the centrosomes play a role in sequestering

positive and negative regulators of mitotic entry.

Budding yeast SPBs

Much is known about the centrosome in higher eukaryotes yet the SPB in budding yeast *S. cerevisiae* remains the most well studied and characterized MTOC to date (Adams and Kilmartin, 2000). By electron microscopy (EM), the *S. cerevisiae* SPB appears as a multi-layered cylindrical structure that is always embedded in the nuclear envelope (NE) (Figure 4B). Each SPB is divided into three layers: the outer plaque on the cytoplasmic face, the central plaque in the plane of the NE, and the inner plaque on the nuclear side of the NE (Adams and Kilmartin, 2000; Jaspersen and Winey, 2004). The site of new SPB formation, called the half-bridge, is joined to the central plaque (Jaspersen and Winey, 2004).

The SPB of budding yeast has been purified and many of its components have been identified through combinations of mass spectrometric analysis, genomic studies, two hybrid screens, synthetic lethal screens and sedimentation analysis. Recent FRET studies have determined how core SPB components are arranged in relation to one another, which provides a better understanding of SPB structure/function (Muller *et al.*, 2005b). At the core of the SPB is the coiled-coil protein Spc42 which forms a hexagonal lattice as seen through EM (Donaldson and Kilmartin, 1996). Overproduction of Spc42 forms a "superplaque" structure where this central lattice is enlarged and extends into the nuclear membrane (Donaldson and Kilmartin, 1996; Bullitt *et al.*, 1997). The N-terminal region of Spc42 interacts with two other proteins that are part of the inner plaque, Spc110 (*Sp* Pcp1, higher eukaryotic pericentrin) and Spc29 (Adams and Kilmartin, 1999; Elliott

et al., 1999). The C-terminal region of Spc110 binds both Cmd1 (calmodulin) and Spc29 (Spang *et al.*, 1996a; Elliott *et al.*, 1999). Spc29 is thought to be the linker between the central core and inner plaque of the SPB but Spc110 appears to control the distance from the inner plaque to the central core (Spang *et al.*, 1996b). The C-terminal region of Spc42 is oriented towards the outer plaque and binds Cnm67 (Adams and Kilmartin, 1999; Muller *et al.*, 2005b). The N-terminal region of Cnm67 binds the outer plaque protein, Nud1 (*Sp* Cdc11 and higher eukaryotic centriolin) (Adams and Kilmartin, 1999; Elliott *et al.*, 1999). In turn, Nud1 and Spc72 interact through their C-terminal regions (Gruneberg *et al.*, 2000). Spc72 binds to γ-TuC members of the outer plaque (Knop and Schiebel, 1998). Spc42 also plays a role in connecting the half-bridge to the core of the SPB (Figure 4B). One of the main proteins that localizes to the half-bridge is Cdc31 (*Sp* Cdc31 and higher eukaryotic centrin). Cdc31 is needed for SPB duplication and maintenance of integrity of the half-bridge (Spang *et al.*, 1993; Vallen *et al.*, 1994).

Both the inner and outer plaques contain γ-TuC and therefore anchor and nucleate MTs throughout the cell cycle. The main components of the γ-TuC are Tub4 (*Sp* Tug1 and higher eukaryotic TUBG1/2), Spc98 (*Sp* Alp6 and higher eukaryotic GCP3), and Spc97 (*Sp* Alp4 and higher eukaryote GCP2) (Sobel and Snyder, 1995; Marschall *et al.*, 1996; Spang *et al.*, 1996a; Knop and Schiebel, 1997). In interphase, cytoplasmic MTs are localized to the outer plaque whereas in mitosis the mitotic spindle is anchored to the inner plaques of the duplicated SPB.

EM studies utilizing cells arrested with mutant alleles of SPB localized proteins, researchers have been able to observe the morphological changes that take place during budding yeast SPB duplication/maturation (Byers and Goetsch, 1975; Rose and Fink,

1987; Jaspersen *et al.*, 2002). In early G1, the SPB is embedded within the NE and is seen as a cylindrical object with an electron dense half-bridge. Next, satellite material is deposited on the cytoplasmic face of the half-bridge as it elongates. The satellite is the immature SPB and contains many of the core SPB proteins such as Spc42, Spc29 and Nud1 (Adams and Kilmartin, 1999). As cells enter S-phase, the satellite enlarges to form the duplication plaque that resembles the outer plaque and core of the SPB. The half-bridge then retracts underneath the duplication plaque as inner plaque components localize to the SPB. As the half-bridge retracts, it forms a hole in the NE where the new SPB is inserted. It is thought that two transmembrane domain containing proteins that localize to the half bridge, Mps2 and Ndc1, play a role in insertion (O'Toole *et al.*, 1999; Schramm *et al.*, 2000). By the end of S-phase, two SPBs are found next to each other within the NE. Then, as cells progress from G2 to M, the bridge connecting the two SPBs is cleaved allowing the SPBs to migrate to opposite sides of the NE. At this same time the SPBs are anchoring and organizing the mitotic spindle between them. Studies have shown that the kinesin-like motor proteins are responsible for SPB migration (Jacobs *et al.*, 1988; Roof *et al.*, 1992). As cells exit mitosis, the mitotic spindle is broken down and each cell receives a SPB with associated half-bridge after cytokinesis.

Much like the duplication cycle of centrosomes in higher eukaryotes, the SPBs in budding yeast are under control of cell cycle regulators. One of the main factors controlling SPB duplication is the Mps1 kinase, which is also a spindle checkpoint protein (Schutz and Winey, 1998; Castillo *et al.*, 2002). Cells with mutant alleles of Mps1 display monopolar spindles due to a lack of SPB duplication. There are three known substrates of Mps1: Spc110, Spc98 and Spc42, yet it is not known exactly what

role their phosphorylation plays (Pereira *et al.*, 1998; Friedman *et al.*, 2001; Castillo *et al.*, 2002). The best answer to date, is that phosphorylation by Mps1 allows its protein substrates to form higher ordered structures within the SPB, which would then allow SPB maturation and duplication. This model is further supported by studies that show that Mps1 activity is needed for Spc42 mediated superplaque formation, which further supports the previous model of Mps1 phosphorylation (Jaspersen *et al.*, 2004).

Another kinase implicated in SPB duplication/maturation is *Sc* Cdk1 (Cdc28). Cells that have a mutant allele of Cdc28 arrest in G1 with a single SPB and half-bridge with associated satellite (Byers and Goetsch, 1974). This SPB morphology might be due to the fact that cells are arrested in G1 rather than a direct phosphorylation event on the SPB. Recent work has elucidated that Cdc28 phosphorylates Mps1 and Spc42 (Jaspersen *et al.*, 2004). The phosphorylation of both these proteins is needed for increased Spc42 assembly within the SPB and therefore SPB duplication.

The fission yeast SPB

Structural studies show that the *S. pombe* SPB is an amorphous tri-laminar structure with an electron dense central line (Figure 4A). As cells start the cell cycle in G1, the SPB is seen with a small electron dense half bridge outside the nucleus. A new SPB begins to grow from this half bridge until the duplicated SPB is fully mature at the G2/M boundary. As cells transition from G2 to M, a dark amorphous material accumulates in a NE invagination that forms underneath the duplicated SPBs. The composition and function of this material still remains unknown yet it is thought that this material helps to incorporate the duplicated SPBs into the NE. By the time cells enter

into mitosis the SPBs are incorporated into the NE (Ding *et al.*, 1997; Uzawa *et al.*, 2004). Then the half-bridge is severed, allowing the SPBs to separate to opposite sides of the NE and form the mitotic spindle between them (Ding *et al.*, 1997; Uzawa *et al.*, 2004).

The structure and composition of the SPB of fission yeast is not as well characterized as the SPB of *S. cerevisiae* or centrosomes of higher eukaryotic cells. The complete composition of the *S. pombe* SPB has not been fully determined mainly because it has not been able to be purified as with the *S. cerevisiae* SPB. All attempts at biochemical purification through gradient columns have not met with much success in our hands or in other labs. This is surprising because the SPB of *S. pombe* is presumably tethered to the NE as is the SPB *S. cerevisiae* that is always embedded in the NE. Therefore, one would not think that attachment to the NE would be problematic for isolation and purification. Perhaps the *S. pombe* SPB is an amorphous concentration of proteins without much internal structure and therefore the SPB falls apart when it is isolated or purified. This could be much like the pericentriolar material surrounding the centrosome that is able to be visualized by light microscopy but is dense cloud of proteins without any structural integrity.

Within the field of *S. pombe* SPB study, there remain several unanswered questions. The most important of these questions is what are the components of the SPB and how are they arranged? Also, how is the duplication/maturation of the SPB regulated? Studies in *S. cerevisiae* have shown us that it is possible to isolate the SPB and determine its protein composition and arrangement. They have also been able, through genetic screens, to identify kinases and their targets that regulate duplication. If all of

these studies have been carried out on the SPB in *S. cerevisiae* why do they need to be performed in *S. pombe*? First, from what we know, the morphology and composition of *S. pombe* and *S. cerevisiae* SPBs are quite different. However, there are still many similarities between the organisms. They all localize signaling proteins to the MTOCs that influence its maturation/duplication. There also appears to be a conserved set of cell cycle regulators that localize to the major MTOCs that also influence cell cycle progression. Furthermore, the SPB of *S. pombe* is outside the nucleus in interphase like higher eukaryotes and also has much of the same γ-tubulin complex members as higher eukaryotes. Therefore, the SPB of *S. pombe* is a good model in which to study the regulation of SPB duplication and MTOC function. This, in turn, can help us determine how the higher eukaryotic centrosome functions.

In an effort to further characterize MTOCs in *S. pombe* my dissertation work has focused on two MTOCs proteins Ppc89 and Mto2. In chapter III, I focus on the characterization of the novel *S. pombe* SPB component, Ppc89 (Rosenberg *et al.*, 2006). It is my hypothesis that this protein is a key structural component needed for the integrity of the SPB. In chapter IV, I examine the phospho-regulation of the novel γ-TuC activator, Mto2. It is my hypothesis that the mitotic phosphorylation of Mto2 inhibits its ability to activate and localize the γ-TuC to non-SPB MTOCs.

CHAPTER II

MATERIALS AND METHODS

Strains, Media, and Genetic Methods

S. pombe strains used in this study (Table 1) were grown in yeast extract (YE) medium or minimal medium with the appropriate supplements (Moreno *et al.*, 1991). Crosses were performed on glutamate medium (minimal medium lacking ammonium chloride and containing 0.01 M glutamate). *S. pombe* transformations were performed by a lithium-acetate method (Keeney and Boeke, 1994). Expression of genes regulated by the *nmt* promoter was achieved by growing cells in the presence of 5 μg/ml thiamine (promoter repressed) and then washing them into medium lacking thiamine (promoter induced) (Siam *et al.*, 2004).

All of the indicated tagged alleles of *ppc89*$^+$, *mto2*$^+$ *cdc11*$^+$, *sid4*$^+$, *alp6*$^+$, *cut11*$^+$, and *pcp1*$^+$ were tagged at the 3' end of their chromosomal loci with sequences encoding 13 copies of the Myc epitope, three copies of the HA epitope, enhanced green fluorescent protein (eGFP), cyan fluorescent protein (CFP), the yellow fluorescent protein (YFP), the tandem affinity purification (TAP) tag (Tasto *et al.*, 2001), or a YFP-CFP double cassette (Tomlin and Gould, unpublished results) by a PCR-mediated strategy as described previously (Bähler *et al.*, 1998). Proper integration of these epitope cassettes was confirmed by PCR.

Deletion of the complete *ppc89*$^+$ open reading frame (ORF) was achieved by PCR-based one-step homologous recombination as described by (Bähler *et al.*, 1998),

using *ura4*$^+$ as a selectable marker.. The amplified fragment was transformed into a *h*$^-$/*h*$^+$ *ade6-M210/ade6-M216 ura4-D18/ura4-D18 leu1-32/leu1-32* diploid strain, and stable integrants were selected. Deletion of one copy of *ppc89*$^+$ in strain KGY774 was confirmed by PCR. Sporulation of KGY774 and tetrad dissection revealed that *ppc89*$^+$ was essential for vegetative growth. *sid4*$^+$ deletion was performed previously (Chang and Gould, 2000).

The *ppc89*$^+$ ORF was amplified from *S. pombe* genomic DNA by PCR and cloned into pSK+. The pSKppc89 clone was sequenced in its entirety to confirm that no mutations had been introduced into the ORF. To clone *ppc89*$^+$ and pieces thereof under control of the *nmt* promoters in the pREP1, pREP81, and pREP81GFP vectors (Basi *et al.*, 1993; Maundrell, 1993; Drummond and Hagan, 1998), *Nde*I and *Bam*HI sites were added to the 5' and 3' ends, respectively, of oligonucleotides used for PCR amplification. The *Nde*I site in each oligonucleotide contributed the initiating methionine codon. Stop codons were incorporated into the oligonucleotides just upstream of the *Bam*HI sites. Similarly, the N-terminal region of *sid4*$^+$ was amplified by PCR using a 5'*Ase*I and 3'*Nde*I site to allow an N-terminal fusion with the C-terminal sequences of *ppc89*$^+$ in the pREP vectors. To facilitate depletion and overproduction of Ppc89, the *nmt81-ppc89* and *nmt1-ppc89* portions of the pREP plasmids were excised with *Pst*I and *Bam*HI and cloned into pJK148 (Keeney and Boeke, 1994). The resultant plasmids were linearized within the *leu1*$^+$ gene by digestion with *Eco*47III and integrated into the *leu1* locus of KGY246 to create strains KGY5328 and KGY5333, respectively. To generate a conditional *ppc89*$^+$ shut-off strain, KGY5328 was crossed to the heterozygous *ppc89*$^+$ deletion strain (KGY774) and allowed to sporulate on glutamate medium. Random spore

analysis was then performed, selecting for haploid cells that were Leu$^+$, Ura$^+$, Ade$^-$, and dead in the presence of thiamine.

Gene Replacement and Site Directed Mutagenesis

Gene replacements involving *mto2* ORF were performed as described (Boeke *et al.*, 1984). Briefly, *mto2::ura4*$^+$ cells were transformed with a mutated genomic construct of *mto2* cloned into the pIRT2 integration vector. Recombinants were selected for on YE agar plates containing the drug, 5-fluoroorotic acid (5-FOA), in order to select for colonies that have lost the *ura4*$^+$gene.

Site directed mutagenesis was performed using Quickchange (Stratagene, La Jolla, CA) per manufacturer's protocol. DNA sequencing confirmed the presence of mutations. A genomic clone of the *mto2*$^+$ ORF containing 500 base pairs upstream and downstream of the coding sequence was cloned into pSK vector (Stratagene, La Jolla, CA) and used as a template for mutagenesis. The mutated copy of *mto2* was then subcloned intop the pIRT2 integration vector.

Fluorescence Microscopy and FRET Analysis

Strains producing YFP- and CFP-tagged proteins were grown in YE medium and visualized live. Images were acquired digitally on a Carl Zeiss MicroImaging, Inc., (Thornwood, NY) Axiovert II inverted microscope equipped with a Plan Apo 100/1.40 lens, a piezo-electric Z-axis stepper objective motor (Physik Instrumente, Auburn, MA), an UltraView LCI real-time scanning-head confocal (Perkin-Elmer, Wellesley, MA), a 488-nm argon ion laser (for YFP excitation), and a 442-nm helium cadmium laser (for

CFP excitation). Images were captured on an Orca-ER charge-coupled-device camera (Hamamatsu, Bridgewater, NJ). Z-series optical sections for each filter set were captured at 0.5-μm intervals using Ultra-View software (Perkin-Elmer). Subsequently, the images were deconvolved, merged, and rendered into a single plane using Volocity 3.5.1 software (Improvision, Lexington, MA).

Cells expressing GFP fused at the N-terminal region of full-length Ppc89 or Ppc89 fragments from the *nmt81* promoter were grown in the absence of thiamine and fixed in methanol or visualized live. To visualize MTs, cells were fixed in methanol and stained with TAT-1 antibodies to α-tubulin (Woods *et al.*, 1989). Microscopy was performed on a Zeiss Axioskop II equipped with a z-focus motor drive and GFP and DAPI filter sets (ChromaTechnology, Rockingham, VT). Images were captured with an Orca II charge-coupled-device camera (Hamamatsu) and processed and analyzed with Open-Lab 4.0.3 software (Improvision).

For fluorescence resonance energy transfer (FRET), cells were imaged on a DeltaVision microscope (Applied Precision, Issaquah, WA) and analyzed as described by (Muller *et al.*, 2005b) (http://depts.washington.edu/~yeastrc/). Briefly, 100 images were captured for each strain. Exposure times were 0.4 sec with 2 x 2 binning and a final image size of 512 x 512. The order of image acquisition was YFP, FRET, CFP, and DIC. Images were analyzed with the SoftWoRx® program from Applied Precision. For each strain, the tagged protein replaced the wild-type protein and was expressed under the control of the native promoter. $FRET_R = FRET\ channel \div Spillover_{Total}$(Muller *et al.*, 2005b). The $Spillover_{YFP}$ factor was determined from the Sid4-YFP strain KGY4334 and was 0.233 ± 0.040 (n=85). The $Spillover_{CFP}$ factor was determined from the Sid4-CFP

strain KGY4439 and was 0.486 ± 0.060. $Spillover_{Total}$ = (*CFPchannel* x $Spillover_{CFP}$) + (*YFPchannel* x $Spillover_{YFP}$). All fluorescence channels were background-subtracted.

Electron Microscopy

Aliquots of cells expressing Ppc89-GFP were prepared for electron microscopy as described previously (Giddings *et al.*, 2001). Briefly, cells were harvested by vacuum filtration onto 0.45-μm Millipore filters and cryofixed by high-pressure freezing in a HPM-010 (BAL-TEC/RMC, Tucson, AZ). Frozen samples were freeze-substituted in 0.25% glutaraldehyde and 0.1% uranyl acetate in acetone at -80 C, infiltrated with liquid Lowicryl HM20 (Electron Microscopy Sciences, Fort Washington, PA) at -20°C, and polymerized under UV at -45°C. For immunolabeling, 60-nm-thick sections were retrieved on formvar-coated nickel slot grids, then floated on a series of drops containing (i) blocking solution of 1% non-fat dry milk in phosphate-buffered saline plus 0.1% Tween 20 (PBST), (ii) primary antibody (affinity-purified rabbit anti-GFP) diluted 1:150 in blocking solution, and (iii) goat-anti-rabbit-IgG secondary antibody conjugated to 15-nm colloidal gold (Ted Pella, Inc., Redding, CA) diluted 1:20 in blocking solution. The labeled grids were rinsed in PBST followed by distilled water. Sections were stained with 2% uranyl acetate and lead citrate, then viewed in a Philips (Mahwah, NJ) CM10 transmission electron microscope operating at 80 kV. Images were recorded with a Gatan (Pleasanton, CA) BioScan digital camera or on Kodak (Rochester, NY) 4489 electron microscope film.

Protein Methods

Total cell extracts of *S. pombe* were prepared in NP-40 buffer (Gould *et al.*, 1991), and immunoprecipitations (McDonald *et al.*, 1999) were carried out using 5 μg of either 12CA5 (anti-HA) or 9E10 (anti-Myc) monoclonal antibodies (both from Vanderbilt Molecular Recognition Shared Resource). After 1 h of incubation, the immunoprecipitates were washed six times in NP-40 buffer and then resuspended in 2X SDS-PAGE sample buffer (McDonald *et al.*, 1999).

For immunoblotting, proteins were resolved by 10% SDS-PAGE and transferred by electroblotting to PVDF membrane (Immobilon P; Millipore Corp., Bedford, MA). Antibodies 12CA5 and 9E10 were used at 2 μg/ml in TBS to detect epitope-tagged proteins. These antibodies were then detected using horseradish-peroxidase–conjugated goat anti-mouse-IgG secondary antibodies (0.8 mg/ml; Jackson ImmunoResearch Laboratories, West Grove, PA) at a dilution of 1:50,000. Immunoblots were visualized using ECL reagents (Amersham Pharmacia Biotech, Piscataway, NJ).

Maltose-binding protein (MBP) and MBP fused to full-length Ppc89 were produced in *Escherichia coli* using plasmid pMAL-c2 (New England Biolabs, Beverly, MA) and purified on amylose beads (New England Biolabs) per the manufacturer's instructions. Briefly, the DNA sequence encoding Ppc89 was amplified by PCR from wild-type genomic DNA using primers that introduced *Eco*RI and *Bam*HI sites at the 5' and 3' ends, respectively. The product was cut with these enzymes and cloned into similarly cut pMAL-c2 to create an *MBP-ppc89* fusion. To create pSK(+)*sid4* (284-660) (pKG3159), DNA was amplified by PCR from wild-type genomic DNA using primers that introduced *Eco*RI and *Bam*HI sites at the 5' and 3' ends, respectively. The product

was cut with these restriction enzymes and cloned into similarly cut pSK(+). pSK(+) containing full-length Prp19 (pKG1781) was constructed previously (Ohi and Gould, 2002). Both pKG1781 and pKG3159 were translated in vitro in the presence of [^{35}S]-Trans label (ICN Pharmaceuticals, Irvine, CA) with the use of the TNT-coupled reticulocyte-lysate system (Promega, Madison, WI). After the transcription/translation reaction was allowed to proceed for 90 min at 30°C, 1 ml of binding buffer (20 mM Tris-HCl, pH 7.0, 150 mM NaCl, 2 mM EDTA, 0.1% NP-40) was added to the lysates. The lysates were then clarified by centrifugation at 14,000 rpm for 15 min. Purified MBP or MBP-Ppc89 bound to amylose beads was mixed with ^{35}S-labeled Sid4 fragment or full-length Prp19 in binding buffer and incubated for 1 h at 4°C. The beads were washed five times in binding buffer, and the proteins were resolved by 10% SDS-PAGE, treated with Amplify (Amersham Pharmacia Biotech), and exposed to film.

Glutathione S-transferase (GST) and GST fused to fragments of full length Mto2 were produced in *Escherichia coli* using plasmid pGEX4T-1 (GE Healthcare, Piscataway, NJ) described previously (Venkatram *et al.*, 2005) and purified on glutathione sepharose beads (Novagen, San Diego, CA) as the manufacturers instructions.

In Vitro Kinase and PAA Analysis

For tryptic peptide mapping and phosphoamino acid analysis ^{32}P-Labeled Mto2-GST (bound to polyvinylidene difluoride membrane) was used for phosphoamino acid analysis or tryptic peptide mapping as described previously (Kamps and Sefton, 1989; Boyle *et al.*, 1991).

For *in vitro* kinase assays, approximately 100 ng of recombinant Cdk1 kinase complex, purified from baculovirus-infected insect cells as described (Yoon *et al.*, 2002), was used to phosphorylate 1 μg of bacterially produced GST-Mto2 in TB1 buffer (50 mM Tris HCL, pH 8.0, 120mM NaCl, 1 mM EDTA, 1 mM DTT) supplemented with either 50 μM unlabeled ATP and 5 μCi of [γ-^{32}P]ATP or 1mM cold ATP. Reactions were incubated at 30 °C for 30 min and terminated by the addition of sample buffer. Samples were boiled and separated by SDS-PAGE. Coomassie Blue staining and autoradiography were performed for the detection of proteins.

Two-hybrid Analyses

The yeast two-hybrid system used in this study was described previously (James *et al.*, 1996). Various portions of *ppc89*$^{+}$ or *sid4*$^{+}$ were amplified by PCR from genomic DNA and cloned into the bait plasmid pGBT9 and/or the prey plasmid pGAD424 (Clontech, Palo Alto, CA). To test for protein interactions, both bait and prey plasmids were co-transformed into *S. cerevisiae* strain PJ69-4A. Leu^{+} and Trp^{+} transformants were selected and then scored for positive interactions by streaking onto synthetic dextrose plates lacking adenine and histidine.

TABLE 1 ***S. pombe*** **strains used in this study**

Strain	Genotype[a]		Source
KGY246	*h*$^-$	*ade6-M210 ura4-D18 leu1-32*	Lab stock
KGY247	*h*$^+$	*ade6-M210 ura4-D18 leu1-32*	Lab stock
KGY248	*h*$^-$	*ade6-M216 ura4-D18 leu1-32*	Lab stock
KGY249	*h*$^+$	*ade6-M216 ura4-D18 leu1-32*	Lab stock
KGY262	*h*$^+$	*ppc89-CFP::Kan*^{R} *sid4-YFP::Kan*^{R} *ade6-M210 ura4-D18 leu1-32*	This study[b]
KGY774	*h*$^+$/ *h*$^-$	*ppc89Δ::ura4*$^+$*/ppc89*$^+$ *ade6-M210/ade6-M216 ura4-D18/ura4-D18 leu1-32/leu1-32*	See text
KGY794	*h*$^+$	*ppc89-YFP::Kan*^{R} *sid4-CFP::Kan*^{R} *ade6-M21X*^{a} *ura4-D18 leu1-32*	This study[b]
KGY1234	*h*$^-$	*sid4-SA1 ade6-M210 ura4-D18 leu1-32*	*(Balasubramanian et al., 1998)*
KGY1341	*h*$^+$	*sid4-myc::Kan*^{R} *ade6-M210 ura4-D18 leu1-32*	Chang and Gould, 2000
KGY1358	*h*$^+$/ *h*$^-$	*sid4Δ::ura4*$^+$*/sid4*$^+$ *ade6-M210/ade6-M216 ura4-D18/ura4-D18 leu1-32/leu1-32*	Chang and Gould, 2000
KGY3271	*h*$^+$	*sid4-YFP::Kan*^{R} *cdc11-CFP::Kan*^{R} *ade6-M21X ura4-D18 leu1-32*	This study[b]
KGY3275	*h*$^-$	*ppc89-YFP::Kan*^{R} *cdc11-CFP::Kan*^{R} *ade6-M210 ura4-D18 leu1-32*	This study[b]
KGY3526	*h*$^-$	*sid4-CFP::Kan*^{R} *cdc11-YFP::Kan*^{R} *ade6-M21X ura4-D18 leu1-32*	This study[b]
KGY3888	*h*$^-$	*cdc11-TAP::Kan*^{R} *ade6-M210 ura4-D18 leu1-32*	See text
KGY4288	*h*$^-$	*ppc89-HA::Kan*^{R} *ade6-M210 ura4-D18 leu1-32*	See text
KGY4293	*h*$^-$	*ppc89-TAP::Kan*^{R} *ade6-M210 ura4-D18 leu1-32*	See text
KGY4294	*h*$^+$	*ppc89-GFP::Kan*^{R} *ade6-M210 ura4-D18 leu1-32*	See text

KGY4297	h^+	*ppc89-HA::Kan^R sid4-myc::Kan^R ade6-M21X ura4-D18 leu1-32*	This study[b]
KGY4318	h^+	*ppc89-CFP::Kan^R cdc11-YFP::Kan^R ade6-M210 ura4-D18 leu1-32*	This study[b]
KGY4325	h^+	*ppc89-GFP::Kan^R sid4-SA1 ade6-M21X ura4-D18 leu1-32*	This study[b]
KGY4334	h^-	*sid4-YFP::Kan^R ade6-M210 ura4-D18 leu1-32*	See text
KGY4439	h^-	*sid4-CFP::Kan^R ade6-M210 ura4-D18 leu1-32*	See text
KGY4608	h^-	*sid4-YFP-CFP::Kan^R ade6-M210 ura4-D18 leu1-32*	See text
KGY4897	h^+	*nda3-KM311 mto2-myc$_{13}$::KanR ade6-M210 ura4-D18 leu1-32*	This Study
KGY5067	*h*	*cdc25-22 mto2-myc$_{13}$::KanR ade6-M210 ura4-D18 leu1-32*	This Study
KGY5185	h^+	*leu1-32::pJK148-nmt81-ppc89$^+$ ppc89Δ::ura4$^+$ ade6-M21X ura4-D18*	See text
KGY5328	h^-	*leu1-32::pJK148-nmt81-ppc89$^+$ ade6-M210 ura4-D18*	See text
KGY5331	h^-	*sid4-GFP::Kan^R leu1-32::pJK148-nmt1-ppc89$^+$ ade6-M210 ura4-D18*	This study[b]
KGY5332	h^-	*ppc89-GFP::Kan^R leu1-32::pJK148-nmt1-ppc89$^+$ ade6-M210 ura4-D18*	This study[b]
KGY5333	h^-	*leu1-32::pJK148-nmt1-ppc89$^+$ ade6-M210 ura4-D18*	See text
KGY5458	h^+	*cdc11-GFP::Kan^R leu1-32::pJK148-nmt1-ppc89$^+$ ade6-M210 ura4-D18*	This study[b]
KGY5459	h^+	*alp6-GFP::Kan^R leu1-32::pJK148-nmt1-ppc89$^+$ ade6-M210 ura4-D18*	This study[b]
KGY5537	h^-	*pcp1-YFP::Kan^R leu1-32::pJK148-nmt1-ppc89$^+$ ade6-M210 ura4-D18*	This study[b]

KGY5576	h^+	*sid4-CFP::Kan^R nmt81-GFP-atb2$^+$::Kan^R leu1-32::pJK148-nmt1-ppc89$^+$ ade6-M210 ura4-D18*	This study[b]
KGY5647	h^-	*cdc11-GFP::Kan^R leu1-32::pJK148-nmt81-ppc89$^+$ ppc89Δ::ura4$^+$ ade6-M21X ura4-D18*	This study[b]
KGY5648	h^+	*sid4-GFP::Kan^R leu1-32::pJK148-nmt81-ppc89$^+$ ppc89Δ::ura4$^+$ ade6-M21X ura4-D18*	This study[b]
KGY5649	h^+	*alp6-GFP::Kan^R leu1-32::pJK148-nmt81-ppc89$^+$ ppc89Δ::ura4$^+$ ade6-M21X ura4-D18*	This study[b]
KGY5650	h^+	*pcp1-GFP::Kan^R leu1-32::pJK148-nmt81-ppc89$^+$ ppc89Δ::ura4$^+$ ade6-M21X ura4-D18*	This study[b]
KGY5762	h^+	*cut11-GFP::ura4$^+$ leu1-32::pJK148-nmt81-ppc89$^+$ ppc89Δ::ura4$^+$ade6-M21X ura4-D18*	This study[b]
KGY6748	h^-	*mto2-10A-myc$_{13}$::KanR ade6-M210 ura4-D18 leu1-32*	This Study
KGY6749	h^-	*cdc25-22 mto2-10A-myc$_{13}$::KanR ade6-M210 ura4-D18 leu1-32*	This Study
KGY6750	h^-	*nda3-KM311 mto2-10A-myc$_{13}$::KanR ade6-M210 ura4-D18 leu1-32*	This Study

[a]Some *ade6* alleles could be either *210* or *216,* and *21X* denotes this uncertainty.

[b] Constructed by crosses among other strains listed here or between such strains and strains described by (West *et al.*, 1998; Chang and Gould, 2000; Flory *et al.*, 2002; Tomlin *et al.*, 2002; Sawin *et al.*, 2004b; Venkatram *et al.*, 2004).

Table 3. **Plasmids**

Plasmid Name	Vector	Insert
pKG 240	pGBT9	sid4 (459-1980)
pKG 367	pREP81	none
pKG 368	pREP1	none
pKG 827	pGAD424	ppc89
pKG 835	pMAL-2c	ppc89
pKG 890	pPREP81	ppc89
pKG 934	pGAD424	ppc89 (1-798)
pKG 954	pGAD424	ppc89 (783-2349)
pKG 955	pGBT9	ppc89 (783-2349)
pKG 982	pGAD424	ppc89 (783-2349)
pKG 1141	pGAD424	ppc89 (783-1650)
pKG 1143	pGBT9	ppc89 (783-1650)
pKG 1162	pGAD424	ppc89 (1-1650)
pKG 1173	pMAL-2c	sid4 (906-1980)
pKG 1227	pREP81	sid4
pKG 1288	pREP81-GFP	ppc89 (783-2349)
pKG 1294	pPREP1	ppc89
pKG 1699	pGEX4T-1	none
pKG 1743	pGAD424	none
pKG 1744	pBGT9	none
pKG 1781	pSK	prp19
pKG 1826	pMAL-2c	none
pKG 2152	pGBT9	sid4 (903-1980)
pKG 2193	pGBT9	sid4 (1455-1980)
pKG 3140	pPREP81-GFP	sid4N-ppc89
pKG 3159	pSK	sid4
pKG 3419	pGEX4T-1	mto2
pKG 4257	pGEX4T-1	mto2-10A

CHAPTER III

PPC89 LINKS MULTIPLE PROTEINS TO THE CORE OF THE FISSION YEAST SPB

(This Chapter was previously published in:
Molecular Biology of the Cell Vol.17, 3793-3805, Sept. 2006)[*]

Introduction

The centrosome is the major microtubule-organizing center (MTOC) in higher eukaryotes (Urbani and Stearns, 1999). Problems in centrosome function such as improper duplication or an inability to anchor MTs lead to defects in chromosome segregation that result in incomplete genome inheritance to the progeny. Furthermore, centrosomal defects resulting in an inability to properly organize MTs cause nuclear positioning, cell polarity and intra-cellular trafficking defects (Jaspersen and Winey, 2004). Additionally, there is a growing list of regulatory and signaling molecules localized to the centrosome that underscores its key role as a signaling center (Doxsey *et al.*, 2005b).

The SPB is the yeast analog of the centrosome; its structure, composition, and organization are well characterized in the budding yeast *Saccharomyces cerevisiae* (Adams and Kilmartin, 2000). The *S. cerevisiae* SPB appears as a multi-layered cylindrical structure that is always embedded in the nuclear envelope (NE) as visualized

[*] Rosenberg, J.A., Tomlin, G.C., McDonald, W.H., Snydsman, B.E., Muller, E.G., Yates, J.R., 3rd, and Gould, K.L. (2006). Ppc89 links multiple proteins, including the septation initiation network, to the core of the fission yeast spindle-pole body. Mol. Biol. Cell *17*, 3793-3805.

by electron microscopy. Each SPB can be divided into three layers: the outer plaque on the cytoplasmic face, the central plaque in the plane of the NE, and the inner plaque on the nuclear side of the NE (Adams and Kilmartin, 2000; Jaspersen and Winey, 2004). The site of new SPB formation, called the half bridge, is joined to the central plaque (Jaspersen and Winey, 2004).

Far less is known about the SPB in the fission yeast *Schizosaccharomyces pombe.* The complete composition of the *S. pombe* SPB has not been determined (see Chapter 1) and there remains some uncertainty even as to when during the cell cycle the *S. pombe* SPB duplicates. Although it was first reported to duplicate in late G2 (Ding *et al.*, 1997), a recent study indicates that the SPB duplicates at the G1/S boundary from a half-bridge (Uzawa *et al.*, 2004), much like the *S. cerevisiae* SPB. Structural studies show that the *S. pombe* SPB is an amorphous body with an electron dense central line. It is tethered to the outside of the NE until mitosis, when it embeds in the NE (Ding *et al.*, 1997; Uzawa *et al.*, 2004). Cut11, which localizes to the NE and nuclear pore complexes throughout the cell cycle, is needed for the SPB to embed in the NE and becomes concentrated at the site of SPB insertion during mitosis (West *et al.*, 1998). During meiosis, the *S. pombe* SPB leads the nucleus in dynamic "horsetail" oscillatory movements (reviewed by (Sawin, 2005), which are necessary for normal rates of recombination, and also serve to initiate spore formation at the end of meiosis (Shimoda, 2004).

Although the full complement of *S. pombe* SPB components has not been determined, some proteins have been identified based on homology to *S. cerevisiae* components or through genetic screens. One structural component identified is Pcp1, the homologue of *S. cerevisiae* Spc110 (Flory *et al.*, 2002). Spc110 binds calmodulin and

links the gamma tubulin complex (γ-TuC) to the central plaque of the SPB (Knop and Schiebel, 1997; Sundberg and Davis, 1997). Another structural element is centrin/Cdc31. This protein is a part of the SPB half bridge and controls SPB duplication (Paoletti *et al.*, 2003). Several proteins have been identified that localize at the SPB between the NE and the SPB. One such component is Sad1. Sad1 contains one transmembrane helix domain and is required for mitotic functions of the SPB (Hagan and Yanagida, 1995). Interacting with Sad1 are Kms1 and Kms2, which contain coil-coiled and transmembrane helices and are not essential for vegetative growth (Niwa *et al.*, 2000; Miki *et al.*, 2004). Kms1 is essential for telomere clustering and SPB function during meiosis (Shimanuki *et al.*, 1997). The less well characterized *kms2* mutant is reported to have mitotic defects (Miki *et al.*, 2004). Another group of SPB proteins has been identified based on their specific requirement during meiosis. Among these proteins are Hrs1/Mcp6, produced specifically during meiosis (Saito *et al.*, 2005; Tanaka *et al.*, 2005), and Ssm4 (Niccoli *et al.*, 2004), a p150-Glued protein, which are both required for horsetail nuclear movement and recombination of sister chromosomes, and Spo15, a meiotic SPB protein involved in spore membrane formation (Ikemoto *et al.*, 2000).

In addition to the MTOC functions discussed above, the SPB in *S. pombe* functions as an assembly site for a signal transduction network, called the septation initiation network (SIN), that coordinates mitosis with cytokinesis (reviewed by (McCollum and Gould, 2001; Simanis, 2003; Krapp *et al.*, 2004b). The SIN is a GTPase-regulated protein kinase pathway that coordinates proper chromosome segregation with mitotic exit and cytokinesis. All components of this pathway localize to the SPB during at least a portion of the cell cycle, and the signal for cytokinesis is thought to emanate

from there (Bardin and Amon, 2001; McCollum and Gould, 2001; Simanis, 2003; Krapp *et al.*, 2004b). Components of the SIN, as well as its regulators, are localized to the SPB through their association with its two scaffolding components, Sid4 and Cdc11, which are constitutively localized to the SPB (Chang and Gould, 2000; Krapp *et al.*, 2001; Tomlin *et al.*, 2002; Krapp *et al.*, 2004a; Morrell *et al.*, 2004). Sid4 appears to be the SIN component most proximal to the SPB, because its function is required for the SPB localization of all other known SIN components. The C-terminal region of Sid4 directs the protein to the SPB, whereas the Sid4 N-terminal region binds directly to the C-terminal region of Cdc11 as well as to the polo-like kinase Plo1 and the SIN inhibitor Dma1 (Guertin *et al.*, 2002; Tomlin *et al.*, 2002; Morrell *et al.*, 2004). The N-terminal region of Cdc11 binds Spg1, Cdc16, Sid2, and Cdk1-Cdc13 (Morrell *et al.*, 2004). However, although Sid4 is stably associated with the SPB, it is not clear how it is integrated into the SPB.

In an effort to reveal additional components, anchors, or regulators of the SIN previously unidentified through genetic screens, we performed a TAP (tandem affinity purification) analysis on Cdc11. Mass spectrometric analysis of proteins co-purifying with Cdc11 identified a previously uncharacterized protein, which we named Ppc89, encoded by the SPAC4H3.11c locus. In this work, we test our hypothesis that Ppc89 is a key structural element of the SPB needed for its integrity. We also go on to characterize the relationship of this protein to the SIN and its role in SPB function.

Results

Identification of Ppc89

In order to identify previously unrecognized SIN components, interactors, or SPB anchors, sequences encoding a TAP cassette were introduced at the 3' end of the *cdc11*$^+$ ORF, to generate strain KGY3888 (see Materials and Methods). Following TAP, the eluate was digested with proteases and subjected to two-dimensional liquid chromatography and tandem mass spectrometry as described (Link *et al.*, 1999; MacCoss *et al.*, 2002). Proteins within the mixture were then identified using the SEQUEST algorithm (Eng *et al.*, 1994). Besides Cdc11, Sid4, and known contaminants of TAP complexes (Gould *et al.*, 2004), the protein identified by the next greatest sequence coverage in this purification encoded by a previously uncharacterized ORF, SPAC4H3.11c. The predicted molecular mass of this protein is 89 kDa. We named this protein Pombe Pole Component 89 (Ppc89) based on its molecular mass and localization (see below). Ppc89 is predicted to contain two blocks of coiled-coils in its central region as well a third coiled-coil region at its C-terminal region [(schematized in Figure 7A and 9A)]. BLAST searches failed to reveal obvious homologs of this protein in any other organism for which a genome sequence is available. We determined that *ppc89*$^+$ is an essential gene by tetrad analysis of diploid cells in which one copy of *ppc89*$^+$ had been replaced with *ura4*$^+$ (see Materials and Methods).

To determine the intracellular localization of Ppc89 and investigate other properties of this protein, sequences encoding eGFP, Myc_{13}, HA_3, YFP, CFP, or the TAP tag were appended to the 3'end of the chromosomal *ppc89*$^+$ ORF so that normal control of fusion-protein expression was maintained. The resultant strains were wild type in morphology and growth rate, indicating that the tags did not disrupt Ppc89 function. Pcp89-GFP was detected as one or two dots adjacent to the nucleus throughout the cell

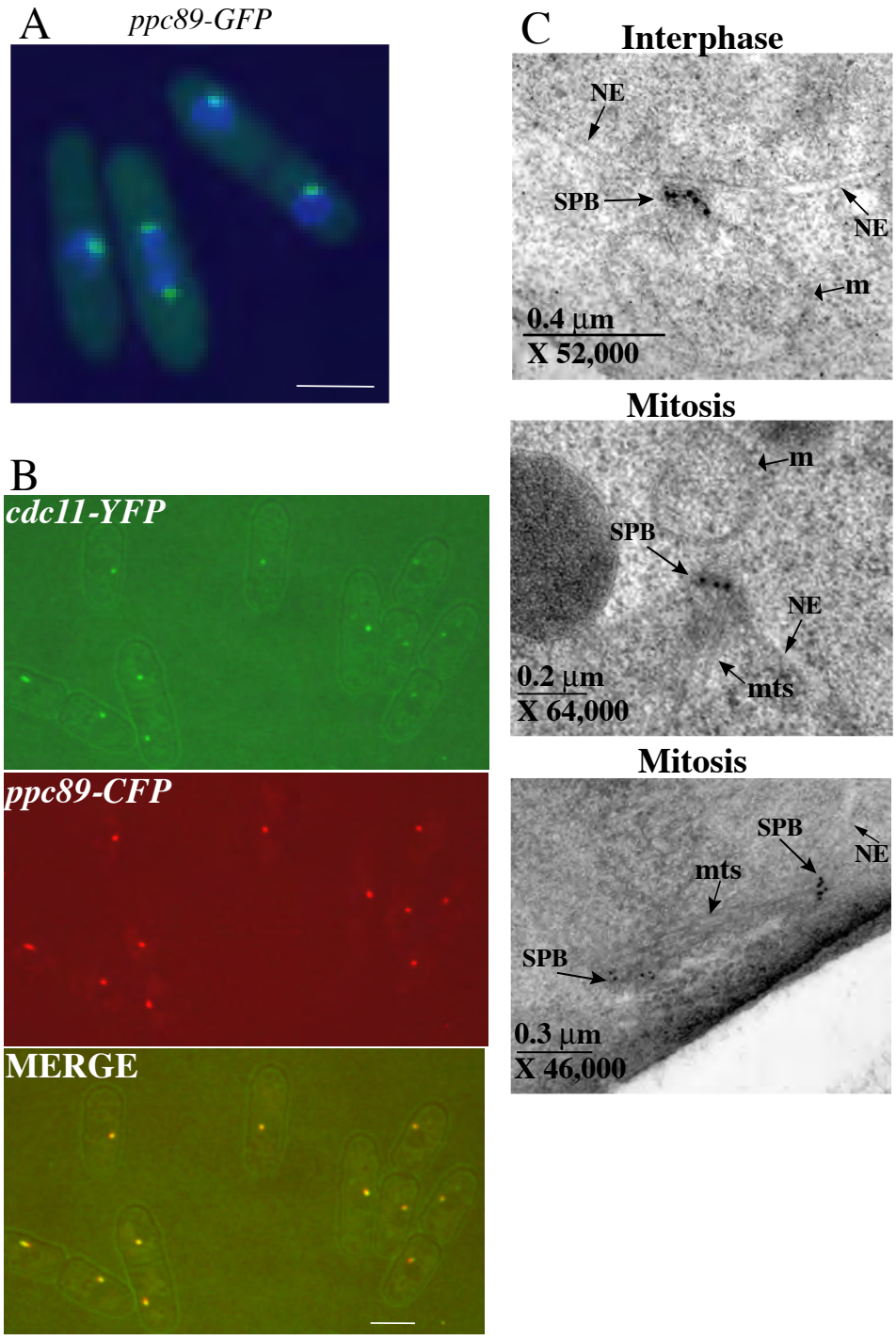

Figure 5. Ppc89 localizes to the SPB throughout the cell cycle. (A) ppc89-GFP cells (KGY 4294) were fixed in ethanol and stained with DAPI to visualize DNA. (B) Live ppc89-CFP cdc11-YFP cells (KGY 4318) were imaged, and the images were then merged. Bars, 5 µm. (C) Immuno-electron micrographs of ppc89-GFP cells (KGY4294). Top panel: gold particles labeling Ppc89-GFP in an interphase cell in which the SPB lies just outside the nuclear envelope. Middle and lower panels: Mitotic cells showing SPBs labeled with gold particles. NE, nuclear envelope; S, spindle; m, mitochondrion; mts, microtubules. (EM performed by Tom Giddings and Erin White, University of Colorado Electron Microscopy Service)

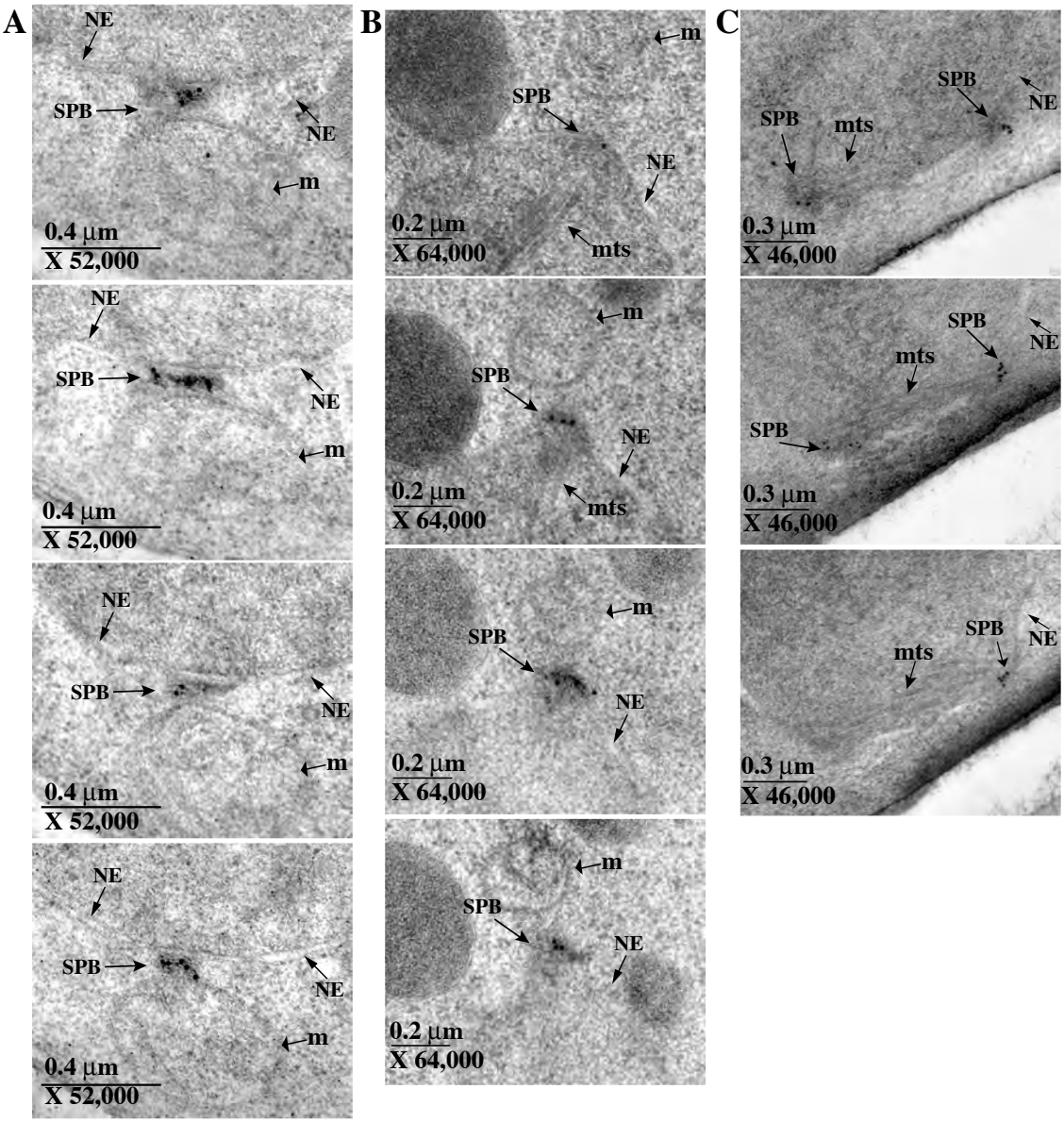

Figure 6. Serial sections from the same immuno-gold labeled ppc89-GFP cells as shown in Figure 5. (A) An interphase cell. Gold particles label Ppc89-GFP in a non-inserted SPB just outside the nuclear envelope. (B and C) Mitotic cells. Both SPBs are labeled with gold particles in C. NE, nuclear envelope; S, spindle; m, mitochondrion; mts, microtubules. (EM performed by Tom Giddings and Erin White, University of Colorado Electron Microscopy Service)

cycle (Figure 5A), a staining pattern indicative of SPB localization. To confirm that these dots corresponded to SPBs, we examined the localization of Pcp89-CFP in cells also producing Cdc11-YFP. Cdc11 is known to reside at SPBs throughout the cell cycle (Krapp *et al.*, 2001; Tomlin *et al.*, 2002). The individual and merged images indicate that Pcp89 and Cdc11 co-localize to SPBs (Figure 5B), an expected result given that the two proteins co-purified. Ppc89 was also found to localize to SPBs through immuno-electron microscopy. *ppc89-GFP* cells in exponential phase were fixed by high-pressure freezing and stained with antibodies to GFP and then with colloidal-gold-labeled secondary antibodies. In interphase cells, gold particles were localized in the central region of the SPB that lay adjacent to the NE (Figure 5C and Figure 6). In mitotic cells, gold particles appeared in the central region of the SPB in the same plane as the NE or slightly towards the cytoplasmic side (Figure 5C, Figure 6, and unpublished observations). A reciprocal TAP experiment was also performed on a *ppc89-TAP* strain (KGY4293), and mass-spectrometric analysis revealed the presence of Ppc89, Sid4, and Cdc11 (unpublished observations). Taken together, these results suggest that Ppc89 is closely associated with the SIN scaffolding proteins Cdc11 and Sid4 at the SPB.

Ppc89 Interacts with Sid4

To understand the basis of the co-purification of Ppc89 with Cdc11 and Sid4, we tested whether it bound to either or both of these proteins directly. First, directed two-hybrid analysis was performed. Although no positive interactions were detected between fragments of Cdc11 and Ppc89, positive interactions were detected between Sid4 and Ppc89 (Figure 7A). The regions within the two proteins responsible for their interaction

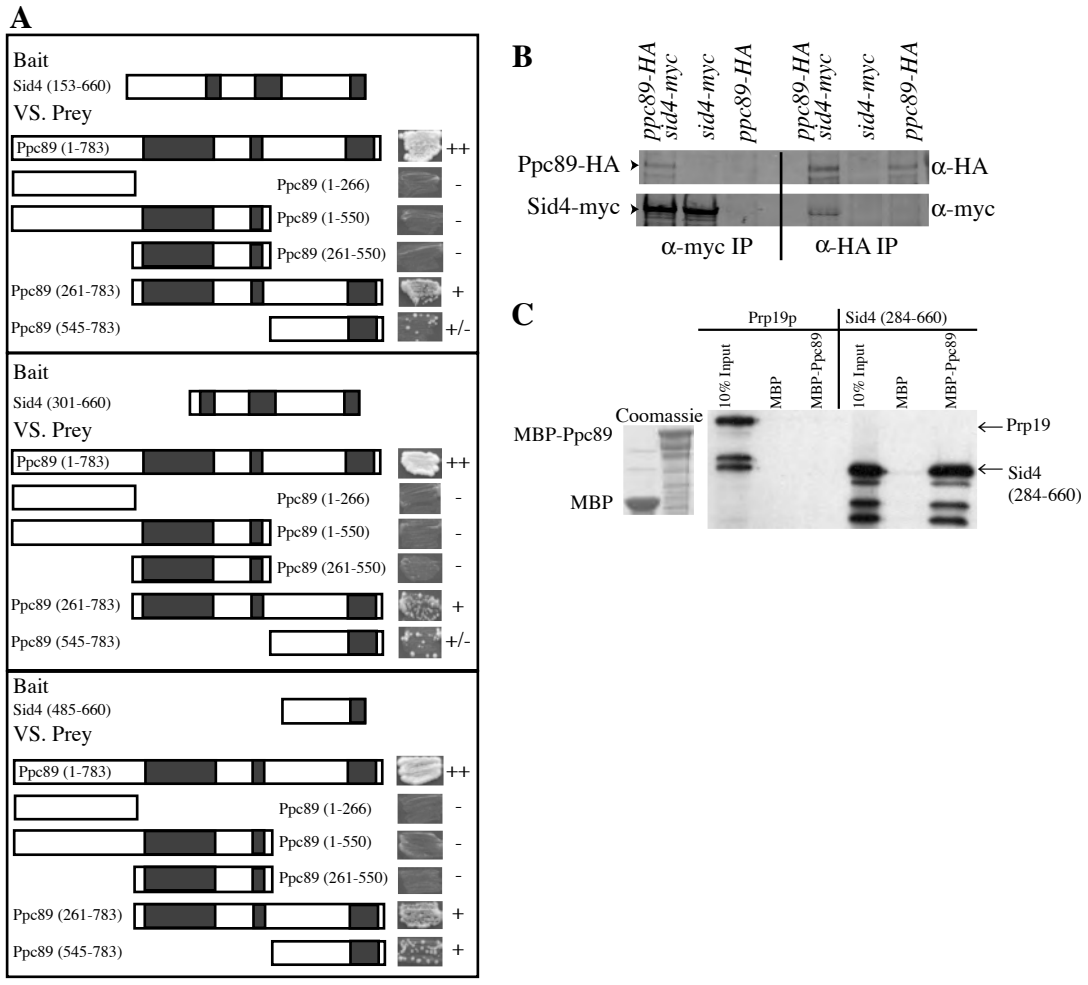

Figure 7. Ppc89 and Sid4 interact directly through their C-termini. (A) S. cerevisiae strain PJ69-4A was co-transformed with plasmids expressing the indicated regions of Sid4 and Ppc89. Transformants carrying both plasmids were scored for growth on –Ade -His plates. Pluses indicate strong growth, plus/minus indicates little growth, and minuses indicate no growth. Shaded areas indicate regions of predicted coiled-coil. (B) Lysates from ppc89-HA3 (KGY4288), sid4-myc13 (KGY1341), or ppc89-HA3 sid4-myc13 (KGY4297) strains were immunoprecipitated using anti-myc (left hand panel) or anti-HA (right hand panel) antibodies. After SDS-PAGE, blots were probed with anti-HA (upper panel) or anti-myc (lower panel) antibodies. (C) MBP and MBP-Ppc89 were produced in E. coli, and the soluble portion was bound to amylose beads. The amounts of recombinant proteins added to the reactions are shown by Coomassie staining in the left panel. Prp19 and Sid4 (284-660) were expressed using an in vitro reticulocyte lysate system in the presence of 35S-methionine, and 10% of the reaction was used in the input lane. Following incubation with proteins bound to beads and washing of the beads, samples were separated by SDS-PAGE, and proteins were detected by autoradiography (right panel). (Sections B and C performed by Greg Tomlin, Vanderbilt University).

were narrowed to their C-terminal regions containing predicted coiled-coils (Figure 7A). As expected from the above results, Sid4 and Ppc89 were able to co-immunoprecipitate from a *sid4-myc$_{13}$ ppc89-HA$_3$* strain (but not from singly-tagged strains) when either an anti-Myc or an anti-HA antibody was used for precipitation (Figure 7B). Moreover, MBP-Ppc89 produced and purified from *E. coli,* but not MBP alone, was able to interact with the C-terminal region of Sid4 (residues 284-660) that was produced in a cell-free coupled transcription/translation system from rabbit reticulocytes, neither MPB nor MBP-Ppc89 interacted with a functionally unrelated control protein, Prp19 (Figure 7C). These results indicate that there is a direct association between Sid4 and Ppc89 mediated by their respective C-terminal regions.

Evidence for the close proximity of the C-terminal regions of Ppc89 and Sid4 *in vivo* was provided by fluorescence resonance energy transfer (FRET). The C-terminal regions of the two proteins were tagged with YFP and CFP, respectively, and examined by fluorescence microscopy (Figure 8, top row). The extent of energy transfer was determined using the $FRET_R$ metric (see Materials and Methods), which measures the relative increase of fluorescence in the FRET channel compared to a baseline calculated from the fluorescence in the CFP and YFP channels. In the absence of energy transfer, $FRET_R$ has a value of 1. $FRET_R$ for the Ppc89-YFP and Sid4-CFP pair was 2.05 (Table 3, row 1). There was no significant change when the tags were reversed (Table 3, row 2). This high FRET was comparable to that of a positive control, Sid4-YFP-CFP, which had a $FRET_R$ of 2.37 (Figure 8, middle row; Table 3, row 3). Neither Ppc89 nor Sid4 was near enough to Cdc11 for FRET (Figure 8, bottom row; Table 3, lines 4-7). From these

Table 3. Summary of FRET results

Row	Strain	CFP Donor	YFP Acceptor	$FRET_R$	N
1	KGY794	Sid4-CFP	Ppc89-YFP	2.05 ± 0.12	126
2	KGY262	Ppc89-CFP	Sid4-YFP	1.86 ± 0.16	58
3	KGY4608	Sid4-YFP-CFP	Sid4-YFP-CFP	2.37 ± 0.20	90
4	KGY4318	Ppc89-CFP	Cdc11-YFP	0.96 ± 0.09	113
5	KGY3275	Cdc11-CFP	Ppc89-YFP	1.02 ± 0.08	104
6	KGY3526	Sid4-CFP	Cdc11-YFP	0.96 ± 0.10	88
7	KGY3271	Cdc11-CFP	Sid4-YFP	0.95 ± 0.09	81

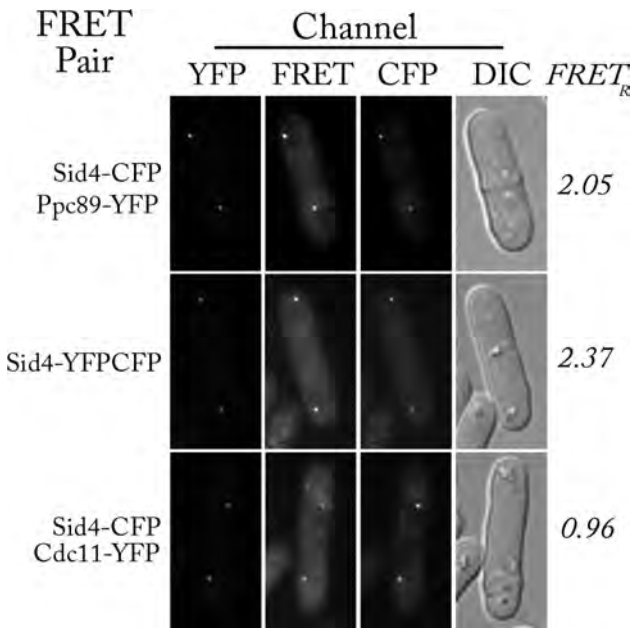

Figure 8. The close proximity of the C-termini of Sid4 and Ppc89 leads to FRET.
Images were captured in four channels: YFP (500-nm excitation, 545-nm emission), FRET (440-nm excitation, 545-nm emission), CFP (440-nm excitation, 480-nm emission), and DIC. For each strain, the images have the same minimum and maximum pixel intensity, allowing visual comparison of the images. FRETR was calculated as described in Methods. Strains were KGY 794, KGY4608, and KGY3526. (FRET strains made by Greg Tomilin, Vanderbilt University. FRET analysis performed by Brian Snydsman and Eric Muller, University of Washington).

values, we conclude that the C-terminal regions of Ppc89 and Sid4 are probably within 100 Å of each other in the cell.

The C-terminus of Ppc89 is a SPB-Binding Module

The overall organization of predicted coiled-coil domains within Ppc89 is very similar to that of Sid4 (Figure 9A). Sid4 dimerizes through its central coiled-coil domain (Chang and Gould, 2000) and binds to the SPB through its very C-terminal region (Tomlin *et al.*, 2002). Furthermore, Sid4 SPB binding is enhanced by its ability to dimerize; residues 300-560 very effectively localize GFP to the SPB in cells that also express full-length Sid4 (Tomlin *et al.*, 2002). To determine if similar regions of Ppc89 have similar functions, we generated a GFP fusion to residues 261-783 of Ppc89 and produced it in wild-type cells. As expected, this fusion protein localized correctly to SPBs (Figure 9B). To determine if Ppc89, like Sid4, is able to self-associate, two-hybrid analysis was performed. As with Sid4, Ppc89 interacted robustly with itself, and this activity could be narrowed to the central coiled-coil region (Figure 9C).

The similarity in architecture between Sid4 and Ppc89 and their similar localization prompted us to generate a fusion between the N-terminal region of Sid4 and the C-terminal self-interaction and SPB-targeting domains of Ppc89 (Figure 9A). We reasoned that if the only region of Sid4 important for SIN signaling was its N-terminal 300 amino acids, then this fusion protein should be able to rescue *sid4* mutant alleles. Consistent with this possibility, the Sid4-Ppc89 fusion protein localized to SPBs (Figure 9D) and rescued *sid4Δ::ura4*$^+$ segregants from strain KGY1358 (unpublished observation) and the temperature-sensitive lethality of *sid4-SA1* cells (Figure 9E). Full-

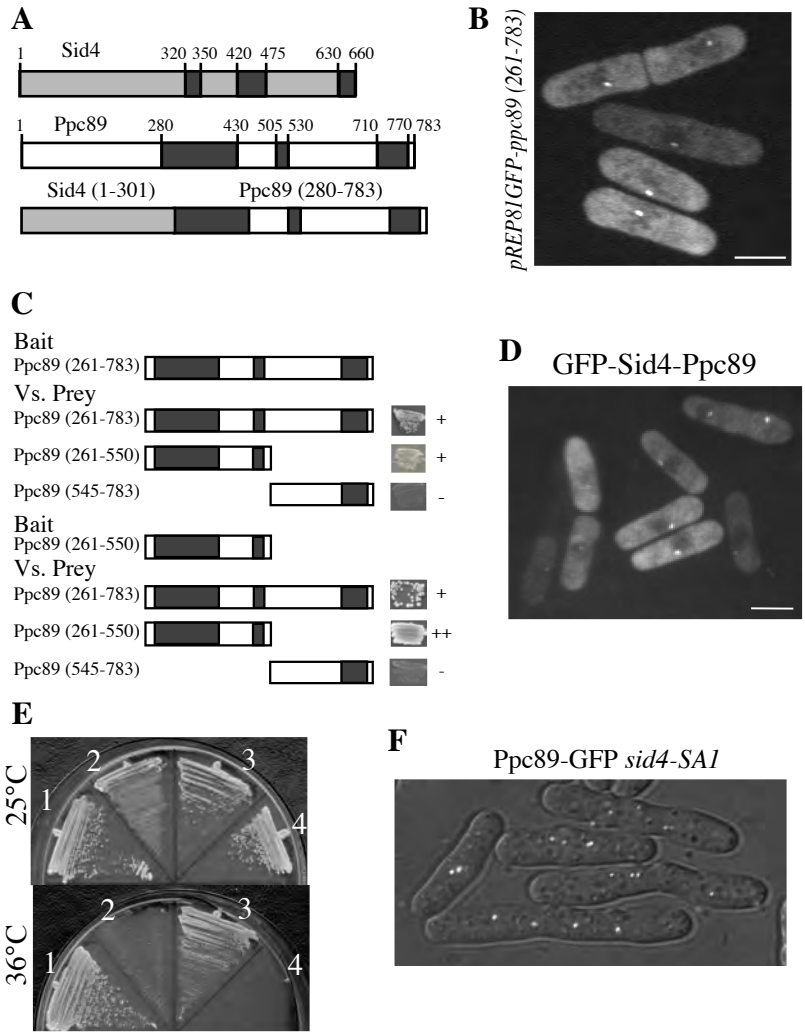

Figure 9. The essential function of the Sid4 C-terminus in SIN signaling is SPB targeting. (A) Schematic representation of Sid4, Ppc89, and a Sid4-Ppc89 fusion. Predicted coiled-coil domains are indicated by black boxes. Numbers indicate amino acids. (B) Wild-type cells (KGY246) expressing GFP-ppc89 (261-783) from the pREP81 vector were grown in the absence of thiamine for 18 h at 32˚C. An image of live cells was captured. (C) Bait and prey vectors expressing the indicated regions of Ppc89 were co-transformed into S. cerevisiae strain PJ69-4A. Transformants carrying both plasmids were scored for growth on a medium selecting for a two-hybrid interaction, as indicated to the right of the schematics. Shaded areas indicate regions of predicted coiled-coil. (D) sid4-SA1 cells (KGY1234) were transformed with pREP81-GFPsid4-ppc89, and live-cell images were captured after 24 h of growth in the absence of thiamine at 25˚C. (E) Strain KGY1234 was transformed with pREP81sid4+ (1), pREP81ppc89+ (2), pREP81sid4-ppc89 (3), and pREP81 (4). Transformants were incubated on medium lacking thiamine at 25˚C (top panel) or 36˚C (bottom panel) for 4 days. (F) ppc89-GFP sid4-SA1 cells (KGY4325) were incubated at the restrictive temperature of 36˚C for 4 h, and live-cell images were captured. Bars, 5 µm. (Panels B, D, E and F performed by Greg Tomlin, Vanderbilt University).

length *ppc89*$^{+}$, the C-terminal portion of Ppc89 used in the fusion protein, and any *sid4* construct lacking its C-terminal coiled-coil region, such as Sid4 (1-300), were not able to rescue growth of *sid4-SA1* cells at 36˚C (Figure 9E; unpublished observations; (Chang and Gould, 2000; Krapp *et al.*, 2001; Tomlin *et al.*, 2002). These data indicate that the first 300 amino acids of Sid4 are the only ones critical for SIN signaling and that the remainder of the molecule is involved in SPB targeting and oligomerization, functions that can be performed by a similar region of Ppc89. These results also suggest that Ppc89 might anchor Sid4 to the SPB rather than Sid4 affecting Ppc89 localization. Consistent with this possibility, Ppc89-GFP was still at SPBs in cells lacking *sid4* function (Figure 9F), in contrast to all known SIN components, which require Sid4 for their localization (Krapp *et al.*, 2001; Tomlin *et al.*, 2002; Morrell *et al.*, 2004).

Ppc89 Is Required For SPB Integrity and Function.

To further elucidate the role of Ppc89, we created a strain containing *ppc89Δ::ura4*$^{+}$ and a copy of *ppc89*$^{+}$ under control of the low- strength, thiamine-repressible *nmt81* promoter integrated at the *leu1* locus (see Materials and Methods). These cells were viable in the absence of thiamine, when *ppc89*$^{+}$ was expressed, but failed to grow when the promoter was repressed (Figure 10A and B). Samples taken 8 h after thiamine addition were stained with DAPI to visualize the nuclei and anti-α-tubulin antibodies to visualize MTs (Figure 10C and D). (Beyond this point, the majority of cells lysed, and no further assessment of phenotype could be performed). The majority of cells (68%) were found to contain a single nucleus, although a minor population (6%; Figure 5D, right panel) contained multiple nuclei, indicative of a SIN phenotype. A significant

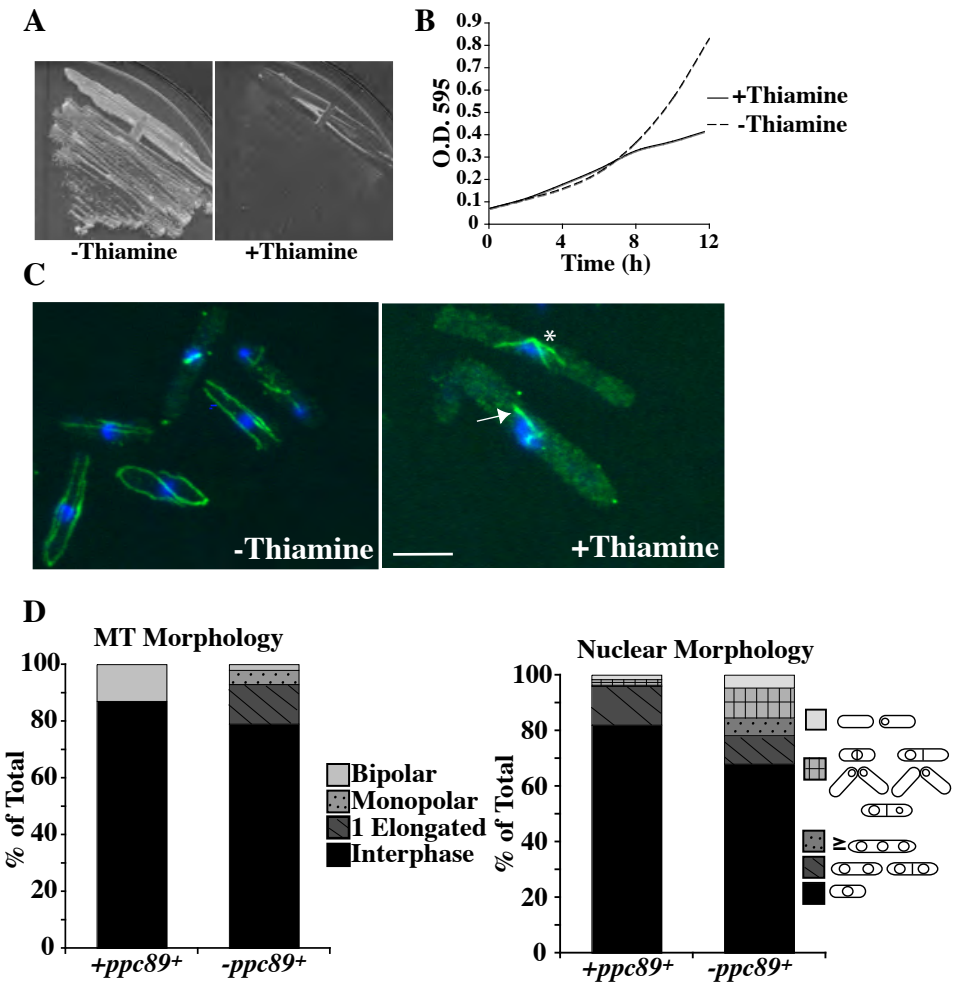

Figure 10. Ppc89 depletion is lethal. (A) Cells containing a single copy of ppc89+ under control of the nmt81 promoter (KGY5185) were incubated on minimal medium lacking thiamine (promoter induced) or containing thiamine (promoter repressed). (B) Strain KGY5185 was grown in minimal medium in the absence of thiamine, and thiamine was added to half the culture at time 0. (C) Cells from the 8-h time point in part B were fixed with ethanol and stained with DAPI (blue) and antibodies to γ-tubulin (green). Arrow indicates single elongated MT bundle; asterisk indicates a monopolar spindle. Bar, 5 μm. (D) Quantification of morphologies of cells from (C). Right, nuclear morphologies; left, MT morphologies. 300 cells were counted in each case.

percentage of the cells (15%; Figure 10D, right panel) displayed a "cut" phenotype in which the septum cleaved through an undivided chromatin mass. By immunofluorescence, the majority (79%; Figure 10D, left panel) of Ppc89-depleted cells appeared to contain a normal interphase array of MTs. Another substantial population (14%; Figure 10D, left panel) arrested with a single elongated MT bundle. Only 7% of the cells appeared to be in mitosis, as judged by the presence of a spindle, and most of these had monopolar rather than bipolar spindles. (The population of cut cells was not represented in cells stained for MTs, probably because cell-wall digestion frequently destroys them). Taken together, these data suggest that cells lacking Ppc89 have defects in organizing SPB MTs, including the mitotic spindle, and that, as a consequence, chromosome segregation fails in those cells that enter mitosis.

To examine the effects of Ppc89 loss on SIN-component localization, it was depleted from strains producing GFP-tagged Sid4 or Cdc11. In both cases, GFP signals were absent from SPBs (Figure 11A, top two rows). This result is consistent with the data implicating Ppc89 as an anchor for Sid4 at the SPB (Figure 9). In similar experiments, the other SPB components Alp6, a γ-tubulin complex (γ-TuC) component (Vardy and Toda, 2000), and Pcp1 (see Introduction) were examined. Again, the GFP signals at SPBs were absent or significantly reduced after 8 h of *ppc89*$^{+}$ repression (Figure 11A, bottom two rows). These data indicate that Ppc89 is required to recruit or maintain a variety of proteins at the SPB and suggest that Ppc89 might be required for SPB integrity.

We next asked whether Ppc89 depletion also affected the integrity of the NE by repressing *ppc89*$^{+}$ expression in a strain producing GFP-tagged Cut11, which normally

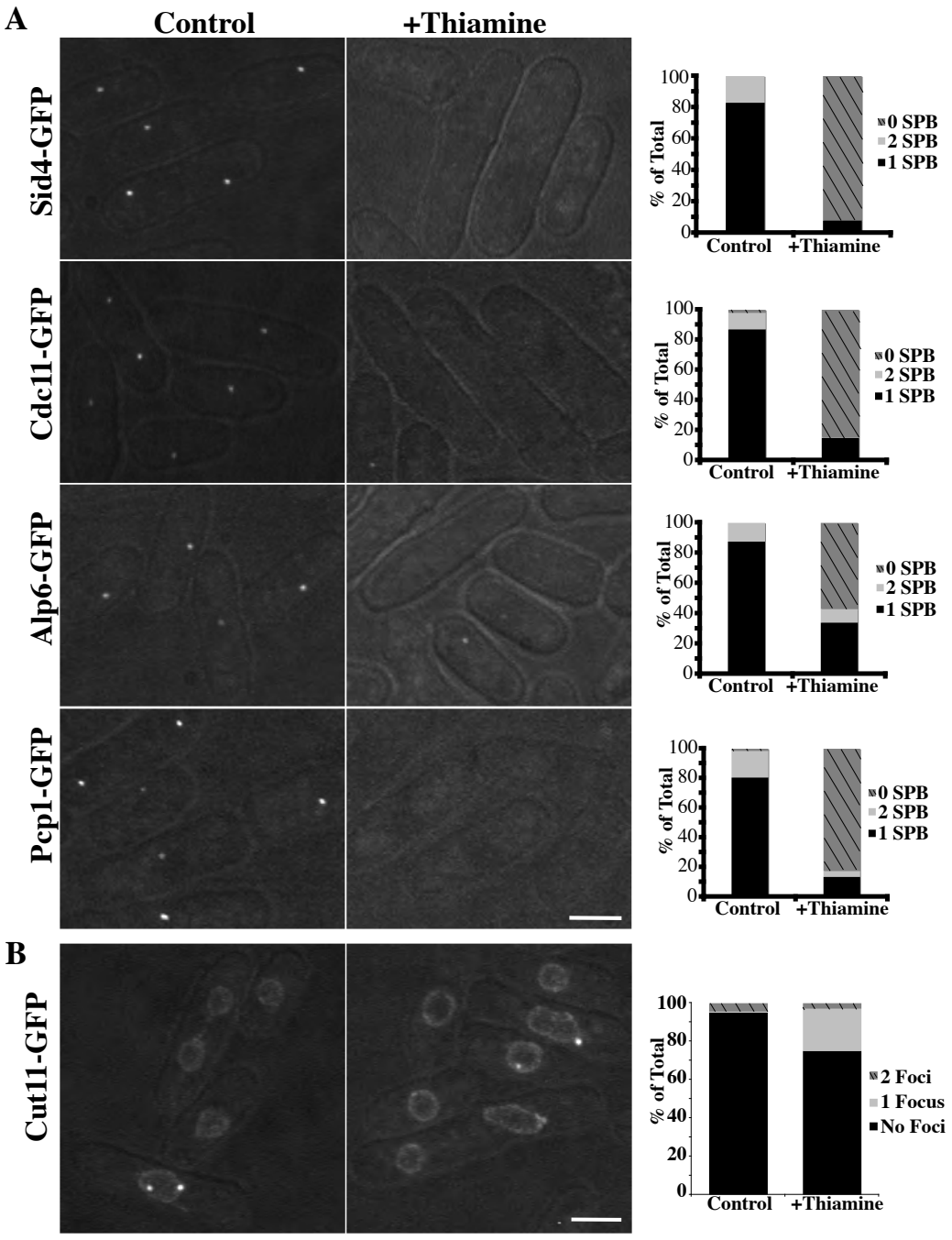

Figure 11. Ppc89 depletion results in the loss of multiple factors from the SPB but not in NE fragmentation. (A) Strains producing the indicated GFP-tagged SPB component and carrying a single, integrated copy of ppc89+ under control of the thiamine-repressible nmt81 promoter (strains KGY5647, KGY5648, KGY5649, and KGY5650) were grown for 16 h at 32°C in the absence of thiamine. Each culture was then split into two portions, thiamine was added to one, incubation was continued for 8 h at 32°C, and live- cell images were captured. The numbers of SPBs visualized per cell were scored (graphs on right). (B) As in A, except using strain KGY5762 (cut11-GFP nmt81-ppc89+). The numbers of foci of Cut11-GFP were quantified (graph on right). Bars, 5 μm.

decorates the NE and nuclear pores as well as concentrating at the site of SPB insertion into the NE in mitosis (West *et al.*, 1998). In cells depleted of Ppc89, the NE appeared intact (Figure 11B). However, 36% of the cells had a misshapen nucleus (versus 2% in control cells), 22% (versus 0.5% in control cells) displayed a single Cut11-GFP focus (Figure 11B). Although we do not yet understand the reason for the altered NE morphology, these results indicate that NE fragmentation does not account for the observed loss of SPB components in cells lacking Ppc89.

Ppc89 Overproduction Is Lethal and Results in SPB Enlargement

To further examine the role of Ppc89 at the SPB, *ppc89*$^{+}$ was placed under the control of the strong, thiamine-regulatable *nmt1* promoter. Overproduction of Ppc89 was lethal (Figure 12A), and FACS analysis revealed that the cells arrested with a 2N content of DNA (unpublished observation). The *nmt1-ppc89* construct was then integrated into the *leu1* locus to facilitate further analysis. To explore the basis of the lethality, Ppc89-overproducing cells were stained with DAPI and antibodies to the known SPB component Sad1 (Hagan and Yanagida, 1995) (Figure 12B). The majority of Ppc89-overproducing cells arrested with a single nucleus, but a significant population (22%) displayed a "cut" phenotype. Interestingly, most cells overproducing Ppc89 contained a single, enlarged focus of Sad1 staining. Ppc89 was also overproduced in strains expressing GFP- or YFP-tagged Sid4, Cdc11, Pcp1, Alp6, or Ppc89 itself. In all cases, single, enlarged GFP or YFP foci were detected that trailed out to give a comet-like appearance (Figure 12C). Immunoblot analysis indicated that the overall levels of these proteins did not change with Ppc89 overproduction (unpublished observation). Taken

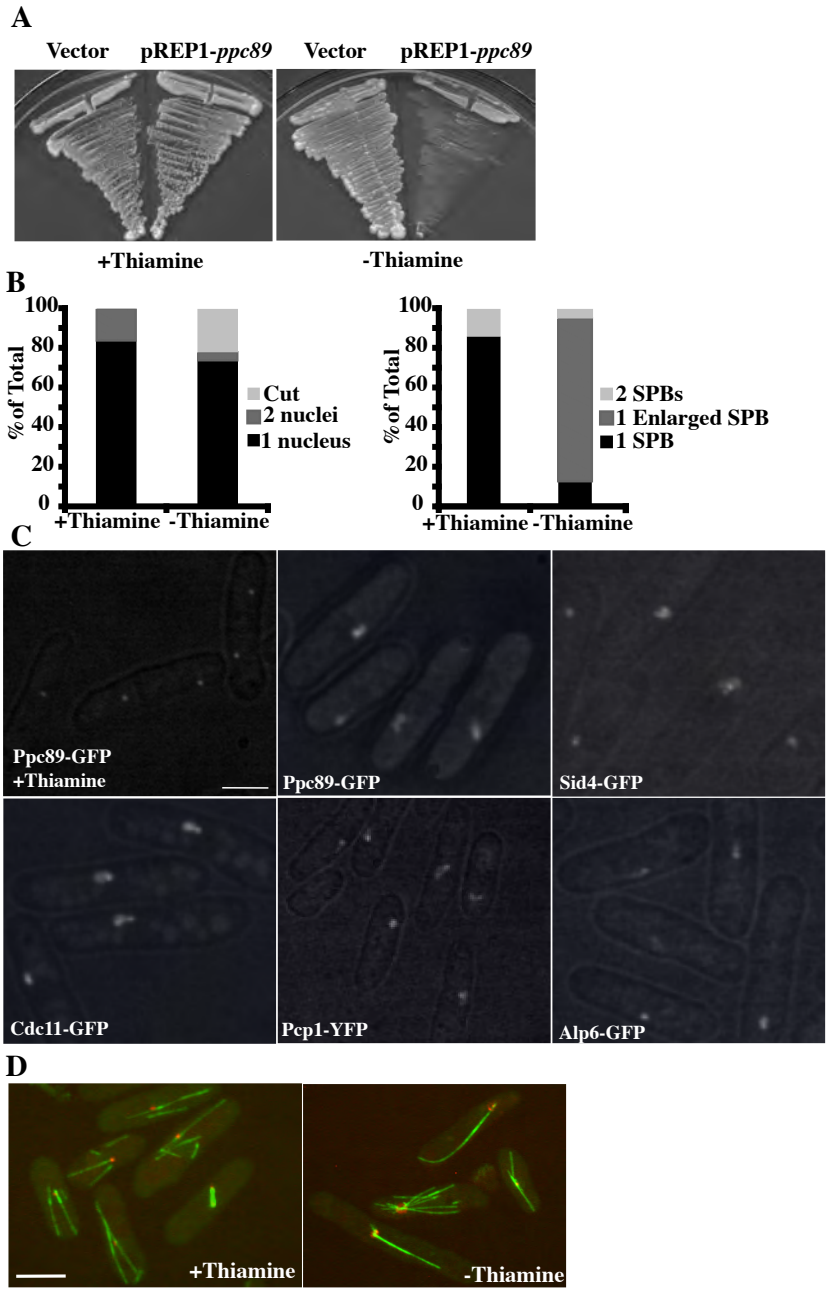

Figure 12 . Ppc89 overproduction results in abnormal SPB morphology. (A) Wild-type cells (KGY246) were transformed with either pREP1 vector alone (left sectors) or pREP1-ppc89 (right sectors), and transformants were incubated on minimal medium containing thiamine (promoter repressed) or lacking thiamine (promoter induced). (B) sid4-GFP nmt1-ppc89+ cells (KGY5331) were grown in the presence or absence of thiamine for 24 h at 32˚C, fixed with methanol, and stained with DAPI and antibodies to Sad1. Left, quantification of the numbers of nuclei per cell; right, quantification of the number of SPBs per cell, based on Sad1 staining. 300 cells were counted in each case. (C) Strains KGY5331, KGY5332, KGY5458, KGY5459, and KGY5537, which produce the indicated GFP- or YFP-tagged SPB component and carry a single, integrated copy of ppc89+ under control of the nmt1 promoter, were grown to mid-exponential phase at 32°C in medium containing thiamine. Cells were then grown in medium lacking thiamine for 24 h at 32°C, and live-cell images were captured. (D) nmt81-GFP-atb2 sid4-CFP nmt1-ppc89+ (KGY5576) cells were grown and imaged as in (C). Bars, 5 µm.

together, these data suggest that Ppc89 overproduction causes a cell-cycle arrest, predominantly in G2/M phase, accompanied by the enlargement of a single SPB.

To examine effects on the MT cytoskeleton, we also overproduced Ppc89 in cells expressing both the GFP-tagged α-tubulin gene, *atb2*$^{+}$, under control of the *nmt81* promoter (Sawin *et al.*, 2004b) and Sid4-CFP. Many cells (24%) were observed with greater-than-normal numbers of cytoplasmic MTs emanating from the SPBs (Figure 12D). There were also many cells (53%) with a single, extremely bright MT (or bundle of MTs) that extended from the edge of the nucleus (Figure 12D).

To examine the effect of Ppc89 overproduction on SPB morphology in greater detail, cells were viewed by electron microscopy. The majority of cells examined contained an elaborate extension of what appeared to be a reasonably normal SPB-like structure, although it extended away from the NE (Figure 13A-C). In some sections, a dark line was visible through this structure, as in normal SPBs (Ding *et al.*, 1997; Uzawa *et al.*, 2004). In cells with this additional SPB-associated material, the SPB itself was not embedded within the NE, and the darkly staining material associated with the SPB on the nuclear side of the NE appeared normal. This extension of SPB material into the cytoplasm is consistent with the localization of various SPB proteins as observed by light microscopy in cells overproducing Ppc89 (Figure 12C). Also consistent with the light-microscopy data, nuclear MTs were not detected adjacent to the enlarged SPBs, but cytoplasmic MTs frequently were (Figure 13C and unpublished observations). Interestingly, in Ppc89-overproducing cells, there were no detectable electron-dense centers or irregularities in the surfaces of the SPBs, such as those typically observed between duplicated but unseparated SPBs (Ding *et al.*, 1997; Uzawa *et al.*, 2004) (Figure

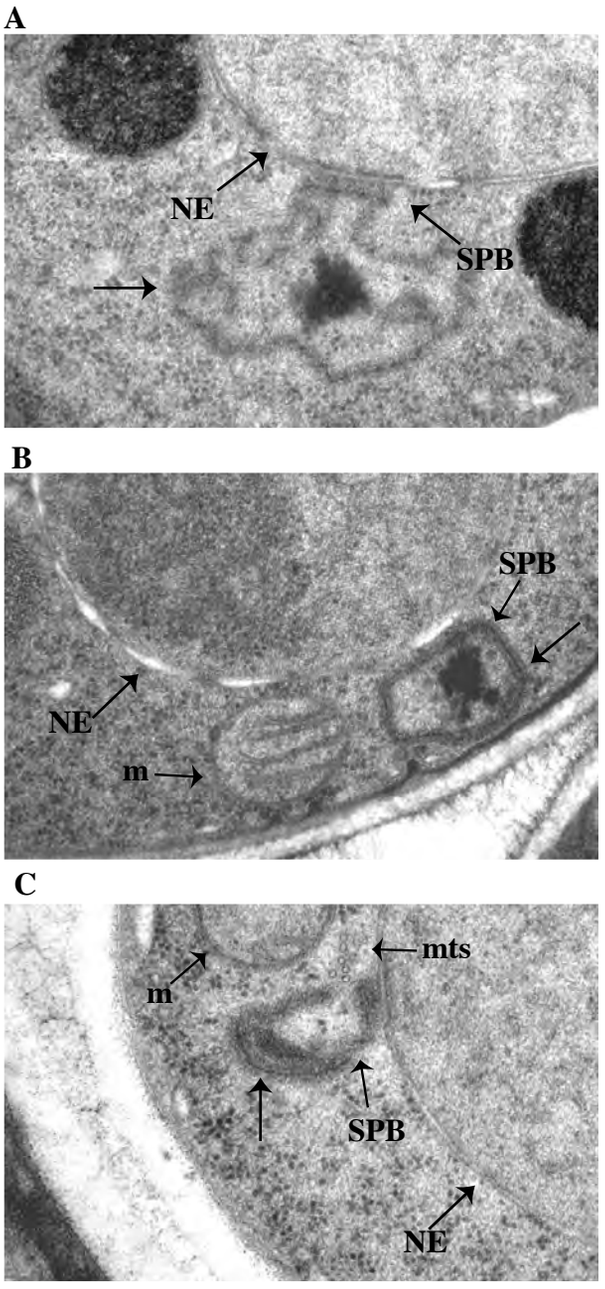

Figure 13. Representative electron micrographs of SPBs in cells overproducing Ppc89. Strain KGY5331 was grown as in Figure 12B. Note elaborate cytoplasmic SPB projections (unlabeled arrows). NE, nuclear envelope; m, mitochondria; mts, microtubules. (EM performed by Tom Giddings and Erin White, University of Colorado Electron Microscopy Service)

13A-C). Therefore, these enlarged SPBs are unlikely to be duplicated.

Discussion

The SPB in yeast functions not only to nucleate and organize MTs but also as a signaling center for coordinating cell-cycle events. Although several *S. pombe* SPB components have been identified, we do not know in detail how they interact with one another to form a functional SPB that organizes signaling modules. One such gap in knowledge is how the SIN signaling complex is tethered to the SPB. It is known that the scaffolding protein Sid4 is the most upstream component of the SIN and a stable SPB component, but it is not known how this protein is integrated into the SPB. In this study, we have identified and characterized a novel component of the *S. pombe* SPB, Ppc89, which has no homologues in any other species. Ppc89 binds directly to Sid4 and appears be the link between the SIN and the SPB. It is also important more globally for the organization of the SPB.

Ppc89 and the SIN

Ppc89 was identified in a TAP analysis of Cdc11, indicating that it associated with one or more SIN components. Through two-hybrid analyses and *in vitro* binding experiments, Ppc89 was determined to bind Sid4 directly, an association mediated by their respective C-terminal regions and one that can be observed by FRET *in vivo*. These data indicate that Ppc89 and Sid4 interact on the outer surface of the SPB, where Sid4 (unpublished observation) and Sid2 (Sparks *et al.*, 1999) have been shown to localize by immuno-EM.

In contrast to all known SIN components and regulators (reviewed by (Balasubramanian *et al.*, 2004; Krapp *et al.*, 2004b; Wolfe and Gould, 2005), Ppc89-GFP remains SPB-associated in *sid4-SA1* cells, suggesting that Ppc89 links the SIN to the SPB through its association with Sid4. Indeed, immunolocalization of Ppc89-GFP by EM indicated that it localizes more centrally within the SPB than SIN components. Further evidence in support of this relative arrangement of proteins is the finding that the Sid4 N-terminal region fused to the Ppc89 coiled-coil domains is fully functional for SIN signaling. This observation not only suggests a SIN tethering role for Ppc89 but indicates that the N-terminal 300 amino acids of Sid4 is solely responsible for its essential function in the SIN. This conclusion is consistent with the evidence that Sid4 residues 1-300 contain the docking sites for the checkpoint protein Dma1p (Guertin *et al.*, 2002), the mitotic kinase Plo1 (Morrell *et al.*, 2004), and also Cdc11, which in turn links to all other SIN components and Cdk1-cyclin B (Krapp *et al.*, 2004a; Morrell *et al.*, 2004). These data also indicate that the central and C-terminal coiled-coil domains of Sid4 serve solely as a SPB targeting module. Other evidence that Ppc89 tethers Sid4 to the SPB is that both Sid4 and Cdc11 were lost from SPBs in the absence of Ppc89 and that some cells with multiple nuclei and no septa, indicative of SIN defects, were observed in Ppc89-depleted cells.

Ppc89 and SPB Functions

Clearly, however, the major defect of cells lacking Ppc89 is not SIN mis-regulation. Depletion and overexpression experiments showed that Ppc89 is necessary for assembling and/or maintaining a variety of proteins at the SPB that perform different

functions. For example, a number of MT defects are caused by Ppc89 overproduction or depletion. This is probably due, at least in part, to changes in the amount of SPB-localized γ-TuC, as measured in this study by the localization of Alp6, a core γ-TuC element. The γ-TuC localizes to the outer and inner faces of the *S. pombe* SPB, as well as to non-SPB interphase microtubule-organizing centers (iMTOCs), and is responsible for nucleating and anchoring MTs (Hagan and Petersen, 2000). The MT defects we observed in Ppc89-depletion and overproduction studies are consistent with defects in SPB MTOC functions. In Ppc89-overproducing cells, a greater number of MTs emanated from the enlarged SPBs, as would be expected if the γ-TuC had been preferentially recruited to SPBs rather than iMTOCs. Reciprocally, most cells depleted of Ppc89 contained a seemingly normal interphase array of MTs that could be generated from non-SPB MTOCs. However, because these non-SPB MTOCs do not contribute to spindle assembly, it is not surprising that bipolar-spindle formation and proper chromosome segregation were disrupted in Ppc89-depleted cells.

Ppc89 and SPB Structure

The aberrant phenotypes arising from overproduction or depletion of Ppc89 differ from those of any previously identified *S. pombe* SPB component. Furthermore, it is different from any morphology seen in any other MTOC of other organisms when components are overproduced. For example, Pcp1 overproduction induces formation of multiple foci throughout the cytoplasm and nucleus but not enlarged SPBs (Flory *et al.*, 2002). Loss of other central SPB components with essential roles during vegetative growth, such as centrin/Cdc31, leads to formation of monopolar spindles in a high

percentage of cells (Paoletti *et al.*, 2003). Because the SPBs can still nucleate MTs in these mutants, it appears that the SPBs remain largely intact in the absence of these proteins. In contrast, our evidence indicates that Ppc89 integrates the assembly of a large number of SPB proteins, including Pcp1, into a well-organized structure. When excess Pcp89 is supplied, at least some portion of the SPB expands. It is interesting that the Ppc89-induced SPB structures extend primarily away from the NE, suggesting that some SPB-NE-tethering factors become limiting. Sad1 appears not to be such a factor, because it appears to be enriched in the non-tethered structures. Reciprocally, when Ppc89 is depleted, the SPB apparently disassembles, because we have yet to identify a single SPB marker that remains concentrated as a spot in such cells (this study and unpublished observation). However, until EM studies are performed, the exact defect in SPB structure in the absence of Ppc89 cannot be known. Given that promoter shut-off experiments lead to heterogeneity in the extent of Ppc89 depletion at any given time point, it will be advantageous to perform EM studies on a tight conditional mutant. Such a temperature-sensitive strain is currently being constructed for these purposes.

The extension of the SPB induced by Ppc89 overproduction bears some similarity to superplaque structures formed by overproduction of *S. cerevisiae* Spc42. These superplaques are formed when the central plaque of the SPB enlarges laterally and bulges out of the NE (Donaldson and Kilmartin, 1996; Jaspersen *et al.*, 2004). This enlargement, and the central role played by Spc42 in SPB organization (Muller *et al.*, 2005a), have led us to consider the possibility that *S. pombe* Ppc89 is a functional analog of *S. cerevisiae* Spc42. It should be noted that neither of these proteins has an evident homologue in the other yeast, although both contain extensive regions of predicted

coiled-coil. Even if Ppc89 and Spc42 are not strictly functional equivalents, it is likely that Ppc89 function or protein level is regulated to control the extent of SPB growth during the cell cycle. This might occur similarly to the regulation of SPB duplication through Cdc28-mediated phosphorylation of Spc42 (Donaldson and Kilmartin, 1996; Jaspersen *et al.*, 2004). Because Sid4 and Cdc11 bind the mitotic kinases Plo1 and Cdc2-Cdc13, respectively (Morrell *et al.*, 2004), Ppc89 would be proximal to these regulators and a potential target.

The overproduction data discussed above leads me to theorize that Ppc89 is the structural core of the *S. pombe* SPB, much like Spc42 is the core of the *S. cerevisiae* SPB. Because components of the core of the *S. pombe* SPB have not been identified before our studies, no data is similar to ours. Our immuno-EM data supports my idea that Ppc89 is at the central region of the SPB, I would even predict that Ppc89 forms the electron dense line seen in EM images. It is an interesting idea that Ppc89 could form a higher ordered lattice through interactions with itself that, in turn, forms the structural core of the SPB like Spc42. If Ppc89 is indeed the core of the SPB that would explain why when Ppc89 is overproduced there are more SPB proteins localized to the SPB without affecting the translation of SPB proteins (unpublished observations). In this model increasing the amount of Ppc89 would increase the size of the SPB and allow more proteins to be incorporated into the organelle. My model further suggests that increasing or decreasing the amount of Ppc89 will affect all SPB components since it comprises the core of the SPB. My data in this chapter supports this idea.

The defects associated with Ppc89 depletion and overproduction suggest that, in addition to Sid4, it interacts with at least one other protein to organize SPBs. Preliminary

mass spectrometric analysis on a Ppc89-TAP preparation indicates that several coil-coil proteins including Pcp1 (Flory *et al.*, 2002), Kms2 (Miki *et al.*, 2004), and Cut12 (Bridge *et al.*, 1998) co-purify (unpublished observation). These are strong candidates for additional direct binding partners and studies are underway to test this possibility.

While our data suggest that Ppc89 anchors the SIN to the SPB, it is not yet clear how Ppc89 is organized within the SPB. Specifically, we do not know if the N-terminal region of Ppc89 is buried within the SPB, facing into the cytoplasm to bind additional proteins, or both. The self-interacting central coiled-coil domain could allow dimerization in a head-to-head or head-to-tail configuration, and it could also allow oligomerization. Determining the configuration of Ppc89 at the SPB will help us understand how it organizes *S. pombe* SPB components into functional units.

CHAPTER IV

MTO2 PHOSPHOREGULATION BY CDK1

Introduction

Microtubule structure and function

MTs are highly dynamic filaments that play essential roles in mitosis, cytokinesis, vesicular transport, nuclear positioning, and cellular polarity. They are highly conserved hollow cylindrical polymers made up of α and β tubulin dimers. The orientation of α and β dimers in a MT are such that the α tubulin of one dimer contacts the β tubulin of the one before it (Figure 14). Laterally, the α tubulin and β tubulin monomers interact with one another and wrap around in a helical formation forming the cylinder of the MT. There is a seam that runs parallel along the longitudinal axis of the MT as the dimers create one turn (Figure 14). At this seam, α and β tubulin monomers interact with one another laterally. This organization of tubulin dimers results in MTs having a polarized configuration with α tubulin at the minus end and β tubulin at the plus end (reviewed in (Valiron *et al.*, 2001)).

Furthermore, tubulins are GTPases in which each tubulin monomer binds GTP. α tubulin has a GTP molecule that is held between the α and β subunits making it non-hydrolyzable. The GTP on the β subunit, however, is exposed, allowing it to be hydrolyzed to GDP and exchanged for GTP. As the tubulin dimers assemble into a MT lattice, GTP is hydrolyzed to GDP increasing the tubulin dimers' dissociation constant. Since the dissociation constant of GDP-bound tubulin is greater than GTP-bound tubulin,

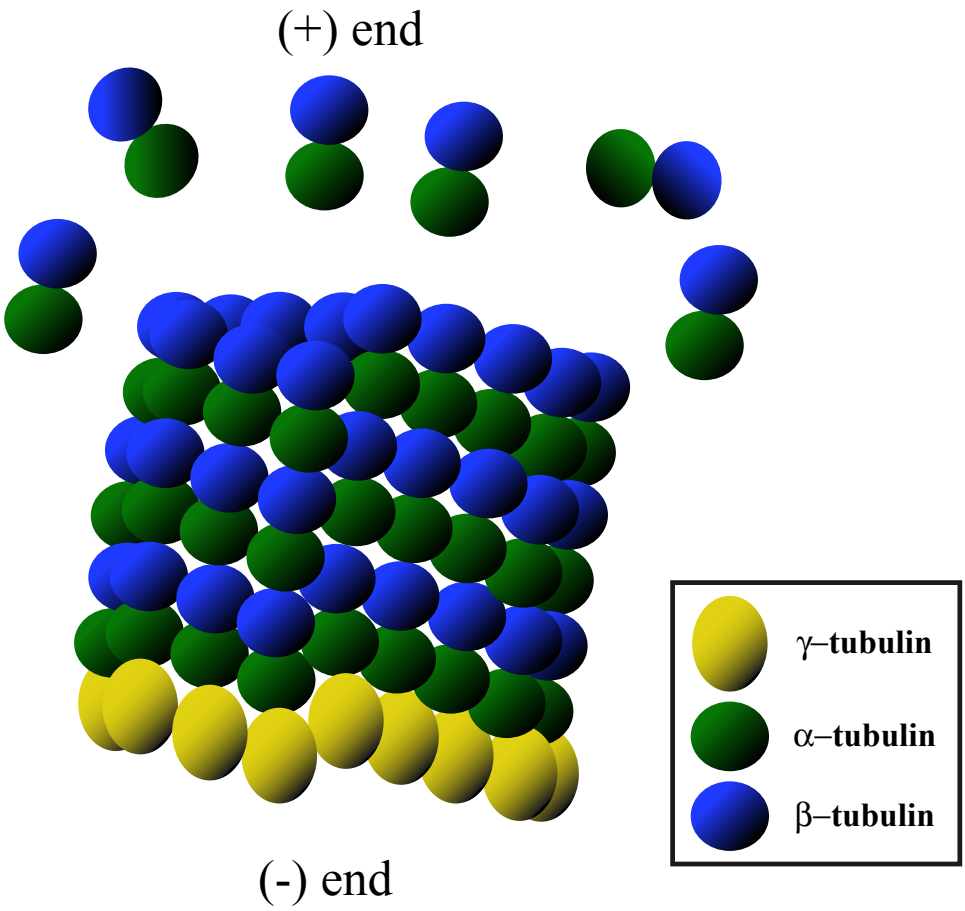

Figure 14. Microtubule structure. Microtubules are hollow filaments made up of tubulin dimers consisting of an α and β subunit (shown at the top of the figure.) These dimers assemble so that α-tubulin from one dimer contacts β-tubulin from another. This creates a polarity for the microtubule where α-tubulin is at the minus end and β-tubulin is at the plus end. α and β subunits interact with themselves laterally and form an asymmetrical helix resulting in a seam where α-tubulin meets β-tubulin. The concentration of α and β tubulin is too low for nucleation *in vitro* and therefore requires γ-tubulin (yellow) to nucleate microtubules.

MTs with GDP-bound dimers shrink and MTs with GTP bound dimers grow. As new dimers are added to the tips of MTs they are GTP bound and form a stable GTP cap at the plus end. The older dimers are GDP bound and therefore less stable and dissociate faster than the newer GTP bound dimers. This causes MTs to shrink from their minus ends and grow from their plus ends.

The concentration of free tubulin in solution determines the rate of MT elongation (Valiron *et al.*, 2001). For this reason MTs undergo dynamic instability where they can suddenly convert from growing to shrinking and back again. When the rates of tubulin assembly are equal to the rates of disassembly the MT undergoes treadmilling, a process in which length stays constant in spite of continuous exchange at either end.

In vitro, the concentration of α and β tubulin is below the required amount for spontaneous nucleation (Moritz and Agard, 2001). Therefore, cells require the activity of γ-tubulin localized to MTOCs in order to nucleate MTs. Exactly how γ-tubulin works to nucleate MTs is not understood but there are two models in the literature: the template model (Zheng *et al.*, 1995) and the protofilament model (Erickson and Stoffler, 1996). The template model suggests that 13 γ-tubulin subunits interact with one another laterally in order to form a ring that serves as a platform for MT nucleation at the MT minus end. The protofilament model suggests that γ-tubulin interacts with itself longitudinally and each γ-tubulin monomer interacts with either an α or β tubulin subunit laterally in the MT seam. This creates a small stable protofilament that serves as a nucleator for the rest of the MT.

γ-tubulin complexes

γ-tubulin serves to nucleate MTs with the activity of γ-tubulin associated proteins localized to MTOCs. γ-tubulin and its associated proteins are known as the γ-tubulin complex (γ-TuC) in yeast. In higher eukaryotes the complex is called the γ-tubulin ring complex (γ-TuRC) because of the ring structure observed throught EM analyses (Luders and Stearns, 2007). Both the γ-TuC and γ-TuRC are homologous to one another, both containing γ-tubulin and two accessory proteins. These accessory proteins are Spc97, Spc98 in *S. cerevisiae* Alp4, Alp6 in *S. pombe* and GCP2, GCP3 in higher eukaryotes respectively. The composition of the yeast γ-TuC appears to be the same as the γ-tubulin small complex (γ-TuSC) that is composed of two units of γ-tubulin and one copy of Spc97 and Spc98. Through biochemical purifications different groups showeed that γ-TuRC is assembled from multiple preformed γ-TuSCs (Murphy *et al.*, 1998; Oegema *et al.*, 1999; Gunawardane *et al.*, 2000). The higher eukaryotic γ-TuRC is composed of many copies of the γ-TuSC plus (additional proteins) GCP4, GCP5, and GCP6 and is more active for MT nucleation than the γ-TuSC alone (Fava *et al.*, 1999; Oegema *et al.*, 1999; Murphy *et al.*, 2001). In *S. pombe* there are homologues of GCP4, GCP5 and GCP6 that are complexed together with γ-tubulin. Therefore, it appears that the *S. pombe* γ-TuC is the same as the higher eukaryotic γ-TuRC (Fujita *et al.*, 2002; Venkatram *et al.*, 2004; Anders *et al.*, 2006). This makes *S. pombe* an excellent model system in which to study γ-tubulin complex function and further increases the relavence of S. pombe γ-tubulin studies.

In *S. pombe*, MTs are nucleated from multiple sites in the cell much like in higher eukaryotes (Figure 15). MTs are localized to the major MTOC, the SPB, as well as to secondary MTOCs, interphase MT organizing centers (iMTOCs) and equatorial MT

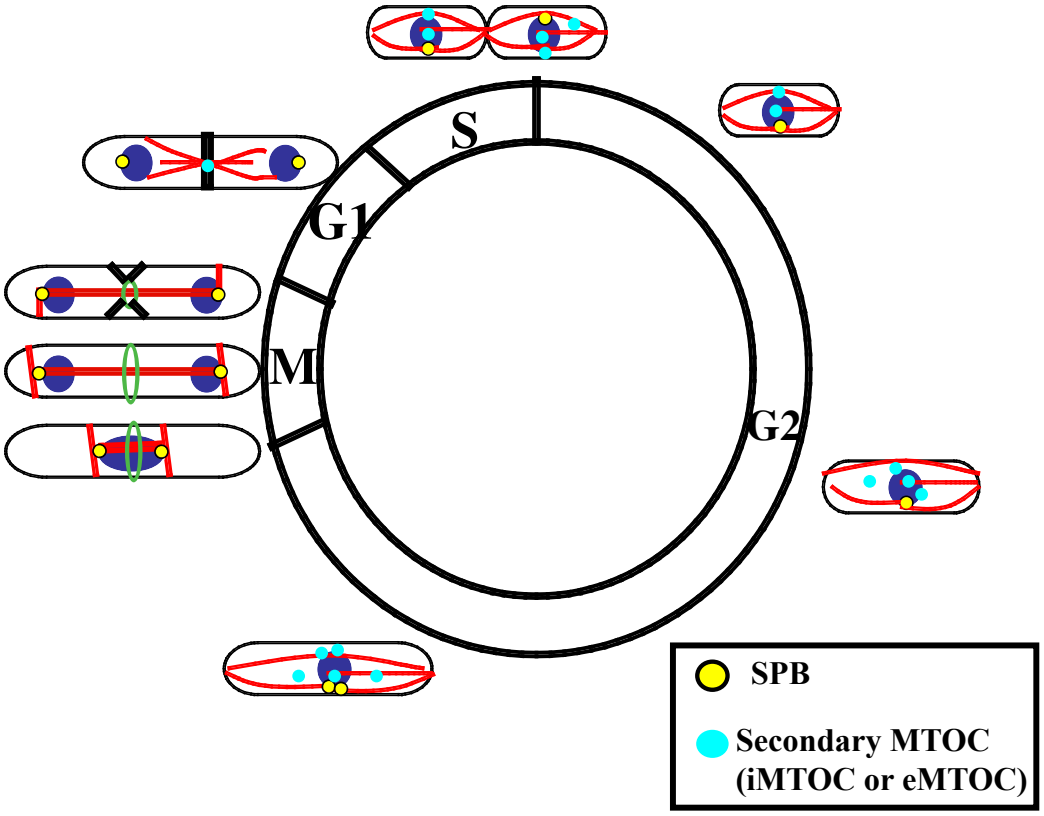

Figure 15. Microtubule organization in *S. pombe*. Schematic of microtubules (red lines) in relation to the nucleus (blue circle), SPBs (yellow circles) iMTOCs and eMTOCs (light blue circles) throughout the cell cycle. Microtubule minus ends are associated with MTOCs and plus ends are towards the cell tips. In interphase, microtubules are associated with the SPB, nuclear envelope, along microtubules and in the cytoplasm. In mitosis, the only site of microtubule organization is from the SPBs where the spindle is formed. In anaphase astral microtubules are nucleated from the SPBs, perpendicular to the spindle. At the end of mitosis, eMTOCs form at the side of division forming the post anaphase array of microtubules.

organizing centers (eMTOCs). As their name implies, iMTOCs are found during interphase and localize to the nuclear envelope, along MTs themselves and within the cytoplasm (Sawin *et al.*, 2004a; Venkatram *et al.*, 2004; Janson *et al.*, 2005; Samejima *et al.*, 2005; Venkatram *et al.*, 2005; Zimmerman and Chang, 2005; Carazo-Salas and Nurse, 2006). At this stage in the cell cycle, MTs appear in 3-5 longitudinal MT bundles with the MT minus ends at MTOCs and the plus ends facing toward the cell tips. As cells enter mitosis the only site of MT nucleation is the SPB where the mitotic spindle is formed from the nuclear face of the SPBs. As cells further progress through mitosis, astral MTs are nucleated from the cytoplasmic side of the SPBs, perpendicular to the spindle. It is thought that astral MTs help orient the spindle longitudinally so the daughter cells each receive half of the duplicated DNA. As mitosis is complete and the actomyosin ring forms, the eMTOC forms at the site of division. The eMTOC nucleates the post anaphase array (PAA) of MTs, a transient MT array thought to keep the duplicated nuclei away from the site of division. This structure has not been well studied in fission yeast but there is some speculation that the eMTOC could be the *S. pombe* equivalent of the higher eukaryotic spindle midbody. It might also serve to anchor the actomyosin ring to the site of division (Hagan and Petersen, 2000; Pardo and Nurse, 2003).

There are two novel interacting proteins responsible for MT nucleation from secondary MTOCs in fission yeast: Mto1 and Mto2 (Sawin *et al.*, 2004a; Venkatram *et al.*, 2004; Janson *et al.*, 2005; Samejima *et al.*, 2005; Venkatram *et al.*, 2005; Zimmerman and Chang, 2005; Carazo-Salas and Nurse, 2006). Neither of these proteins are essential for viability or mitotic spindle formation but they are needed for non-SPB, cytoplasmic,

MT nucleation. *mto1Δ* cells lose γ-TuC localization to iMTOCs and eMTOCs and no longer nucleate astral MTs in anaphase or the PAA after mitosis. Furthermore, in cells lacking Mto2, the phenotype is the same as in *mto1Δ* cells except that they still nucleate astral MTs. Since *mto1Δ* and *mto2Δ* cells have defects in nucleating cytoplasmic MTs, they display defects in cellular polarity, nuclear positioning and therefore cleavage plane specification. Mto1 and Mto2 interact directly with the γ-TuC, which would explain the MT defects seen in *mto1Δ* and *mto2Δ* cells, yet the defects seen in *mto1Δ* cells are more severe than in *mto2Δ*. However, in *mto2Δ* cells, Mto1 cannot Co-IP with γ-TuC. These data suggest that Mto1 and Mto2 work together to recruit γ-TuC to iMTOCs and eMTOCs with Mto1 as the primary recruiting factor for γ-TuC and Mto2 as a regulator for the interaction of Mto1 with the γ-TuC.

Non-centrosomal MTOCs are not just a phenomenon in *S. pombe*. They are also seen in mammalian cells where MTs are nucleated around the nuclear envelope and in the cytoplasm. In higher eukaryotic cells, such as myotubes, MTs are nucleated from around the nuclear envelope (Tassin *et al.*, 1985). A similar pattern to the cytoplasmic nucleation observed in *S. pombe* is observed in mammalian cells where the *trans*-Golgi network functions as a non-centrosomal MTOC. The MTs localized to the trans-Golgi network set up an asymmetric array of MTs extending towards the leading edge of polarized cells (Chabin-Brion *et al.*, 2001; Efimov *et al.*, 2007). It is thought that these MT arrays transport vesicles and their cargo to the leading edge of the cell. This, in turn, could cause protrusions in the cell membrane at its leading edge. Therefore, these MT arrays could drive the movement of cells at its leading edge.

MTOCs in *S. pombe* play an essential role in anchoring and nucleating MTs

throughout the cell cycle as well as serving as signaling centers. In mitosis, the major MTOC, known as the SPB, is needed for the formation of a bipolar spindle to properly segregate sister chromosomes. In interphase, cytoplasmic MTs are anchored to the SPB as well as to secondary MTOCs (called iMTOCs), which are found on the nuclear periphery, in the cytoplasm and along MTs. Furthermore, after anaphase is complete MTs are nucleated and anchored to another secondary MTOC called the eMTOC, which localizes to the site of division. In order for these MTOCs to anchor and nucleate MTs they need to localize the γ-TuC that performs the essential function of nucleating MTs. The composition of the γ-TuC is beginning to be elucidated in *S. pombe* and higher eukaryotes even though the exact mode of activating and localizing the γ-TuC to MTOCs is not known. It is my belief that in *S. pombe* Mto1 and Mto2 function together to activate the γ-TuC and localize it to MTOCs during interphase.

The second part of by dissertation, and this chapter, focuses on identifying a novel method for regulation of the γ-TuC. During our previous studies of Mto2 (Venkatram *et al.*, 2005) we noted that epitope tagged versions of this protein migrated as several species on SDS-PAGE analysis, a behavior typical of phosphoproteins. Therefore, I hypothesize that Mto2 phosphorylation plays a role in its ability to activate the γ-TuC iMTOCs and eMTOCs. To test this idea, we first examined Mto2 throughout the cell cycle and find that Mto2 is hyperphosphorylated during mitosis by Cdk1. Mutation of these sites to nonphosphorylatable alanine residues eliminates the mitotic phosphorylation but does not alter function.

Results

Mto2 is a phosphoprotein

In order to determine if Mto2 function might be regulated by phosphorylation, we examined whether the multiple forms of Mto2 were in fact due to phosphorylation and whether they varied during the cell cycle. The mobilities of Mto2 from cells blocked at either at the G2/M boundary with a temperature sensitive allele of *cdc25* or in prometaphase using the β-tubulin temperature sensitive mutant, *nda3-KM311* could be collapsed by treatment with λ-phosphatase confirming that Mto2 is a phosphoprotein (Figure 16A). Mto2 phosphorylation appeared to change significantly between G2 and prometaphase (Figure 16A). This suggests that Mto2 might be phosphorylated in a cell cycle dependent manner. To test this, we performed a block and release experiment using Mto2-myc$_{13}$ cells blocked at the G2/M boundary. We observed that Mto2 became hyper-phosphorylated in mitosis and this phosphorylation declined as cells exit mitosis (Figure 16B). Therefore, it appears that Mto2 is phosphorylated in a cell cycle dependent manner.

Cdk1 is responsible for mitotic Mto2 phosphorylation

Cdk1 activity drives cells into mitosis and its activity remains high until anaphase onset (reviewed in (Berry and Gould, 1996)) Since the peak of Mto2 phosphorylation corresponds temporally with the peak of Cdk1 activity (Booher and Beach, 1986; Simanis and Nurse, 1986; Moreno *et al.*, 1989), we tested whether Mto2 might be a Cdk1 substrate *in vitro*. Cdk1 phosphorylated GST-Mto2 but did not phosphorylate GST and catalytically inactive Cdk1 did not phosphorylate GST-Mto2 (Figure 17A). Phosphoamino acid (PAA) analysis of Cdk1-phosphorylated Mto2 revealed that

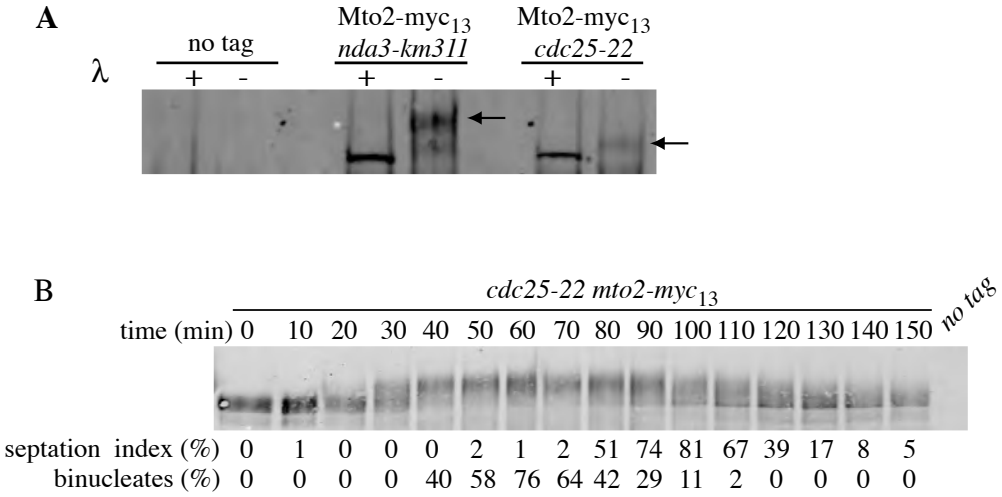

Figure 16. Mto2 is hyper-phosphorylated in mitosis. (A) Anti-Myc IPs from an untagged strain (KGY246), Mto2-myc13 cdc25-22 (KGY5067) cells or Mto2-myc13 nda3-km311 (KGY4897) cells and then immunoblotted in the presence or absence (+/-) of lambda phosphatase (λ). Arrows indicate the position of Mto2-myc13 bands. (B) cdc25-22 mto2-myc13 cells (KGY5067) were synchronized at the G2/M boundary by shifting to 36° C for 4 hours. They were then released to the permissive temperature at 25° C and samples were taken at the indicated time points. Mto2 levels were determined by immunoblot analysis and the percentage of binucleated and septated cells were determined by light microscopy.

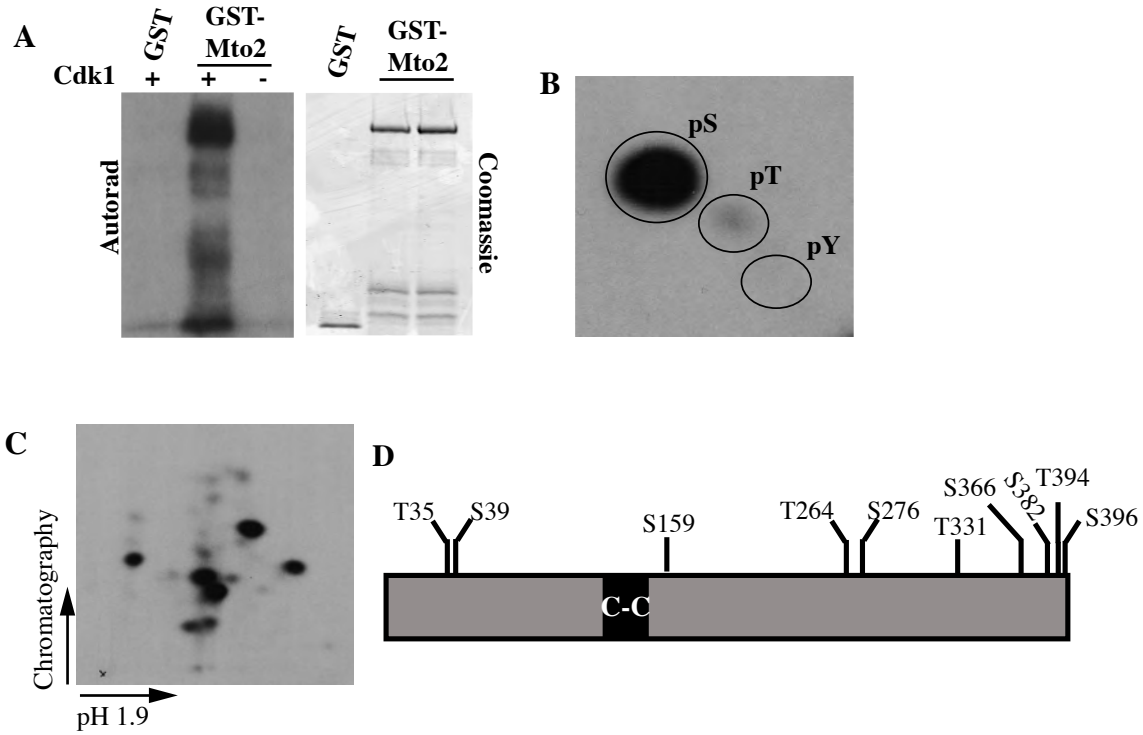

Figure 17. Cdk1 phosphorylates Mto2 in vitro. (A) Recombinant GST and GST-Mto2 were incubated in vitro with kinase active or kinase dead (KD) Cdk1 and then resolved by SDS-PAGE. Labeled proteins were detected by autoradiography (left panel) and the input was visualized by coomassie staining (right panel). (B) ^{32}P-labeled Mto2 from (A) was subjected to partial acid hydrolysis, and the resultant phosphoamino acids were separated by two-dimensional thin-layer electrophoresis and detected by autoradiography. Circles indicate position of phosphoserine (pS), phosphothreonine (pT) or phosphotyrosine (pY). (C) ^{32}P-labeled GST-Mto2 from (A) was also digested with trypsin. 500 cpm of tryptic peptides were spotted and resolved in two dimensions on cellulose thin-layer plates by electrophoresis at pH1.9 with the anode on the left followed by ascending chromatography. (D) Schematic of Mto2 showing phosphorylation sites identified by mass spectrometric analysis of Mto2 phosphorylated by Cdk1 in vitro.

phosphorylation occurred primarily on serine residues and to a lesser extent on threonine residues (Figure 17B). Mto2 contains 16 minimum Cdk1 consensus phosphorylation sites (Ser/Thr-Pro), 4 threonines and 12 serines. To determine which of these residues Cdk1 phosphorylates *in vitro*, a combination of mass spectrometric analysis and tryptic peptide mapping was used to reveal that Mto2 is phosphorylated on six serine and four threonine residues (Figure 17C and 17D). These ten sites were mutated to nonphosphorylatable alanine residues (Mto2-10A). GST-Mto2-10A could not be phosphorylated significantly by Cdk1 *in vitro* suggesting that we had correctly identified the major Cdk1 sites within Mto2 (Figure 18A). To verify that these 10 sites removed the mitotic phosphorylation seen *in vivo*, we generated a strain in which the 10 sites on Mto2 were replaced with alanine (*mto2-10A*) at the *mto2*$^{+}$ genomic locus. The locus was then tagged with Myc_{13} to allow detection of the mutant protein. Mto2-10A-myc_{13} migrated as a smaller band as compared to Mto2-myc_{13} when both strains were blocked in prometaphase with *nda3-KM311* (Figure 18B). Furthermore, Mto2-10A-Myc_{13} *nda3-KM311* appeared to have the same mobility as Mto2-myc_{13} arrested at G2/M with *cdc25-22*. This indicates that Mto2-10A abolishes the mitotic phosphorylation seen with wild-type Mto2 and it appears to have the same basal phosphorylation as wild-type Mto2 in interphase. The *mto2-10A* strain does not display any morphological defects such as loss of polarity seen in the *mto2Δ* strain, indicating that there were no MT defects.

To examine whether Mto2-10A's phosphorylation changed throughout the cell cycle or stayed constant, we performed a block and release experiment using Mto2-10A-myc_{13} cells blocked at the G2/M boundary. We observed that Mto2-10A migrated with a higher mobility in mitosis and this subsequently declined in late mitosis (Figure 19A).

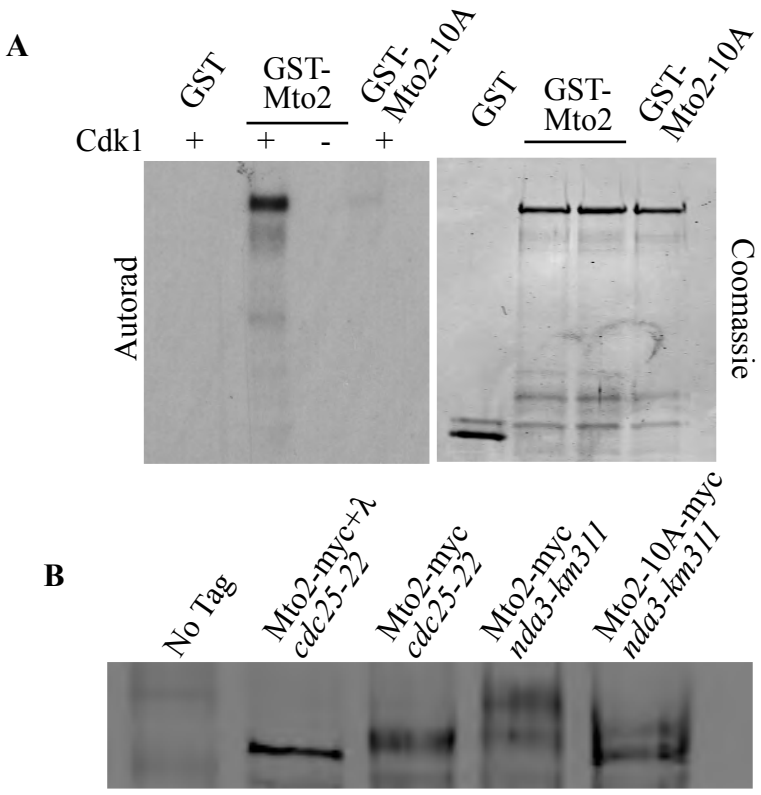

Figure 18. Mto2 10A is not phosphorylated by Cdk1 *in vitro* or *in vivo*. (A) Recombinant GST, GST- Mto2 or GST-Mto2 10A were labeled in vitro by either kinase active Cdk1 (+) or kinase dead Cdk1 (-), resolved by SDS-PAGE and detected by autoradiography (left panel) and coomassie staining (right panel). (B) Anti-Myc IPs from an untagged strain, Mto2-myc13 cdc25-22 in the presence of lambda phosphatase (λ), Mto2-myc13 cdc25-22 cells, Mto2-myc13 nda3-km311 cells or Mto2-10A-myc13 nda3-km311 and then immunoblotted.

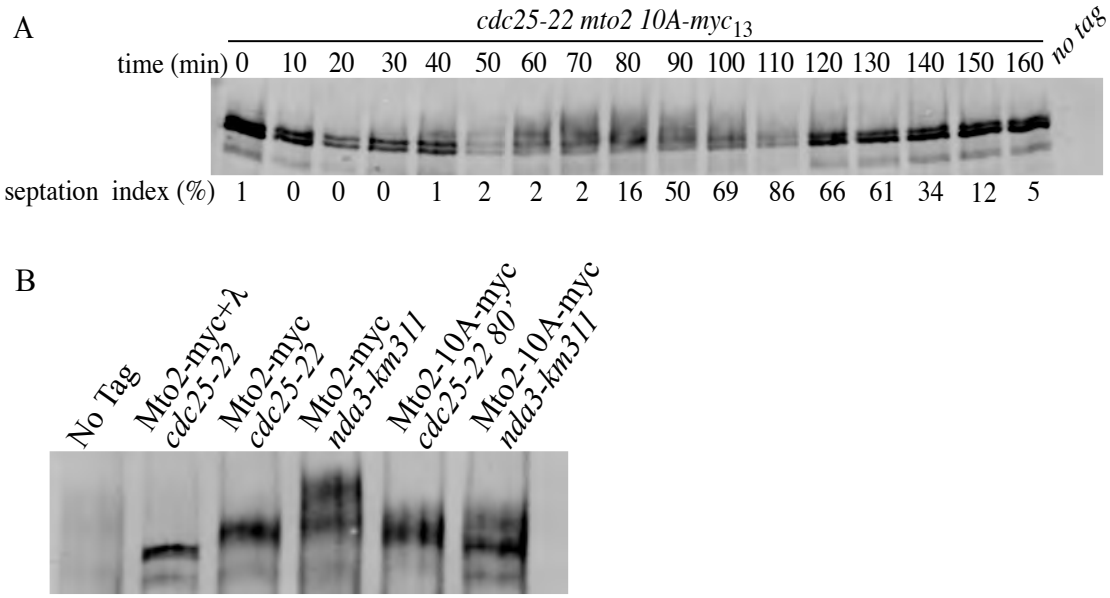

Figure 19. Mto2-10A displays an increased mobility in mitosis (A) cdc25-22 mto2-10A-myc13 cells were synchronized at the G2/M boundary by shifting to 36° C for 4 hours. They were then released to the permissive temperature at 25° C and samples were taken at the indicated time points. Mto2 levels were determined by immunoblot analysis and the percentage septated cells was determined by light microscopy. (B) Anti-Myc IPs from an untagged strain, Mto2-myc13 cdc25-22 in the presence of lambda phosphatase (λ), Mto2-myc13 cdc25-22 cells, Mto2-myc13 nda3-km311 cells, Mto2-10A-myc13 nda3-km311 from the 80 minute time point in (A) or Mto2-10A-myc13 nda3-km311 and then immunoblotted.

However, when comparing the highest mobility of Mto2-10A-myc$_{13}$ in mitosis (time point 80 minutes) with Mto2-myc$_{13}$ arrested at prometaphase or at the G2/M boundary, Mto2-10A-myc$_{13}$ 80' had close to the same mobility as wild-type Mto2 arrested at the G2/M boundary (Figure 19B). These results indicate that even though there is some phosphorylation of Mto2-10A in mitosis it is at the same basal level seen with wild type cells in interphase.

Discussion

Cytoplasmic MTOCs need Mto2 to recruit the γ-TuC in interphase. In order to determine if this function is cell cycle regulated, we examined the mobility of Mto2 by SDS-PAGE at different points in the cell cycle. We found that Mto2 is post-translationally modified and confirmed that Mto2 is hyperphosphorylated during mitosis. The peak of phosphorylation corresponded to when Cdk1 was maximally active. Therefore, we tested and confirmed that Mto2 is a Cdk1 target *in vitro*. Further mass spectrometric analysis identified ten residues, 6 serines and 4 threonines phosphorylated by Cdk1. Mutating these residues to nonphosphorylatable alanine residues abolished the hyperphosphorylation in mitosis but did not alter Mto2's function.

Regulation of *S. pombe* γ-TuC

During the cell cycle of fission yeast, dynamic changes take place with the MT cytoskeleton much like that of higher eukaryotes. Understanding the regulation of these changes in *S. pombe* can serve as a model for understanding the dynamics in more complex organisms. In yeast and higher eukaryotes the γ-TuC and γ-TuRC, respectively,

are required for nucleating and organizing both cytoplasmic and nuclear MTs at MTOCs. In *S. pombe* Mto1 and Mto2 are required for the cytoplasmic localization of the γ-TuC to these MTOCs with Mto1 being the major protein and Mto2 binding to it and the γ-TuC (Sawin *et al.*, 2004a; Venkatram *et al.*, 2004; Janson *et al.*, 2005; Samejima *et al.*, 2005; Venkatram *et al.*, 2005; Zimmerman and Chang, 2005; Carazo-Salas and Nurse, 2006). Here, I investigated the role of phosphorylation on Mto2 as a potential means of regulating the localization of the γ-TuC to cytoplasmic MTOCs. While Mto2 does not have any homologues in other organisms this is the first study to examine the possible link between cell cycle regulation and loss of cytoplasmic MTs during mitosis.

In order to determine if Mto2 is regulated in a cell cycle dependent manner, we examined the mobility by SDS-PAGE through the cell cycle and verified that Mto2 is hyperphosphorylated during mitosis. Since the peak of phosphorylation coincides with the peak of Cdk1 activity, we examined if Mto2 is a Cdk1 substrate *in vitro*. Indeed, Mto2 is phosphorylated by Cdk1, which contributes to its hyperphosphorylation in mitosis. The question remains, what is the role of mitotic phosphorylation of Mto2? Since the timing of phosphorylation correlates to the absence of cytoplasmic MTOCs, I hypothesize that this phosphorylation is a negative regulatory event that inhibits Mto2's ability to activate the γ-TuC and localize it to iMTOCs or eMTOCs during mitosis. My model is that once Mto2 is dephosphorylated at the end of mitosis, it would then be able to activate and localize the γ-TuC to the eMTOC, which nucleates the PAA. As Mto2 is in a dephosphorylated form throughout interphase, it can activate the γ-TuC to iMTOCs as well. In order to test my hypothesis a Mto2-10A mutant was constructed to mimic Mto2 in a dephosphorylated state. This 10A mutant was not hyperphosphorylated in

mitosis like wild type Mto2. However, cells with an integrated copy of Mto2-10A did not display any MT or polarity defects. This is not surprising since Mto2-10A is not able to be inhibited by phosphorylation and therefore remains in its active form throughout the cell cycle. I conclude that this mutant is still able to activate and recruit the γ-TuC to cytoplasmic MTOCs through the cell cycle.

In order further characterize the role of mitotic phosphorylation on Mto2, a phosphomimetic version of Mto2 where the ten Cdk1 sites are mutated to aspartic acid needs to be created. This allele would mimic Mto2 being constitutively phosphorylated by Cdk1. Such a strain is currently being constructed. If my theory is correct and mitotic phosphorylation truly inhibits Mto2 function, then the Mto2-10D phosphomimetic version would be inactive throughout the cell cycle and might display the same cytoplasmic MT nucleation and polarity defects as the Mto2Δ strain.

CHAPTER V

Future Directions

Ppc89

Two hybrid, *in vitro* binding and fluorescence resonance energy transfer (FRET) analyses have shown that Ppc89p and Sid4p interact directly through their C-terminal regions. Yet it is unknown what orientation Ppc89p is in relative to Sid4p, which is tethered to the SPB through its C-terminus (Figure 20). Answering this question will help distinguish between possible functions for Ppc89p. For example if it is orientated as diagrammed in Figure 20B, then Ppc89p could be acting as a scaffolding protein mediating interactions between the SIN and cell cycle regulators. In contrast if it is organized as diagrammed in Figure 20A, then it is perhaps acting as a central structural component of the SPB that is responsible for tethering many different types of signaling pathways to the SPB. Once the orientation of Ppc89 is determined, other SPB proteins could be incorporated into these studies. This will help to determine how the SPB is structurally organized. Similar studies have been done in *S. cerevisiae* to determine how components within its SPB are organized in relation to one another (Muller *et al.*, 2005b).

Another aspect worth investigating is to examine the SPB morphology through EM when Ppc89 is depleted. My hypothesis, as stated in chapter III is that when Ppc89 is depleted, the SPB falls apart. This would be the true test for my original hypothesis that Ppc89 is a key structural element of the SPB. It will be interesting to see if there is any SPB left in the absence of Ppc89. I would imagine that the γ-TuC at the nuclear face of the SPB is still present because monopolar spindles are nucleated in our Ppc89 shutoff

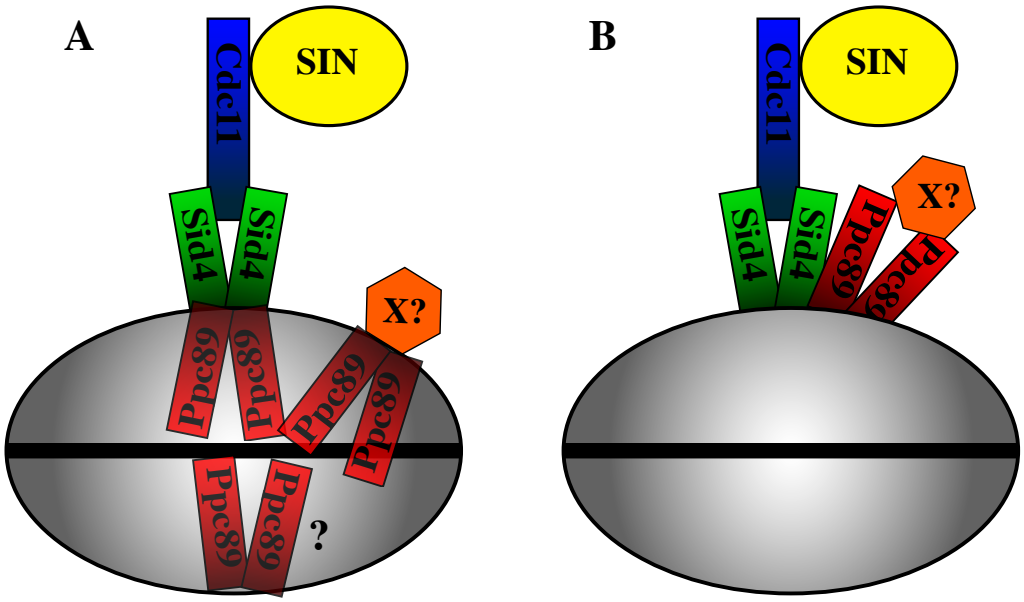

Figure 20. Two possible orientations of Ppc89p in respect to Sid4p, SPB and integral pole components. (A) In this conformation Ppc89 is acting as a structural component of the SPB. (B) In this conformation Ppc89 is a scaffolding protein that anchors signaling molecules to the SPB.

experiments. Still, a temperature sensitive version of Ppc89 is needed to address this theory since the shut-off experiments are pleiotropic. Furthermore, if a conditional mutant of Ppc89 were available then multiple outstanding questions about Ppc89 could be answered. Once such question is at what stage in the cell cycle is Ppc89 needed for SPB function? Execution point analyses using the conditional *ppc89* allele and cell cycle mutants could address this question. These studies would have to be in conjunction with EM analysis to determine the SPB morphology. Our data indicate that Ppc89 is at the core of the SPB and needed for its integrity, therefore I would expect that Ppc89 is needed for SPB integrity at all stages of the cell cycle. Another question is: what functions do the different domains of Ppc89 perform? We know from our studies in Chapter III, that the C-terminal region of Ppc89 is needed for localization to the SPB and interaction with Sid4. Also, the central coiled-coil domains are needed for self-interaction. What is the N-terminal region needed for? It has no homology to any other domains in *S. pombe* or in any other genome. Does it regulate the localization of other proteins to the SPB? Structure function analysis with different domains of Ppc89 in the presence of the conditional mutant could address these questions.

Lastly, to test our hypothesis that Ppc89 is the functional homologue of Spc42 we can determine if Spc42 can rescue a Ppc89Δ strain. Furthermore, we can overproduce Ppc89 in S. cerevisiae to determine if Ppc89 causes the formation of a superplaque in *S. cerevisiae* like Spc42. It is my belief that Ppc89 overproduction will form a superplaque but EM analysis on *S. cerevisiae* cells overproducing Ppc89 will need to be studies to address this theory.

Mto2

Our study of Mto2 has uncovered the mitotic sites of phosphorylation. These sites were then mutated to nonphosphorylatable alanines to abolish this phosphorylation. The Mto2-10A mutant was not significantly phosphorylated in mitosis and there were no defects in MT nucleation or organization. It is our hypothesis that Mto2 is phosphoregulated in a cell cycle dependent manner and this mitotic phosphorylation is inhibitory. To test this hypothesis, a phosphomimetic version of Mto2 is currently being constructed. It will be interesting to see if in this strain the γ-TuC is able to localize to cytoplasmic MTOCs in interphase. Therefore, we would expect the Mto2-10D mutant to have the same phenotype as the Mto2Δ if our hypothesis is true.

It is also possible that other kinases are acting on Mto2 to regulate its function besides Cdk1. We know that Mto2 localizes to eMTOCs at the medial region of the cell after mitosis is complete. What is the signal that localizes Mto2 to the eMTOC? One possibility might be Sid2 (*Sc* Dbf2 homologue) kinase. Our unpublished data shows that Sid2 can phosphorylate Mto2 *in vitro* but the functional significance of this remains unknown.

Along these lines, it is not known how interactions between Mto1, Mto2 and the γ-TuC change throughout the cell cycle. In mitosis, where there are no iMTOCs or eMTOCs, is Mto2 still able to bind to Mto1 and the γ-TuC or is it just not able to activate the γ-TuC at cytoplasmic MTOCs due to a regulatory event? Co-IP experiments are currently underway to define the nature of Mto2's interactions throughout the cell cycle. Interpretation of these data might be difficult do to the fact that Mto2 is always at the SPB presumably interacting with Mto1 and the γ-TuC.

CHAPTER VI

CONCLUDING REMARKS

Work over the past few years has changed the way that we view MTOCs. Once viewed solely as areas for MT nucleation and organization, MTOCs are now are being viewed as key sites for localizing signaling events required for cell cycle regulation. *S. cerevisiae* and *S. pombe* serve as excellent models as to these signaling pathways are localized to the major MTOCs. The structure and composition of SPBs and centrosomes seem distinct from each other yet we are beginning to find homologous proteins in these structures.

The first part of my work describes the discovery of a novel structural protein, Ppc89, which is needed for SPB integrity and function. It is also needed to tether the SIN signaling pathway to the *S. pombe* SPB. Previous studies have only focused on how SPB proteins affect overall SPB morphology or MT organization. This study focused on multiple SPB proteins from all different parts of the SPB. My results show that Ppc89 affects multiple SPB proteins and therefore overall SPB morphology and SPB function. It will be interesting to determine if there is a functional homologue in higher eukaryotes and its effect on centrosome size and MT organization. Further studies of how *S. pombe* SPBs are regulated through the cell cycle will yield insights into how maturation/duplication of our own centrosomes is regulated.

SPBs and centrosomes are the most well known and well characterized sites for MT organization yet there are also less well studied secondary sites of MT organization. All of these sites require γ-tubulin for MT organization but the exact composition and

mode of regulation is not well understood. In *S. pombe*, Mto1 and Mto2 are required for proper MT organization at cytoplasmic MTOCs. The second part of my work has focused on how Mto2 is phosphoregulated by Cdk1 for γ-TuC's localization and activation to cytoplasmic MTOCs. I hypothesize that this phosphorylation is an inhibitory event during mitosis that prevents Mto2 from activating the γ-TuC. Elucidating the regulation of Mto2 and how it affects the γ-TuC may serve as a model for how the γ-TuRC is regulated and activated in higher eukaryotes.

REFERENCES

Adams, I.R., and Kilmartin, J.V. (1999). Localization of core spindle pole body (SPB) components during SPB duplication in Saccharomyces cerevisiae. J Cell Biol *145*, 809-823.

Adams, I.R., and Kilmartin, J.V. (2000). Spindle pole body duplication: a model for centrosome duplication? Trends Cell Biol. *10*, 329-335.

Anders, A., Lourenco, P.C., and Sawin, K.E. (2006). Noncore components of the fission yeast gamma-tubulin complex. Mol. Biol. Cell *17*, 5075-5093.

Balasubramanian, M.K., Bi, E., and Glotzer, M. (2004). Comparative analysis of cytokinesis in budding yeast, fission yeast and animal cells. Curr. Biol. *14*, R806-818.

Bardin, A.J., and Amon, A. (2001). MEN and SIN: what's the difference? Nat. Rev. Mol. Cell Biol. *2*, 815-826.

Basi, G., Schmid, E., and Maundrell, K. (1993). TATA box mutations in the *Schizosaccharomyces pombe* nmt1 promoter affect transcription efficiency but not the transcription start point or thiamine repressibility. Gene *123*, 131-136.

Beisson, J., and Wright, M. (2003). Basal body/centriole assembly and continuity. Curr Opin Cell Biol *15*, 96-104.

Berry, L.D., and Gould, K.L. (1996). Regulation of Cdc2 activity by phosphorylation at T14/Y15. Prog Cell Cycle Res *2*, 99-105.

Bettencourt-Dias, M., and Glover, D.M. (2007). Centrosome biogenesis and function: centrosomics brings new understanding. Nat Rev Mol Cell Biol *8*, 451-463.

Boeke, J.D., LaCroute, F., and Fink, G.R. (1984). A positive selection for mutants lacking orotidine-5'-phosphate decarboxylase activity in yeast: 5-fluoro-orotic acid resistance. Mol Gen Genet *197*, 345-346.

Boleti, H., Karsenti, E., and Vernos, I. (1996). Xklp2, a novel Xenopus centrosomal kinesin-like protein required for centrosome separation during mitosis. Cell *84*, 49-59.

Booher, R., and Beach, D. (1986). Site-specific mutagenesis of cdc2+, a cell cycle control gene of the fission yeast Schizosaccharomyces pombe. Mol Cell Biol *6*, 3523-3530.

Boyle, W.J., van der Geer, P., and Hunter, T. (1991). Phosphopeptide mapping and phosphoamino acid analysis by two-dimensional separation on thin-layer cellulose plates. Methods Enzymol *201*, 110-149.

Brenner, S., Branch, A., Meredith, S., and Berns, M.W. (1977). The absence of centrioles from spindle poles of rat kangaroo (PtK2) cells undergoing meiotic-like reduction division in vitro. J Cell Biol *72*, 368-379.

Bridge, A.J., Morphew, M., Bartlett, R., and Hagan, I.M. (1998). The fission yeast SPB component Cut12 links bipolar spindle formation to mitotic control. Genes Dev. *12*, 927-942.

Bullitt, E., Rout, M.P., Kilmartin, J.V., and Akey, C.W. (1997). The yeast spindle pole body is assembled around a central crystal of Spc42p. Cell *89*, 1077-1086.

Byers, B., and Goetsch, L. (1974). Duplication of spindle plaques and integration of the yeast cell cycle. Cold Spring Harb Symp Quant Biol *38*, 123-131.

Byers, B., and Goetsch, L. (1975). Behavior of spindles and spindle plaques in the cell cycle and conjugation of *Saccharomyces cerevisiae*. J. Bacteriol. *124*, 511-523.

Bähler, J., Wu, J.-Q., Longtine, M.S., Shah, N.G., McKenzie, A., 3rd, Steever, A.B., Wach, A., Philippsen, P., and Pringle, J.R. (1998). Heterologous modules for efficient and versatile PCR-based gene targeting in *Schizosaccharomyces pombe*. Yeast *14*, 943-951.

Carazo-Salas, R.E., and Nurse, P. (2006). Self-organization of interphase microtubule arrays in fission yeast. Nat Cell Biol *8*, 1102-1107.

Castillo, A.R., Meehl, J.B., Morgan, G., Schutz-Geschwender, A., and Winey, M. (2002). The yeast protein kinase Mps1p is required for assembly of the integral spindle pole body component Spc42p. J Cell Biol *156*, 453-465.

Chabin-Brion, K., Marceiller, J., Perez, F., Settegrana, C., Drechou, A., Durand, G., and Pous, C. (2001). The Golgi complex is a microtubule-organizing organelle. Mol Biol Cell *12*, 2047-2060.

Chang, L., and Gould, K.L. (2000). Sid4p is required to localize components of the septation initiation pathway to the spindle pole body in fission yeast. Proc. Natl. Acad. Sci. USA *97*, 5249-5254.

Cowan, C.R., and Hyman, A.A. (2006). Cyclin E-Cdk2 temporally regulates centrosome assembly and establishment of polarity in Caenorhabditis elegans embryos. Nat Cell Biol *8*, 1441-1447.

Dammermann, A., Muller-Reichert, T., Pelletier, L., Habermann, B., Desai, A., and Oegema, K. (2004). Centriole assembly requires both centriolar and pericentriolar material proteins. Dev Cell *7*, 815-829.

de Saint Phalle, B., and Sullivan, W. (1998). Spindle assembly and mitosis without centrosomes in parthenogenetic Sciara embryos. J Cell Biol *141*, 1383-1391.

Delattre, M., Leidel, S., Wani, K., Baumer, K., Bamat, J., Schnabel, H., Feichtinger, R., Schnabel, R., and Gonczy, P. (2004). Centriolar SAS-5 is required for centrosome duplication in C. elegans. Nat Cell Biol *6*, 656-664.

Ding, R., West, R.R., Morphew, D.M., Oakley, B.R., and McIntosh, J.R. (1997). The spindle pole body of *Schizosaccharomyces pombe* enters and leaves the nuclear envelope as the cell cycle proceeds. Mol. Biol. Cell *8*, 1461-1479.

Donaldson, A.D., and Kilmartin, J.V. (1996). Spc42p: a phosphorylated component of the *S. cerevisiae* spindle pole body (SPB) with an essential function during SPB duplication. J. Cell Biol. *132*, 887-901.

Doxsey, S., McCollum, D., and Theurkauf, W. (2005a). Centrosomes in cellular regulation. Annu Rev Cell Dev Biol *21*, 411-434.

Doxsey, S., McCollum, D., and Theurkauf, W. (2005b). Centrosomes in cellular regulation. Annu. Rev. Cell Dev. Biol. *21*, 411-434.

Doxsey, S., Zimmerman, W., and Mikule, K. (2005c). Centrosome control of the cell cycle. Trends Cell Biol *15*, 303-311.

Drummond, D.R., and Hagan, I.M. (1998). Mutations in the bimC box of Cut7 indicate divergence of regulation within the bimC family of kinesin related proteins. J Cell Sci *111 (Pt 7)*, 853-865.

Efimov, A., Kharitonov, A., Efimova, N., Loncarek, J., Miller, P.M., Andreyeva, N., Gleeson, P., Galjart, N., Maia, A.R., McLeod, I.X., Yates, J.R., 3rd, Maiato, H., Khodjakov, A., Akhmanova, A., and Kaverina, I. (2007). Asymmetric CLASP-Dependent Nucleation of Noncentrosomal Microtubules at the trans-Golgi Network. Dev. Cell *12*, 917-930.

Elliott, S., Knop, M., Schlenstedt, G., and Schiebel, E. (1999). Spc29p is a component of the Spc110p subcomplex and is essential for spindle pole body duplication. Proc Natl Acad Sci U S A *96*, 6205-6210.

Eng, J.K., McCormack, A.L., and Yates, J.R. (1994). An approach to correlate tandem mass spectral data of peptides with amino acid sequences in a protein database. J. Amer. Soc. Mass Spectrom. *5*, 976-989.

Erickson, H.P., and Stoffler, D. (1996). Protofilaments and rings, two conformations of the tubulin family conserved from bacterial FtsZ to alpha/beta and gamma tubulin. J Cell Biol *135*, 5-8.

Fankhauser, C., Marks, J., Reymond, A., and Simanis, V. (1993). The S. pombe cdc16 gene is required both for maintenance of p34cdc2 kinase activity and regulation of septum formation: a link between mitosis and cytokinesis? Embo J *12*, 2697-2704.

Fava, F., Raynaud-Messina, B., Leung-Tack, J., Mazzolini, L., Li, M., Guillemot, J.C., Cachot, D., Tollon, Y., Ferrara, P., and Wright, M. (1999). Human 76p: A new member of the gamma-tubulin-associated protein family. J Cell Biol *147*, 857-868.

Feierbach, B., and Chang, F. (2001). Cytokinesis and the contractile ring in fission yeast. Curr Opin Microbiol *4*, 713-719.

Flory, M.R., Morphew, M., Joseph, J.D., Means, A.R., and Davis, T.N. (2002). Pcp1p, an Spc110p-related calmodulin target at the centrosome of the fission yeast *Schizosaccharomyces pombe*. Cell Growth Differ. *13*, 47-58.

Flory, M.R., Moser, M.J., Monnat, R.J., Jr., and Davis, T.N. (2000). Identification of a human centrosomal calmodulin-binding protein that shares homology with pericentrin. Proc Natl Acad Sci U S A *97*, 5919-5923.

Forrest, A.R., McCormack, A.K., DeSouza, C.P., Sinnamon, J.M., Tonks, I.D., Hayward, N.K., Ellem, K.A., and Gabrielli, B.G. (1999). Multiple splicing variants of cdc25B regulate G2/M progression. Biochem Biophys Res Commun *260*, 510-515.

Friedman, D.B., Kern, J.W., Huneycutt, B.J., Vinh, D.B., Crawford, D.K., Steiner, E., Scheiltz, D., Yates, J., 3rd, Resing, K.A., Ahn, N.G., Winey, M., and Davis, T.N. (2001). Yeast Mps1p phosphorylates the spindle pole component Spc110p in the N-terminal domain. J Biol Chem *276*, 17958-17967.

Fujita, A., Vardy, L., Garcia, M.A., and Toda, T. (2002). A fourth component of the fission yeast gamma-tubulin complex, Alp16, is required for cytoplasmic microtubule integrity and becomes indispensable when gamma-tubulin function is compromised. Mol Biol Cell *13*, 2360-2373.

Giddings, T.H., Jr., O'Toole, E.T., Morphew, M., Mastronarde, D.N., McIntosh, J.R., and Winey, M. (2001). Using rapid freeze and freeze-substitution for the preparation of yeast cells for electron microscopy and three-dimensional analysis. Methods Cell Biol. *67*, 27-42.

Gould, K.L., Moreno, S., Owen, D.J., Sazer, S., and Nurse, P. (1991). Phosphorylation at Thr167 is required for *Schizosaccharomyces pombe* $p34^{cdc2}$ function. EMBO J. *10*, 3297-3309.

Gould, K.L., Ren, L., Feoktistova, A.S., Jennings, J.L., and Link, A.J. (2004). Tandem affinity purification and identification of protein complex components. Methods *33*, 239-244.

Gruneberg, U., Campbell, K., Simpson, C., Grindlay, J., and Schiebel, E. (2000). Nud1p links astral microtubule organization and the control of exit from mitosis. Embo J *19*, 6475-6488.

Guertin, D.A., Venkatram, S., Gould, K.L., and McCollum, D. (2002). Dma1 prevents mitotic exit and cytokinesis by inhibiting the septation initiation network (SIN). Dev. Cell *3*, 779-790.

Gunawardane, R.N., Lizarraga, S.B., Wiese, C., Wilde, A., and Zheng, Y. (2000). gamma-Tubulin complexes and their role in microtubule nucleation. Curr Top Dev Biol *49*, 55-73.

Hagan, I., and Yanagida, M. (1995). The product of the spindle formation gene *sad1*$^{+}$ associates with the fission yeast spindle pole body and is essential for viability. J. Cell Biol. *129*, 1033-1047.

Hagan, I.M., and Petersen, J. (2000). The microtubule organizing centers of *Schizosaccharomyces pombe*. Curr. Top. Dev. Biol. *49*, 133-159.

Hartwell, L.H., and Weinert, T.A. (1989). Checkpoints: controls that ensure the order of cell cycle events. Science *246*, 629-634.

Hinchcliffe, E.H., Li, C., Thompson, E.A., Maller, J.L., and Sluder, G. (1999). Requirement of Cdk2-cyclin E activity for repeated centrosome reproduction in Xenopus egg extracts. Science *283*, 851-854.

Humbel, B.M., Konomi, M., Takagi, T., Kamasawa, N., Ishijima, S.A., and Osumi, M. (2001). In situ localization of beta-glucans in the cell wall of Schizosaccharomyces pombe. Yeast *18*, 433-444.

Ikemoto, S., Nakamura, T., Kubo, M., and Shimoda, C. (2000). *S. pombe* sporulation-specific coiled-coil protein Spo15p is localized to the spindle pole body and essential for its modification. J. Cell Sci. *113*, 545-554.

Jacobs, C.W., Adams, A.E., Szaniszlo, P.J., and Pringle, J.R. (1988). Functions of microtubules in the Saccharomyces cerevisiae cell cycle. J Cell Biol *107*, 1409-1426.

James, P., Halladay, J., and Craig, E.A. (1996). Genomic libraries and a host strain designed for highly efficient two-hybrid selection in yeast. Genetics *144*, 1425-1436.

Janson, M.E., Setty, T.G., Paoletti, A., and Tran, P.T. (2005). Efficient formation of bipolar microtubule bundles requires microtubule-bound gamma-tubulin complexes. J. Cell Biol. *169*, 297-308.

Jaspersen, S.L., Giddings, T.H., Jr., and Winey, M. (2002). Mps3p is a novel component of the yeast spindle pole body that interacts with the yeast centrin homologue Cdc31p. J. Cell Biol. *159*, 945-956.

Jaspersen, S.L., Huneycutt, B.J., Giddings, T.H., Jr., Resing, K.A., Ahn, N.G., and Winey, M. (2004). Cdc28/Cdk1 regulates spindle pole body duplication through phosphorylation of Spc42 and Mps1. Dev. Cell *7*, 263-274.

Jaspersen, S.L., and Winey, M. (2004). The budding yeast spindle pole body: structure, duplication, and function. Annu. Rev. Cell Dev. Biol. *20*, 1-28.

Kamps, M.P., and Sefton, B.M. (1989). Acid and base hydrolysis of phosphoproteins bound to immobilon facilitates analysis of phosphoamino acids in gel-fractionated proteins. Anal Biochem *176*, 22-27.

Keeney, J.B., and Boeke, J.D. (1994). Efficient targeted integration at *leu1-32* and *ura4-294* in *Schizosaccharomyces pombe*. Genetics *136*, 849-856.

Khodjakov, A., and Rieder, C.L. (2001). Centrosomes enhance the fidelity of cytokinesis in vertebrates and are required for cell cycle progression. J Cell Biol *153*, 237-242.

Kirkham, M., Muller-Reichert, T., Oegema, K., Grill, S., and Hyman, A.A. (2003). SAS-4 is a C. elegans centriolar protein that controls centrosome size. Cell *112*, 575-587.

Knop, M., and Schiebel, E. (1997). Spc98p and Spc97p of the yeast γ-tubulin complex mediate binding to the spindle pole body via their interaction with Spc110p. EMBO J. *16*, 6985-6995.

Knop, M., and Schiebel, E. (1998). Receptors determine the cellular localization of a gamma-tubulin complex and thereby the site of microtubule formation. Embo J *17*, 3952-3967.

Kramer, A., Mailand, N., Lukas, C., Syljuasen, R.G., Wilkinson, C.J., Nigg, E.A., Bartek, J., and Lukas, J. (2004). Centrosome-associated Chk1 prevents premature activation of cyclin-B-Cdk1 kinase. Nat Cell Biol *6*, 884-891.

Krapp, A., Cano, E., and Simanis, V. (2004a). Analysis of the *S. pombe* signalling scaffold protein Cdc11p reveals an essential role for the N-terminal domain in SIN signalling. FEBS Lett. *565*, 176-180.

Krapp, A., Gulli, M.P., and Simanis, V. (2004b). SIN and the art of splitting the fission yeast cell. Curr. Biol. *14*, R722-730.

Krapp, A., Schmidt, S., Cano, E., and Simanis, V. (2001). *S. pombe* cdc11p, together with sid4p, provides an anchor for septation initiation network proteins on the spindle pole body. Curr. Biol. *11*, 1559-1568.

Kubo, A., Sasaki, H., Yuba-Kubo, A., Tsukita, S., and Shiina, N. (1999). Centriolar satellites: molecular characterization, ATP-dependent movement toward centrioles and possible involvement in ciliogenesis. J Cell Biol *147*, 969-980.

Lacey, K.R., Jackson, P.K., and Stearns, T. (1999). Cyclin-dependent kinase control of centrosome duplication. Proc Natl Acad Sci U S A *96*, 2817-2822.

Leidel, S., Delattre, M., Cerutti, L., Baumer, K., and Gonczy, P. (2005). SAS-6 defines a protein family required for centrosome duplication in C. elegans and in human cells. Nat Cell Biol *7*, 115-125.

Leidel, S., and Gonczy, P. (2003). SAS-4 is essential for centrosome duplication in C elegans and is recruited to daughter centrioles once per cell cycle. Dev Cell *4*, 431-439.

Leidel, S., and Gonczy, P. (2005). Centrosome duplication and nematodes: recent insights from an old relationship. Dev. Cell *9*, 317-325.

Link, A.J., Eng, J., Schieltz, D.M., Carmack, E., Mize, G.J., Morris, D.R., Garvik, B.M., and Yates, J.R., 3rd. (1999). Direct analysis of protein complexes using mass spectrometry. Nat. Biotechnol. *17*, 676-682.

Luders, J., and Stearns, T. (2007). Microtubule-organizing centres: a re-evaluation. Nat Rev Mol Cell Biol *8*, 161-167.

Lutz, W., Lingle, W.L., McCormick, D., Greenwood, T.M., and Salisbury, J.L. (2001). Phosphorylation of centrin during the cell cycle and its role in centriole separation preceding centrosome duplication. J Biol Chem *276*, 20774-20780.

MacCoss, M.J., Wu, C.C., and Yates, J.R., 3rd. (2002). Probability-based validation of protein identifications using a modified SEQUEST algorithm. Anal. Chem. *74*, 5593-5599.

Margolis, S.S., Walsh, S., Weiser, D.C., Yoshida, M., Shenolikar, S., and Kornbluth, S. (2003). PP1 control of M phase entry exerted through 14-3-3-regulated Cdc25 dephosphorylation. Embo J *22*, 5734-5745.

Marschall, L.G., Jeng, R.L., Mulholland, J., and Stearns, T. (1996). Analysis of Tub4p, a yeast gamma-tubulin-like protein: implications for microtubule-organizing center function. J Cell Biol *134*, 443-454.

Marshall, W.F. (2001). Centrioles take center stage. Curr Biol *11*, R487-496.

Maundrell, K. (1993). Thiamine-repressible expression vectors pREP and pRIP for fission yeast. Gene *123*, 127-130.

McCollum, D., and Gould, K.L. (2001). Timing is everything: regulation of mitotic exit and cytokinesis by the MEN and SIN. Trends Cell Biol. *11*, 89-95.

McDonald, W.H., Ohi, R., Smelkova, N., Frendewey, D., and Gould, K.L. (1999). Myb-related fission yeast cdc5p is a component of a 40S snRNP-containing complex and is essential for pre-mRNA splicing. Mol. Cell. Biol. *19*, 5352-5362.

Miki, F., Kurabayashi, A., Tange, Y., Okazaki, K., Shimanuki, M., and Niwa, O. (2004). Two-hybrid search for proteins that interact with Sad1 and Kms1, two membrane-bound

components of the spindle pole body in fission yeast. Mol. Genet. Genomics *270*, 449-461.

Moreno, S., Hayles, J., and Nurse, P. (1989). Regulation of p34cdc2 protein kinase during mitosis. Cell *58*, 361-372.

Moreno, S., Klar, A., and Nurse, P. (1991). Molecular genetic analysis of fission yeast *Schizosaccharomyces pombe*. Methods Enzymol. *194*, 795-823.

Moritz, M., and Agard, D.A. (2001). Gamma-tubulin complexes and microtubule nucleation. Curr Opin Struct Biol *11*, 174-181.

Morrell, J.L., Tomlin, G.C., Rajagopalan, S., Venkatram, S., Feoktistova, A.S., Tasto, J.J., Mehta, S., Jennings, J.L., Link, A., Balasubramanian, M.K., and Gould, K.L. (2004). Sid4p-Cdc11p assembles the septation initiation network and its regulators at the *S. pombe* SPB. Curr. Biol. *14*, 579-584.

Muller, E.G., Snydsman, B.E., Novik, I., Hailey, D.W., Gestaut, D.R., Niemann, C.A., O'Toole, E.T., Giddings, T.H., Jr., Sundin, B.A., and Davis, T.N. (2005a). The organization of the core proteins of the yeast spindle pole body. Mol. Biol. Cell *16*, 3341-3352.

Muller, E.G., Snydsman, B.E., Novik, I., Hailey, D.W., Gestaut, D.R., Niemann, C.A., O'Toole, E.T., Giddings, T.H., Jr., Sundin, B.A., and Davis, T.N. (2005b). The organization of the core proteins of the yeast spindle pole body. Mol Biol Cell *16*, 3341-3352.

Murphy, S.M., Preble, A.M., Patel, U.K., O'Connell, K.L., Dias, D.P., Moritz, M., Agard, D., Stults, J.T., and Stearns, T. (2001). GCP5 and GCP6: two new members of the human gamma-tubulin complex. Mol Biol Cell *12*, 3340-3352.

Murphy, S.M., Urbani, L., and Stearns, T. (1998). The mammalian gamma-tubulin complex contains homologues of the yeast spindle pole body components spc97p and spc98p. J Cell Biol *141*, 663-674.

Murray, A.W., and Hunt, T. (1993). The cell cycle: an introduction. W.H. Freeman: New York.

Murray, A.W., and Kirschner, M.W. (1989). Cyclin synthesis drives the early embryonic cell cycle. Nature *339*, 275-280.

Nasmyth, K., and Nurse, P. (1981). Cell division cycle mutants altered in DNA replication and mitosis in the fission yeast Schizosaccharomyces pombe. Mol Gen Genet *182*, 119-124.

Niccoli, T., Yamashita, A., Nurse, P., and Yamamoto, M. (2004). The p150-Glued Ssm4p regulates microtubular dynamics and nuclear movement in fission yeast. J. Cell Sci. *117*, 5543-5556.

Nigg, E.A. (1995). Cyclin-dependent protein kinases: key regulators of the eukaryotic cell cycle. Bioessays *17*, 471-480.

Niwa, O., Shimanuki, M., and Miki, F. (2000). Telomere-led bouquet formation facilitates homologous chromosome pairing and restricts ectopic interaction in fission yeast meiosis. EMBO J. *19*, 3831-3840.

Nurse, P. (1975). Genetic control of cell size at cell division in yeast. Nature *256*, 547-551.

Nurse, P., Thuriaux, P., and Nasmyth, K. (1976). Genetic control of the cell division cycle in the fission yeast Schizosaccharomyces pombe. Mol Gen Genet *146*, 167-178.

O'Toole, E.T., Winey, M., and McIntosh, J.R. (1999). High-voltage electron tomography of spindle pole bodies and early mitotic spindles in the yeast Saccharomyces cerevisiae. Mol Biol Cell *10*, 2017-2031.

Oegema, K., Wiese, C., Martin, O.C., Milligan, R.A., Iwamatsu, A., Mitchison, T.J., and Zheng, Y. (1999). Characterization of two related Drosophila gamma-tubulin complexes that differ in their ability to nucleate microtubules. J Cell Biol *144*, 721-733.

Ohi, M.D., and Gould, K.L. (2002). Characterization of interactions among the Cef1p-Prp19p-associated splicing complex. RNA *8*, 798-815.

Paoletti, A., Bordes, N., Haddad, R., Schwartz, C.L., Chang, F., and Bornens, M. (2003). Fission yeast cdc31p is a component of the half-bridge and controls SPB duplication. Mol. Biol. Cell *14*, 2793-2808.

Pardo, M., and Nurse, P. (2003). Equatorial retention of the contractile actin ring by microtubules during cytokinesis. Science *300*, 1569-1574.

Pereira, G., Knop, M., and Schiebel, E. (1998). Spc98p directs the yeast gamma-tubulin complex into the nucleus and is subject to cell cycle-dependent phosphorylation on the nuclear side of the spindle pole body. Mol Biol Cell *9*, 775-793.

Roof, D.M., Meluh, P.B., and Rose, M.D. (1992). Kinesin-related proteins required for assembly of the mitotic spindle. J Cell Biol *118*, 95-108.

Rose, M.D., and Fink, G.R. (1987). KAR1, a gene required for function of both intranuclear and extranuclear microtubules in yeast. Cell *48*, 1047-1060.

Rosenberg, J.A., Tomlin, G.C., McDonald, W.H., Snydsman, B.E., Muller, E.G., Yates, J.R., 3rd, and Gould, K.L. (2006). Ppc89 links multiple proteins, including the septation initiation network, to the core of the fission yeast spindle-pole body. Mol Biol Cell *17*, 3793-3805.

Saito, T.T., Tougan, T., Okuzaki, D., Kasama, T., and Nojima, H. (2005). Mcp6, a meiosis-specific coiled-coil protein of *Schizosaccharomyces pombe*, localizes to the

spindle pole body and is required for horsetail movement and recombination. J. Cell Sci. *118*, 447-459.

Samejima, I., Lourenco, P.C., Snaith, H.A., and Sawin, K.E. (2005). Fission yeast mto2p regulates microtubule nucleation by the centrosomin-related protein mto1p. Mol. Biol. Cell *16*, 3040-3051.

Sawin, K.E. (2005). Meiosis: organizing microtubule organizers. Curr. Biol. *15*, R633-635.

Sawin, K.E., Lourenco, P.C., and Snaith, H.A. (2004a). Microtubule nucleation at non-spindle pole body microtubule-organizing centers requires fission yeast centrosomin-related protein mod20p. Curr Biol *14*, 763-775.

Sawin, K.E., Lourenco, P.C.C., and Snaith, H.A. (2004b). Microtubule nucleation at non-spindle pole body microtubule-organizing centers requires fission yeast centrosomin-related protein mod20p. Curr. Biol. *14*, 763-775.

Schramm, C., Elliott, S., Shevchenko, A., and Schiebel, E. (2000). The Bbp1p-Mps2p complex connects the SPB to the nuclear envelope and is essential for SPB duplication. Embo J *19*, 421-433.

Schutz, A.R., and Winey, M. (1998). New alleles of the yeast MPS1 gene reveal multiple requirements in spindle pole body duplication. Mol Biol Cell *9*, 759-774.

Shimanuki, M., Miki, F., Ding, D.Q., Chikashige, Y., Hiraoka, Y., Horio, T., and Niwa, O. (1997). A novel fission yeast gene, *kms1*$^{+}$, is required for the formation of meiotic prophase-specific nuclear architecture. Mol. Gen. Genet. *254*, 238-249.

Shimoda, C. (2004). Forespore membrane assembly in yeast: coordinating SPBs and membrane trafficking. J. Cell Sci. *117*, 389-396.

Siam, R., Dolan, W.P., and Forsburg, S.L. (2004). Choosing and using *Schizosaccharomyces pombe* plasmids. Methods *33*, 189-198.

Simanis, V. (2003). Events at the end of mitosis in the budding and fission yeasts. J. Cell Sci. *116*, 4263-4275.

Simanis, V., and Nurse, P. (1986). The cell cycle control gene cdc2+ of fission yeast encodes a protein kinase potentially regulated by phosphorylation. Cell *45*, 261-268.

Sobel, S.G., and Snyder, M. (1995). A highly divergent gamma-tubulin gene is essential for cell growth and proper microtubule organization in Saccharomyces cerevisiae. J Cell Biol *131*, 1775-1788.

Song, K., Mach, K.E., Chen, C.Y., Reynolds, T., and Albright, C.F. (1996). A novel suppressor of ras1 in fission yeast, byr4, is a dosage-dependent inhibitor of cytokinesis. J Cell Biol *133*, 1307-1319.

Spang, A., Courtney, I., Fackler, U., Matzner, M., and Schiebel, E. (1993). The calcium-binding protein cell division cycle 31 of Saccharomyces cerevisiae is a component of the half bridge of the spindle pole body. J Cell Biol *123*, 405-416.

Spang, A., Geissler, S., Grein, K., and Schiebel, E. (1996a). gamma-Tubulin-like Tub4p of Saccharomyces cerevisiae is associated with the spindle pole body substructures that organize microtubules and is required for mitotic spindle formation. J Cell Biol *134*, 429-441.

Spang, A., Grein, K., and Schiebel, E. (1996b). The spacer protein Spc110p targets calmodulin to the central plaque of the yeast spindle pole body. J Cell Sci *109 (Pt 9)*, 2229-2237.

Sparks, C.A., Morphew, M., and McCollum, D. (1999). Sid2p, a spindle pole body kinase that regulates the onset of cytokinesis. J. Cell Biol. *146*, 777-790.

Stegmeier, F., and Amon, A. (2004). Closing mitosis: the functions of the Cdc14 phosphatase and its regulation. Annu Rev Genet *38*, 203-232.

Sundberg, H.A., and Davis, T.N. (1997). A mutational analysis identifies three functional regions of the spindle pole component Spc110p in *Saccharomyces cerevisiae*. Mol. Biol. Cell *8*, 2575-2590.

Szollosi, D., Calarco, P., and Donahue, R.P. (1972). Absence of centrioles in the first and second meiotic spindles of mouse oocytes. J Cell Sci *11*, 521-541.

Tanaka, K., Kohda, T., Yamashita, A., Nonaka, N., and Yamamoto, M. (2005). Hrs1p/Mcp6p on the meiotic SPB organizes astral microtubule arrays for oscillatory nuclear movement. Curr. Biol. *15*, 1479-1486.

Tassin, A.M., Maro, B., and Bornens, M. (1985). Fate of microtubule-organizing centers during myogenesis in vitro. J. Cell Biol. *100*, 35-46.

Tasto, J.J., Carnahan, R.H., McDonald, W.H., and Gould, K.L. (2001). Vectors and gene targeting modules for tandem affinity purification in *Schizosaccharomyces pombe*. Yeast *18*, 657-662.

Tomlin, G.C., Morrell, J.L., and Gould, K.L. (2002). The spindle pole body protein Cdc11p links Sid4p to the fission yeast septation initiation network. Mol. Biol. Cell *13*, 1203-1214.

Tsou, M.F., and Stearns, T. (2006). Mechanism limiting centrosome duplication to once per cell cycle. Nature *442*, 947-951.

Urbani, L., and Stearns, T. (1999). The centrosome. Curr. Biol. *9*, R315-317.

Uzawa, S., Li, F., Jin, Y., McDonald, K.L., Braunfeld, M.B., Agard, D.A., and Cande, W.Z. (2004). Spindle pole body duplication in fission yeast occurs at the G1/S boundary

but maturation is blocked until exit from S by an event downstream of *cdc10*$^{+}$. Mol. Biol. Cell *15*, 5219-5230.

Valiron, O., Caudron, N., and Job, D. (2001). Microtubule dynamics. Cell Mol Life Sci *58*, 2069-2084.

Vallen, E.A., Ho, W., Winey, M., and Rose, M.D. (1994). Genetic interactions between CDC31 and KAR1, two genes required for duplication of the microtubule organizing center in Saccharomyces cerevisiae. Genetics *137*, 407-422.

Vardy, L., and Toda, T. (2000). The fission yeast γ-tubulin complex is required in G_1 phase and is a component of the spindle assembly checkpoint. EMBO J. *19*, 6098-6111.

Venkatram, S., Jennings, J.L., Link, A., and Gould, K.L. (2005). Mto2p, a novel fission yeast protein required for cytoplasmic microtubule organization and anchoring of the cytokinetic actin ring. Mol. Biol. Cell *16*, 3052-3063.

Venkatram, S., Tasto, J.J., Feoktistova, A., Jennings, J.L., Link, A.J., and Gould, K.L. (2004). Identification and characterization of two novel proteins affecting fission yeast γ-tubulin complex function. Mol. Biol. Cell *15*, 2287-2301.

West, R.R., Vaisberg, E.V., Ding, R., Nurse, P., and McIntosh, J.R. (1998). *cut11*$^{+}$: A gene required for cell cycle-dependent spindle pole body anchoring in the nuclear envelope and bipolar spindle formation in *Schizosaccharomyces pombe*. Mol. Biol. Cell *9*, 2839-2855.

Wolfe, B.A., and Gould, K.L. (2004). Inactivating Cdc25, mitotic style. Cell Cycle *3*, 601-603.

Wolfe, B.A., and Gould, K.L. (2005). Split decisions: coordinating cytokinesis in yeast. Trends Cell Biol. *15*, 10-18.

Wong, C., and Stearns, T. (2003). Dispatch. Centrosome biology: a SAS-sy centriole in the cell cycle. Curr Biol *13*, R351-352.

Wood, V., Gwilliam, R., Rajandream, M.A., Lyne, M., Lyne, R., Stewart, A., Sgouros, J., Peat, N., Hayles, J., Baker, S., Basham, D., Bowman, S., Brooks, K., Brown, D., Brown, S., Chillingworth, T., Churcher, C., Collins, M., Connor, R., Cronin, A., Davis, P., Feltwell, T., Fraser, A., Gentles, S., Goble, A., Hamlin, N., Harris, D., Hidalgo, J., Hodgson, G., Holroyd, S., Hornsby, T., Howarth, S., Huckle, E.J., Hunt, S., Jagels, K., James, K., Jones, L., Jones, M., Leather, S., McDonald, S., McLean, J., Mooney, P., Moule, S., Mungall, K., Murphy, L., Niblett, D., Odell, C., Oliver, K., O'Neil, S., Pearson, D., Quail, M.A., Rabbinowitsch, E., Rutherford, K., Rutter, S., Saunders, D., Seeger, K., Sharp, S., Skelton, J., Simmonds, M., Squares, R., Squares, S., Stevens, K., Taylor, K., Taylor, R.G., Tivey, A., Walsh, S., Warren, T., Whitehead, S., Woodward, J., Volckaert, G., Aert, R., Robben, J., Grymonprez, B., Weltjens, I., Vanstreels, E., Rieger, M., Schafer, M., Muller-Auer, S., Gabel, C., Fuchs, M., Dusterhoft, A., Fritzc, C., Holzer, E., Moestl, D., Hilbert, H., Borzym, K., Langer, I., Beck, A., Lehrach, H., Reinhardt, R.,

Pohl, T.M., Eger, P., Zimmermann, W., Wedler, H., Wambutt, R., Purnelle, B., Goffeau, A., Cadieu, E., Dreano, S., Gloux, S., Lelaure, V., Mottier, S., Galibert, F., Aves, S.J., Xiang, Z., Hunt, C., Moore, K., Hurst, S.M., Lucas, M., Rochet, M., Gaillardin, C., Tallada, V.A., Garzon, A., Thode, G., Daga, R.R., Cruzado, L., Jimenez, J., Sanchez, M., del Rey, F., Benito, J., Dominguez, A., Revuelta, J.L., Moreno, S., Armstrong, J., Forsburg, S.L., Cerutti, L., Lowe, T., McCombie, W.R., Paulsen, I., Potashkin, J., Shpakovski, G.V., Ussery, D., Barrell, B.G., and Nurse, P. (2002). The genome sequence of Schizosaccharomyces pombe. Nature *415*, 871-880.

Woods, A., Sherwin, T., Sasse, R., MacRae, T.H., Baines, A.J., and Gull, K. (1989). Definition of individual components within the cytoskeleton of *Trypanosoma brucei* by a library of monoclonal antibodies. J. Cell Sci. *93*, 491-500.

Yoon, H.J., Feoktistova, A., Wolfe, B.A., Jennings, J.L., Link, A.J., and Gould, K.L. (2002). Proteomics analysis identifies new components of the fission and budding yeast anaphase-promoting complexes. Curr Biol *12*, 2048-2054.

Zheng, Y., Wong, M.L., Alberts, B., and Mitchison, T. (1995). Nucleation of microtubule assembly by a gamma-tubulin-containing ring complex. Nature *378*, 578-583.

Zimmerman, S., and Chang, F. (2005). Effects of {gamma}-tubulin complex proteins on microtubule nucleation and catastrophe in fission yeast. Mol. Biol. Cell *16*, 2719-2733.